

https://dspace.org/

# Group Invariant Solution for the Hydraulic fracture of two closely spaced beams

**khoza, Confide**

**2019**
https://hdl.handle.net/10539/28763

Downloaded from a DSpace repository. https://dspace.org/

# Group Invariant Solution for the Hydraulic Fracture of Two Closely Spaced Beams




**CONFIDE KHOZA**

A dissertation submitted to the Faculty of Science, University of the Witwatersrand, Johannesburg, South Africa, in fulfilment of the requirements for the degree of Master of Science.

**Declaration**

I, **Confide Khoza** Student number **566760**, am a student registered for the degree of Master in Science, year 2018.

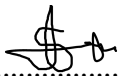
I hereby declare the following :

i) I am aware that plagiarism (the use of someone else's work without permission and acknowledging the original source) is wrong

ii) I confirm that the work submitted for assessment for the above degree is my own unaided work except where I have explicitly indicated otherwise

iii) I have followed the required conventions in referencing the thoughts and ideas of others.

iv) I understand that the University of the Witwatersrand may take disciplinary action against me if there is a belief that this is not my own unaided work or that I failed to acknowledge the source of the ideas or words in my writing.

Signature:

Date : 27 / 05 / 2019

# Abstract

The hydraulic fracture of two closely spaced beams, due to an ultra-high pressure fluid which is injected into the space between the beams, is considered. The fluid is Newtonian and the flow is laminar. The objective of this study is to investigate how the beams deform when the fluid under high pressure is injected. The mathematical model consists of the fourth order time dependent Euler-Bernoulli beam equation and a nonlinear diffusion equation derived using lubrication theory and relating the half-width of the fracture to the difference in pressure between the fluid pressure and the normal compressive stress on the beam. The Lie point symmetries of this system of two partial differential equations are derived and used to reduce the two partial differential equations and associated boundary conditions to a boundary value problem for a system of ordinary differential equations. The case of finite bending moment at the fracture tip is considered. The asymptotic solution of the ordinary differential equations at the fracture tip are derived. A shooting method is used to derive the numerical solution. It is found that the beams tend to "buckle" during the hydraulic fracturing.

# Acknowledgements

Firstly, I would like to give thanks to my God, Ebenezer. Secondly I am thankful to my supervisors, Dr A G Fareo and Prof D P Mason, for their support throughout my research. They have taught me countless things which have given me the ability to obtain the desired results. I am thankful for their kindness and financial assistance.

# Contents

**1 Introduction** **12**

1.1 Background to hydraulic fracturing . . . . . 12

1.2 Research aims and objectives . . . . . 14

1.3 Literature review . . . . . 15

1.4 Dissertation outline . . . . . 16

**2 Background to Lie group theory** **17**

2.1 Introduction . . . . . 17

2.2 Lie symmetry methods . . . . . 17

2.3 Numerical methods for solving non-linear boundary value problems . . . . . 19

2.3.1 Shooting method . . . . . 19

2.4 Conclusions . . . . . 20

**3 Mathematical modelling of hydraulic fracturing** **21**

3.1 Introduction . . . . . 21

3.2 Assumptions . . . . . 21

3.3 Euler-Bernoulli beam equation . . . . . 22

3.4 Thin fluid film equations . . . . . 23

3.5 Nondimensional variables . . . . . 29

3.6 Boundary and initial conditions . . . . . 31

3.7 Conclusions . . . . . 34

**4 Lie point symmetries and invariant solutions 35**

4.1 Introduction . . . . . 35

4.2 Lie point symmetry . . . . . 35

4.3 Invariant solution : general case $c_2 \neq 0$ . . . . . 49

4.4 Invariant solution: special case $c_2 = 0$ . . . . . 53

4.5 Boundary and initial conditions for the invariant solution: general case $c_2 \neq 0$ . . . . . 55

4.6 Boundary and initial conditions for the invariant solution : special case $c_2 = 0$ . . . . . 62

**5 Asymptotic and numerical solutions 67**

5.1 Introduction . . . . . 67

5.2 Asymptotic solution at the fracture tip for $c_2 \neq 0$ . . . . . 67

5.3 Width average fluid velocity: $c_2 \neq 0$. . . . . 69

5.4 Numerical values for the parameters . . . . . 71

5.5 Numerical solution for the general case: $c_2 \neq 0$ with finite bending moment at the fracture tip . . . . . 74

5.6 Results for the silicic magma fracture . . . . . 81

5.7 Conclusions . . . . . 107

**6 Conclusions 110**

6.1 Mathematical model . . . . . 110

6.2 Lie group analysis . . . . . 111

6.3 Numerical solution . . . . . 111

6.4 Results . . . . . 111

6.5 Future work . . . . . 112

**A Lie point symmetries of the system of ordinary differential equations**

**for the general case $c_2 \neq 0$. 113**

**B Lie point symmetries of the system of ordinary differential equations for $c_2 = 0$. 123**

# List of Figures


1.1 Injection of high pressure fluid leading to bending of the beams. . 13

3.1 Bending beams due to injection of high pressure fluid . . . . . 32

5.1 Graph of $c_1^{\frac{2}{3}} F(0)$ plotted against $E_3$ for $M_0 = 10^2$ and $c_1 = 10^5$. . . . 85

5.2 Graph of $c_1^{\frac{2}{3}} F(0)$ x $10^3$ plotted against $E_4$ for $M_0 = 10^2$ and $c_1 = 10^5$. 85

5.3 Graph of $c_1^{\frac{2}{3}} F(u)$ plotted against $u$ for $M_0 = 2.2$ x $10^2$ for a silicic magma fracture. . . . . 86

5.4 Graph of half-width $h(t,u)$ plotted against $u$ for $M_0 = 2.2$ x $10^2$ for a silicic magma fracture at times $t^* = \frac{t}{c_1} = 0.$ 20, 40, 60, 80. 100 . . 86

5.5 Graph of $c_1^{-\frac{4}{3}} G(u)$ plotted against $u$ for $M_0 = 2.2$ x $10^2$ for a silicic magma fracture . . . . . 87

5.6 Graph of pressure difference $P(t,u)$ plotted against $u$ for $M_0 = 2.2$ x $10^2$ and $t^* = \frac{t}{c_1} = 0$, 20, 40, 60, 80. 100 for a silicic magma fracture. 87

5.7 Graph of ratio of width average fluid velocity to the speed of propagation of the fracture $\frac{dL}{dt}$ plotted against $u$ for a silicic magma fracture. At the end points, $R(0) = 1.487$ x $10^2$ and $R(1) = 0$. . . . . 88

5.8 The length $L(t)$ of the fracture plotted against time $t^* = \frac{t}{c_1}$ for $c_1 = 10^5$. The length is independent of $M_0$ and $L(0) = 1$. . . . . 88

5.9 Graph of $c_1^{\frac{2}{3}} F(u)$ plotted against $u$ for $M_0 = 2.6105$ x $10^2$ for a silicic magma fracture. . . . . 90

5.10 Graph of half-width $h(t,u)$ plotted against $u$ for $M_0 = 2.6105 \text{ x } 10^2$ for a silicic magma fracture at times and $t^* = \frac{t}{c} = 0$, 20, 40, 60, 80 and 100 . . . . . 90

5.11 Graph of $c_1^{-\frac{4}{3}} G(u)$ plotted against $u$ for $M_0 = 2.26105 \text{ x } 10^2$ for a silicic magma fracture . . . . . 91

5.12 Graph of pressure difference $P(t,u)$ plotted against $u$ for $M_0 = 2.6105 \text{ x } 10^2$ and $t^* = \frac{t}{c} = 0$, 20, 40, 60, 80 and 100 for a silicic magma fracture. . . . . 91

5.13 Graph of ratio of width average fluid velocity to the speed of propagation of the fracture $\frac{dL}{dt}$ plotted against $u$ for $M_0 = 2.6105 \text{ x } 10^2$ for a silicic magma fracture. At the end points, $R(0) = 14.184028$ and $R(1) = 0$. . . . . 92

5.14 Graph of $c_1^{\frac{2}{3}} F_1(0)$ plotted against $E_3$ for $M_0 = 2.8 \text{ x } 10^2$ and $c_1 = 10^5$ 96

5.15 Graph of $c_1^{\frac{2}{3}} F_1(0) \text{ x } 10^{-3}$ plotted against $E_4$ for $M_0 = 2.8 \text{ x } 10^2$ and $c_1 = 10^5$ . . . . . 96

5.16 Graph of $h(0,u) = c_1^{\frac{2}{3}} F_1(u)$ plotted against $u$ for $M_0 = 2.618 \text{ x } 10^2$ for silicic magma fracture. . . . . 97

5.17 Graph of half-width $h(t,u)$ plotted against $u$ for $M_0 = 2.618 \text{ x } 10^2$ for a silicic magma fracture at a range of times from $t^* = \frac{t}{c_1} = 0$ to $t^* = \frac{t}{c_1} = 100$. . . . . 97

5.18 Graph of pressure difference $P(0,u) = c_1^{-\frac{4}{3}} G_1(u)$ plotted against $u$ for $M_0 = 2.618 \text{ x } 10^2$ for a silicic magma fracture. . . . . 98

5.19 Graph of the ratio R(u) of the width average fluid velocity to the speed of propagation of the fracture $\frac{dL}{dt}$ plotted against $u$ for $M_0 = 2.618 \text{ x } 10^2$ for silicic magma fracture. At the entry $R(0) = 10.1851$ while the asymptotic results with $Q_0 = 9.0945 \text{ x } 10^{-5}$ gives $R(0) = c_1 Q_0 = 9.0945$. . . . . 98

5.20 Graph of $h(0,u) = c_1^{\frac{2}{3}} F_1(u)$ plotted against $u$ for $M_0 = 1.05 \text{ x } 10^3$ for a silicic magma fracture. . . . . 99

5.21 Graph of half-width $h(t,u)$ plotted against $u$ for $M_0 = 1.05 \text{ x } 10^3$ for a silicic magma fracture at a range of times from $t^* = \frac{t}{c_1} = 0$ to $t^* = \frac{t}{c_1} = 100$. . . . . 99

5.22 Graph of pressure difference $P(0,u) = c_1^{-\frac{4}{3}} G_1(u)$ plotted against $u$ for $M_0 = 1.05 \text{ x } 10^3$ for a silicic magma fracture. . . . . 100

5.23 Graph of the ratio R(u) of the width average fluid velocity to the speed of propagation of the fracture $\frac{dL}{dt}$ plotted against $u$ for $M_0 = 1.05 \text{ x } 10^3$ for silicic magma fracture. At the entry $R(0) = 37.0540$ while the asymptotic results with $Q_0 = 3.64557 \text{ x } 10^{-4}$ gives $R(0) = c_1 Q_0 = 36.4557$. . . . . 100

5.24 Graph of $h(0,u) = c_1^{\frac{2}{3}} F_1(u)$ plotted against $u$ for $M_0 = 2.8 \text{ x } 10^2$ for silicic magma fracture. The shooting method cannot reach $c_1^{\frac{2}{3}} F_1(0) = 1$ and the curve is not a numerical solution. . . . . 101

5.25 Graph of half-width $h(t,u)$ plotted against $u$ for $M_0 = 2.8 \text{ x } 10^2$ for a silicic magma fracture at a range of times from $t^* = \frac{t}{c_1} = 0$ to $t^* = \frac{t}{c_1} = 100$. The shooting method cannot reach $c_1^{\frac{2}{3}} F_1(0) = 1$ and the figure does not show a numerical solution. . . . . 101

5.26 Graph of pressure difference $P(0,u) = c_1^{-\frac{4}{3}} G_1(u)$ plotted against $u$ for $M_0 = 2.8 \text{ x } 10^2$ for a silicic magma fracture. The curve does not describe a numerical solution because $c_1^{\frac{2}{3}} F_1(0) \neq 1$. . . . . 102

5.27 Graph of the ratio R(u) of the width average fluid velocity to the speed of propagation of the fracture $\frac{dL}{dt}$ plotted against $u$ for $M_0 = 2.8 \text{ x } 10^2$ for a silicic magma fracture. At the entry $R(0) = 0.339792$ while the asymptotic result with $Q_0 = 3.441743 \text{ x } 10^{-11}$ gives $R(0) = c_1 Q_0 = 3.441743 \text{ x } 10^{-6}$. The large difference is because the shooting method could not reach $c_1 F_1(0) = 1$. . . . . 102

5.28 Graph of $c_1^{\frac{2}{3}} F_1(0) \text{ x } 10^{-3}$ plotted against $E_3$ for $M_0 = 6 \text{ x } 10^3$ and $c_1 = 10^5$. . . . . 103

5.29 Graph of $h(0,u) = c_1^{\frac{2}{3}} F_1(u)$ plotted against $u$ for $M_0 = 6 \text{ x } 10^3$ for a silicic magma fracture. . . . . 103

5.30 Graph of half-width $h(t,u)$ plotted against $u$ for $M_0 = 6 \text{ x } 10^3$ for a silicic magma fracture at a range of times from $t^* = \frac{t}{c_1} = 0$ to $t^* = \frac{t}{c_1}$.104

# List of Tables

5.1 Maximum values for the characteristic volume flux per unit breadth $Q_0$ and the characteristic velocity $U$ along the fracture for the fluid flow in the fracture to be laminar [7]. . . . . 72

5.2 Values of the characteristic numbers $A$ and $B$ and the characteristic maximum depth below the surface. The values of the parameters were taken from Emerman et al. [7]. . . . . 75

5.3 The values of the parameters in the numerical solution for $c_1 = 10^5$ 82

5.4 Numerical values for $\frac{dG}{du}(0)$ and $Q_0$ for a range of values of bending moment $M_0$. . . . . 95

# Chapter 1

# Introduction

## 1.1 Background to hydraulic fracturing

Hydraulic fracturing, which was first introduced in the 1940's, has proved to be a very useful technique for the enhancement of the production of oil and natural gas from underground reservoirs. Most investigations on hydraulic fracturing have been done on rocks. The process of hydraulic fracturing occurs when an ultra-high pressure fluid is injected into a crack in the rock to facilitate the opening of the crack in the rock formation [7].

The purpose of hydraulic fracturing in the petroleum industry is to increase the permeability of the rock formation by using injected water with some additives to open existing fractures and create new ones in order to enhance the extraction of gas and oil. Fracturing is designed to maximise the permeability of the rock, increase the accessibility and production of oil and gas.

In the hydraulic fracturing of two closely spaced beams [20], ultra-high pressure viscous incompressible Newtonian fluid is injected in the space between the beams which causes the beams to bend symmetrically away from the axis of the two beams. The injected viscous incompressible fluid supplies a force per unit length acting transversely along the length of the beams.

The aim of this research is to use Lie symmetry analysis to investigate the deformation of two closely spaced beams when an incompressible fluid is injected into the space between the beams. The fluid flow in the fracture is modelled using the lubrication equations.

There has been significant work involving beam bending [16, 18].The investigation by Please et al.[16] considered a beam which is clamped at each end at a pillar. Lie group analysis of the Euler Bernoulli beam has being investigated by several authors [18]

The study will derive the Lie point symmetries of the coupled system of partial differential equations consisting of the nonlinear diffusion equation for the half-width of the fracture and the Euler-Bernoulli beam equation. We will then use a linear combination of the Lie point symmetries to reduce the partial differential equations to a system of two ordinary differential equations and derive the general invariant form for the fracture half-width and pressure.

Two boundary conditions on the bending moment at the fracture tip are found. They are the finite bending moment and the infinite bending moment.The infinite bending moment corresponds to the infinite curvature which causes the beam to fracture at the tip. The hydraulic fracture of the two closely spaced beams and the coordinate system are illustrated in Figure 1.1. The $z$ - axis is orthogonal the $x$, $y$ - plane.

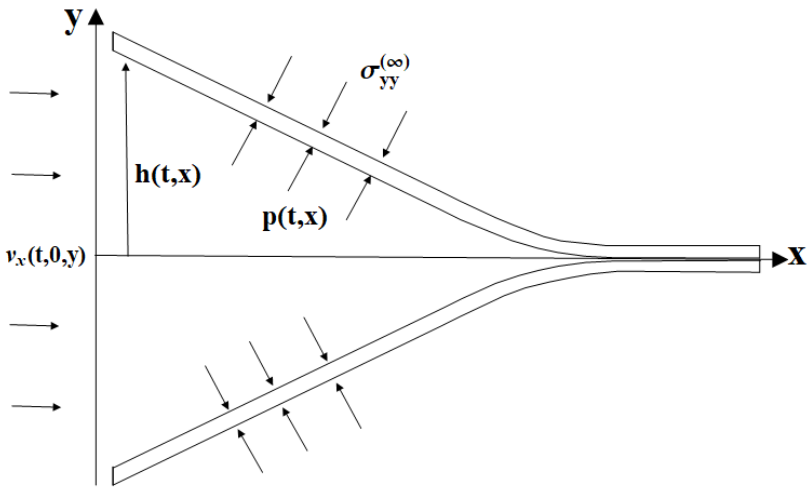



Figure 1.1: Injection of high pressure fluid leading to bending of the beams.

In this dissertation, our investigation focuses on the upper half of the fracture $0 \leq y \leq h(t,x)$. The upper beam is acted on by a normal compressive stress $\sigma_{yy}^{(\infty)}$. For a beam underground this would be the compressive stress due to the

overburden rock. The rock mass underground may be modelled as a layered system of beams which interact through normal surface stresses. The time dependent Euler-Bernoulli beam equation is

$$EI\frac{\partial^4 h}{\partial x^4} + \hat{\rho}\frac{\partial^2 h}{\partial t^2} = P, \tag{1.1}$$

where $E$ is the Young's modulus of the beam, $I$ is the second moment of area, $\hat{\rho}$ is the mass of the beam per unit length, $h(t,x)$ is the half-width, also the deflection of the beam from the centerline and $P$ is the net force per unit length on the beam in the upward direction. $P$ is related to the fluid pressure $p$ and the normal stress on the upper surface of the beam, $\sigma_{yy}^{(\infty)}$, by

$$\frac{P(t,y)}{b} = p(t,x) - \sigma_{yy}^{(\infty)}, \tag{1.2}$$

where $b$ is the thickness of the beam. Further details on the beam equation will be given in Chapter 3.

The lubrication approximation will be used to derive the nonlinear diffusion equation relating the fracture half-width $h(t,x)$ to the fluid pressure $p(t,x)$,

$$\frac{\partial h}{\partial t} = \frac{1}{3\mu}\frac{\partial}{\partial x}\Big(h^3\frac{\partial p}{\partial x}\Big), \tag{1.3}$$

where $\mu$ is the viscosity of the fluid. The derivation of equation (1.3) will be provided in Chapter 3.

## 1.2 Research aims and objectives

In this research , we aim to do the following:

- Model the time dependent Euler-Bernoulli beam equation [17].
- Model the fluid flow between the beams using lubrication theory and derive a partial differential equation relating half-width of the fracture to the fluid pressure.

- Employ Lie symmetry analysis to reduce the system of two governing partial deferential equations to a system of two ordinary differential equations and find the general form of the group invariant solution which describes the hydraulic fracture between two closely spaced beams.
- Find analytical solutions for special cases when the bending moments is finite at the fracture tip.
- Look for numerical solutions of reduced models.

## 1.3 Literature review

A number of investigations have been made on the Euler-Bernoulli beam equation. Wafo Soh [18] considered the Euler-Bernoulli beam equation from a symmetry standpoint. His goal was to study the symmetry breaking of the Euler-Bernoulli beam equation. Wafo Soh believed that Da Vinci and Galileo foresaw the need for a theory of a vibrating thin beam.

An extension of the work of Wafo Soh was made by Fatima, Bokhari, Mahomed and Zaman [8]. They agreed that Wafo Soh had solved the equivalence problem using symmetry analysis for the Euler-Bernoulli equation. In their study they performed the complete Lie group classification of the ordinary differential equation(ODE) that resulted from the reduction of the static Euler-Bernoulli beam partial differential equation. The isospectral properties of the Euler-Bernoulli beam equation and its nonhomogeneous variant have been studied [10]. Ndogmo [15] obtained the complete equivalence transformations of the Euler-Bernoulli beam equation which was initialy attempted by Morozov and Wafo Soh. Naz and Mohamed [14] studied the dynamic Euler-Bernoulli beam equation from the symmetry point of view. Zvyagin and Gevorkyan [20] worked on the self-similar solution of the hydraulic fracture problem for two closely spaced beams and the numerical results obtained when solving the corresponding system of differential equations with various boundary conditions.

## 1.4 Dissertation outline

This research includes six chapters.

- In Chapter 1, the Introduction, the background to hydraulic fracturing and the governing equations for the beam and fluid flow in the fracture are given.
- In Chapter 2 the background to the theory of Lie symmetry analysis of coupled partial differential equations is presented. An outline of the theory of the shooting method is described.
- In Chapter 3 the mathematical model is developed and the derivation of the governing equations and boundary conditions is given.
- In Chapter 4 calculation of the Lie point symmetries of the coupled system of two partial differential equations and derivation of the general form of the group invariant solution is presented.
- In Chapter 5 the asymptotic solution at the fracture tip is derived and the numerical solution for finite bending moment at the fracture tip using a shooting method is obtained.
- Finally, the general conclusions from the results obtained in all chapters are given in Chapter 6.

# Chapter 2

# Background to Lie group theory

## 2.1 Introduction

In this chapter the analytical and numerical methods used in this dissertation are outlined. The analytical method is Lie symmetry analysis of partial differential equations and it will be used to reduce the coupled differential equations derived in this research. Lie symmetry analysis of differential equations has been considered in several books [11, 12]. The shooting method for solving non-linear boundary value problems will be briefly described.

## 2.2 Lie symmetry methods

This study considers the Lie point symmetries of the coupled system of partial differential equations

$$F(t,x,h,h_t,h_x,h_{tx},h_{tt},h_{xx},P_t,P_x,P_{tx},P_{tt},P_{xx}) = 0, \tag{2.1}$$

$$G(t,x,h,h_t,h_x,h_{tx},h_{tt},h_{xx},P_t,P_x,P_{tx},P_{tt},P_{xx}) = 0, \tag{2.2}$$

where a subscript denotes partial differentiation, $t$ and $x$ are independent variables and $h$ and $P$ are dependent variables, which are the fracture half-width and fluid pressure respectively.

A Lie point symmetry of the system of partial differential equations (2.1) and (2.2) has the form

$$X = \xi^1(t,x,h,P)\frac{\partial}{\partial t} + \xi^2(t,x,h,P)\frac{\partial}{\partial x} + \eta^1(t,x,h,P)\frac{\partial}{\partial h} + \eta^2(t,x,h,P)\frac{\partial}{\partial P}. \quad (2.3)$$

The operator (2.3) is prolonged to as many derivatives as required. For the nonlinear diffusion equation the second prolongation is taken while for the Euler-Bernoulli equation the fourth prolongation is used. The extension formulae are defined as [3, 4, 5, 11, 12]

$$\zeta_i^\alpha = D_i(\eta^\alpha) - u_s^\alpha D_i(\xi^s), \quad (2.4)$$

$$\zeta_{ij}^\alpha = D_j(\zeta_i^\alpha) - u_{is}^\alpha D_j(\xi^s), \quad (2.5)$$

$$\zeta_{ijk}^\alpha = D_k(\zeta_{ij}^\alpha) - u_{ijs}^\alpha D_k(\xi^s), \quad (2.6)$$

$$\zeta_{ijkl}^\alpha = D_l(\zeta_{ijk}^\alpha) - u_{ijks}^\alpha D_l(\xi^s), \quad (2.7)$$

where $\alpha = 1$ and 2 with $u^1 = h$ and $u^2 = P$. The total derivative operators are

$$D_1 = D_t = \frac{\partial}{\partial t} + h_t\frac{\partial}{\partial h} + P_t\frac{\partial}{\partial P} + h_{tt}\frac{\partial}{\partial h_t} + h_{xt}\frac{\partial}{\partial h_x} + P_{tt}\frac{\partial}{\partial P_t} + P_{xt}\frac{\partial}{\partial P_x} + \cdots, \quad (2.8)$$

$$D_2 = D_x = \frac{\partial}{\partial x} + h_x\frac{\partial}{\partial h} + P_x\frac{\partial}{\partial P} + h_{xx}\frac{\partial}{\partial h_x} + h_{tx}\frac{\partial}{\partial h_t} + P_{xx}\frac{\partial}{\partial P_x} + P_{tx}\frac{\partial}{\partial P_t} + \cdots \quad (2.9)$$

The invariant criteria for the system of partial differential equations, (2.1) and (2.2), is given by:

$$X(F)\,|_{F=0,G=0)} = 0, \quad (2.10)$$

$$X(G)\,|_{F=0,G=0} = 0, \tag{2.11}$$

where $X$ is prolonged to as many partial derivatives as necessary. The first prolongation is given in (2.12)

$$X^{[1]} = X + \zeta_1^1 \frac{\partial}{\partial h_t} + \zeta_1^2 \frac{\partial}{\partial P_t} + \zeta_2^1 \frac{\partial}{\partial h_x} + \zeta_2^2 \frac{\partial}{\partial P_x}. \tag{2.12}$$

The group invariant solutions of the system of partial differential equations (2.1) and (2.2) are $h = \psi(t,x)$ and $P = \phi(t,x)$ provided

$$X(h - \psi(t,x))_{h=\psi(t,x)} = 0, \tag{2.13}$$

$$X(P - \psi(t,x))_{P=\psi(t,x)} = 0. \tag{2.14}$$

The invariant solutions is then substituted into the two partial differential equations, reducing them to two ordinary differential equations.

## 2.3 Numerical methods for solving non-linear boundary value problems

### 2.3.1 Shooting method

The shooting method is a much used way of solving non-linear boundary value problems. It is based on replacing the boundary value problem (BVP) with an initial value problem(IVP). The IVP is obtained using the asymptotic solution at one of the ends of the range of integration.

We start with a guess of the initial values and "shoot" to a target at the other end of the range if the target is not attained we adjust the estimate of the initial values and "shoot" again. We continue in this way until the target is reached. This technique is called a "shooting method".

## 2.4 Conclusions

In this chapter the background to Lie group analysis and the shooting method were briefly outlined. The Lie group analysis will be used to reduce the system of coupled partial differential equations to system of coupled ordinary differential equations. The shooting method will be used to derived a numerical solution of the system of ordinary differential equations by transforming a boundary value problem into an initial value problem.

# Chapter 3

# Mathematical modelling of hydraulic fracturing

## 3.1 Introduction

In this chapter the problem of hydraulic Fracturing of a Euler - Bernoulli beam is formulated mathematically. The Euler-Bernoulli beam equation is introduced and the thin fluid film equation for the half-width of the fracture is derived. The boundary and initial conditions are also specified. Dimensionless variables are introduced and the partial differential equations and the boundary and initial conditions are written in the dimensionless form.

## 3.2 Assumptions

The assumptions are as follows.

- The beams are able to be bent and are modelled using Euler-Bernoulli beam theory [17].
- The cross-sections are flat before deformation. The study assume that they return to their original shape after the fluid is removed.
- The axial line of each beam is inextensible.

- The width of the cross-section is assumed to be small compared to the length of the beam and to the curvature radius of the axial line.
- The injected fluid is Newtonian, viscous, incompressible and supplies a force that is able to bend the beam.
- The fluid flow is modelled using lubrication theory.

## 3.3 Euler-Bernoulli beam equation

The hydraulic fracture and coordinate system are illustrated in Figure 1.1. The study considers the upper half of the fracture, $0 \leq y \leq h(x,t)$. The time dependent Euler-Bernoulli beam equation is

$$EI\frac{\partial^4 h}{\partial x^4} + \hat{\rho}\frac{\partial^2 h}{\partial t^2} = f, \tag{3.1}$$

where $E$ is the Young's modulus of the beam, $\hat{\rho}$ is the mass of the beam per unit length, $f(t,x)$ is the applied force per unit length in the upward vertical direction on the internal surface of the beam and $I$ is the second moment of area about the $z$-axis,

$$I = \frac{bd^3}{12}, \tag{3.2}$$

where $b$ is the breath of the beam and $d$ is the thickness of the beam. The derivation of (3.1) is very complicated and detailed. The full derivation of the time dependent Euler- Bernoulli beam equation is given by Segel and Handelman [17].

For the upper beam,

$$f(t,x) = P(t,x), \tag{3.3}$$

where

$$\frac{P(t,x)}{b} = p(t,x) - \sigma_{yy}^{(\infty)}. \tag{3.4}$$

In (3.4), $p(t,x)$ is the fluid pressure acting on the lower surface of the beam and $\sigma_{yy}^{(\infty)}$ is the normal compressive stress on the upper surface of the beam due to surrounding rock which may be in the form of an adjacent beam. The beam equation (3.1) becomes

$$EI\frac{\partial^4 h}{\partial x^4} + \hat{\rho}\frac{\partial^2 h}{\partial t^2} = P. \tag{3.5}$$

The deformation of the beam is governed by the pressure difference per unit length $P(t,x)$, not by $p(t,x)$. We will therefore develop the theory in terms of $P(t,x)$ instead of $p(t,x)$. The spatial gradient of $\frac{P}{b}$ and $p$ are equal and therefore $p$ can be replaced by $\frac{P}{b}$ in the Navier-Stokes equation.

## 3.4 Thin fluid film equations

To derive the two-dimensional nonlinear diffusion equation for the flow of the injected viscous incompressible Newtonian fluid in the closely spaced beams, we start with the Navier-Stokes equation for an incompressible fluid and conservation of mass equation:

$$\nabla.\mathbf{v} = 0, \tag{3.6}$$

$$\frac{\partial \mathbf{v}}{\partial t} + (\mathbf{v}.\nabla)\mathbf{v} = -\frac{\nabla P}{b\rho} + \nu\nabla^2\mathbf{v}, \tag{3.7}$$

where $\mathbf{v}$ is the fluid velocity, $P$ defined by (3.4), $\rho$ is the fluid density and $\nu = \frac{\mu}{\rho}$ the kinematic viscosity of the fluid.

Consider a thin film of viscous incompressible fluid, bounded above by $y = h(x,t)$ and below by $y = 0$. In order to simplify equations (3.6) and (3.7), we introduce the characteristic quantities [1]:

characteristic length in $x$-direction $=L_0$,

characteristic length in $y$-direction $=H$,

characteristic fluid velocity in $x$-direction $= U$,

characteristic fluid velocity in $y$-direction $W = \frac{H}{L_0}U$,

characteristic force per unit length $P_0 = b\left(\frac{\mu U L_0}{H^2} - \sigma_{yy}^{(\infty)}\right)$,

characteristic time $T = \frac{L_0}{U}$.

The characteristic length $L_0$ is the initial length of the fracture and $H$ is the initial half-width of the fracture at the fracture entry which satisfy

$$\frac{H}{L_0} \ll 1. \tag{3.8}$$

The characteristic velocity $U$ will be specified later. The characteristic fluid pressure is the characteristic fluid pressure of lubrication theory [1].

We now justify the expression for the characteristic velocity in the $y$-direction. The continuity equation, (3.6), written in Cartesian coordinates, is

$$\frac{\partial v_x}{\partial x} + \frac{\partial v_y}{\partial y} = 0. \tag{3.9}$$

The order of magnitude of terms in (3.9) must balance because we do not make an approximation in the conservation of mass equation. Thus

$$\frac{U}{L_0} \sim \frac{W}{H} \tag{3.10}$$

and therefore

$$W = \frac{H}{L_0}U. \tag{3.11}$$

To justify the expression for the characteristic fluid pressure, consider the $x$-component of the Navier-Stokes equation expressed in terms of $p(x,t)$,

$$\rho\frac{Dv_x}{Dt} = -\frac{\partial p}{\partial x} + \mu\left(\frac{\partial^2 v_x}{\partial x^2} + \frac{\partial^2 v_x}{\partial y^2}\right). \tag{3.12}$$

The order of magnitude of the terms in (3.12) is

$$\rho\frac{U}{T}\sim-\frac{P_0}{L_0}+\mu\Big(\frac{U}{L_0^2}+\frac{U}{H^2}\Big). \tag{3.13}$$

In the thin fluid-film theory, which is also called lubrication theory, the pressure gradient must balance the viscous term $\frac{U}{H^2}$, that is

$$\frac{P_0}{L_0}\sim\mu\frac{U}{H^2}, \tag{3.14}$$

that is,

$$P_0\sim\mu\frac{UL_0}{H^2} \tag{3.15}$$

which is the characteristic net fluid pressure in the thin fluid film.

We write the mass conservation equation and the $x$ and $y$ components of the Navier-Stokes equation in dimensionless form. The fluid variables are

$$v_x=v_x(t,x,y),\qquad v_y=v_y(t,x,y),\qquad v_z=0,\qquad P=P(t,x,y). \tag{3.16}$$

We introduce the dimensionless variables:

$$\bar{t}=\frac{Ut}{L_0},\qquad \bar{x}=\frac{x}{L_0},\qquad \bar{y}=\frac{y}{H},\qquad \bar{v}_x=\frac{v_x}{U},\qquad ,\bar{v}_y=\frac{v_yL_0}{UH},\qquad \bar{P}=\frac{P}{P_0}. \tag{3.17}$$

This gives conservation of mass:

$$\frac{\partial\bar{v}_x}{\partial\bar{x}}+\frac{\partial\bar{v}_y}{\partial\bar{y}}=0. \tag{3.18}$$

The $x$ - component of Navier-Stokes equation (3.7) gives

$$Re\Big(\frac{H}{L_0}\Big)^2\Big(\frac{\partial\bar{v}_x}{\partial\bar{t}}+\bar{v}_x\frac{\partial\bar{v}_x}{\partial\bar{x}}+\bar{v}_y\frac{\partial\bar{v}_x}{\partial\bar{y}}\Big)=-\frac{1}{b}\Big(1-\frac{\sigma_{yy}^{(\infty)}H^2}{\mu uL}\Big)\frac{\partial\bar{P}}{\partial\bar{x}}+\Big(\frac{H}{L_0}\Big)^2\frac{\partial^2\bar{v}_x}{\partial\bar{x}^2}+\frac{\partial^2\bar{v}_x}{\partial\bar{y}^2}, \tag{3.19}$$

and the $y$- component of Navier-Stokes equation is

$$Re\Big(\frac{H}{L_0}\Big)^4\Big(\frac{\partial \bar{v}_y}{\partial \bar{t}}+\bar{v}_x\frac{\partial \bar{v}_y}{\partial \bar{y}}+\bar{v}_y\frac{\partial \bar{v}_y}{\partial \bar{y}}\Big)=-\Big(1-\frac{\sigma_{yy}^{(\infty)}H^2}{\mu UL_0}\Big)\frac{\partial \bar{P}}{\partial \bar{y}}+\Big(\frac{H}{L_0}\Big)^4\frac{\partial^2 \bar{v}_y}{\partial \bar{x}^2}+\Big(\frac{H}{L_0}\Big)^2\frac{\partial^2 \bar{v}_y}{\partial \bar{y}^2}, \tag{3.20}$$

where the Reynolds number Re is defined by

$$Re=\frac{UL_0}{\nu}. \tag{3.21}$$

We assume that although

$$1-\frac{\sigma^{(\infty)}H^2}{\mu UL_0}$$

is small, it still satisfies

$$1-\frac{\sigma^{(\infty)}H^2}{\mu UL_0}\gg\Big(\frac{H}{L_0}\Big)^2.$$

By imposing the thin film approximation

$$\frac{H}{L_0}\ll 1 \qquad \text{and} \qquad Re\Big(\frac{H}{L_0}\Big)^2\ll 1, \tag{3.22}$$

we obtain

$$\frac{1}{b}\Big(1-\frac{\sigma_{(yy)}^{(\infty)}H^2}{\mu UL}\Big)\frac{\partial \bar{P}}{\partial \bar{x}}=\frac{\partial^2 \bar{v}_x}{\partial \bar{y}^2}, \tag{3.23}$$

$$\frac{\partial \bar{P}}{\partial \bar{y}}=0. \tag{3.24}$$

Expressed in terms of the original dimensional variables, equations (3.18), (3.23) and (3.24) are respectively

$$\frac{\partial v_x}{\partial x}+\frac{\partial v_y}{\partial y}=0, \tag{3.25}$$

$$\frac{\partial P}{\partial x}=b\mu\frac{\partial^2 v_x}{\partial y^2}, \tag{3.26}$$

$$\frac{\partial P}{\partial y} = 0. \tag{3.27}$$

For the beam to move apart,

$$\frac{\mu U L_0}{H^2} > \sigma_{yy}^{(\infty)} \tag{3.28}$$

and therefore

$$1 - \frac{\sigma_{yy}^{(\infty)} H^2}{\mu U L_0} > 0. \tag{3.29}$$

We consider the upper half of the fluid, $0 \le y \le h(t,x)$. The boundary conditions are:

$$y = h(t,x): \qquad v_x(t,x,h) = 0 \qquad (\text{no slip}), \tag{3.30}$$

$$y = h(x,t): \ v_y(t,x,h) = \frac{\partial h}{\partial t} + v_x(t,x,h)\frac{\partial h}{\partial x} = \frac{\partial h}{\partial t} \ (\text{no cavities}), \tag{3.31}$$

$$y = 0: \quad v_y(t,x,0) = 0 \quad (\text{symmetry about the } x\text{-axis}), \tag{3.32}$$

$$y = 0: \quad \frac{\partial v_x(t,x,0)}{\partial y} = 0 \ \ (\text{local maximum of } \ v_x(t,x,y)). \tag{3.33}$$

We now outline the derivation of the nonlinear diffusion equation relating $h(t,x)$ and $P(t,x)$ in the upper half of the fluid.

Integrate the conservation of mass equation(3.25) with respect to $y$ from $y = 0$ to $y = h$:

$$\int_0^h \frac{\partial v_x(t,x,y)}{\partial x} dy + \int_0^h \frac{\partial v_y(t,x,y)}{\partial y} dy = 0. \tag{3.34}$$

Now using the boundary conditions (3.30) and (3.31),

$$\begin{aligned}\int_0^h \frac{\partial v_y(t,x,y)}{\partial y} dy &= \Big[ v_y(t,x,y) \Big]_0^h \\ &= \frac{\partial h}{\partial t} + v_x(t,x,h)\frac{\partial h}{\partial x} \\ &= \frac{\partial h}{\partial t}. \end{aligned} \tag{3.35}$$

Also using the Leibniz rule for differentiation under the integral sign [9] and the boundary condition (3.31),

$$\begin{aligned}\int_0^{h(t,x)} \frac{\partial v_x(t,x,y)}{\partial x} dy &= \frac{\partial}{\partial x}\int_0^{h(t,x)} v_x(t,x,y)\,dy - v_x(t,x,h)\frac{\partial h}{\partial x} \\ &= \frac{\partial}{\partial x}\int_0^{h} v_x(t,x,y)\,dy. \end{aligned} \tag{3.36}$$

Substituting (3.35) and (3.36) into (3.34) gives

$$\frac{\partial h}{\partial t} + \frac{\partial}{\partial x}\int_0^{h(t,x)} v_x(t,x,y)\,dy = 0. \tag{3.37}$$

We now derive an expression for $v_x(t,x,y)$ using from (3.26). Noting that

$$P = P(t,x), \tag{3.38}$$

we integrate (3.26) twice with respect to $y$ we obtain,

$$v_x(t,x,y) = \frac{1}{2\mu b}\frac{\partial P(t,x)}{\partial x} y^2 + A(t,x)\,y + B(t,x). \tag{3.39}$$

Imposing the boundary conditions (3.30) and (3.31) gives

$$A(t,x) = 0, \qquad B(t,x) = -\frac{1}{2\mu b}\frac{\partial P(t,x)}{\partial x} h^2 \tag{3.40}$$

and therefore

$$v_x(t,x,y) = -\frac{1}{2\mu b}\frac{\partial P(t,x)}{\partial x}(h^2(t,x) - y^2). \tag{3.41}$$

Substituting (3.41) into (3.37) and integrating, we obtain

$$\frac{\partial h}{\partial t} = \frac{1}{3\mu b}\frac{\partial}{\partial x}\Big(h^3\frac{\partial P}{\partial x}\Big). \tag{3.42}$$

Equations (3.5) and (3.42) form the coupled system of partial differential equations which describes the hydraulic fracturing of the two closely spaced beams.

Finally, consider the flux of fluid in the region bounded by the two beams defined by

$$Q(t,x) = 2\int_0^{h(t,x)} v_x(t,x,y)\,dy. \tag{3.43}$$

Substituting (3.41) into (3.43) and integrating gives

$$Q(t,x) = -\frac{2}{3\mu b}h^3(t,x)\frac{\partial}{\partial x}P(t,x). \tag{3.44}$$

A related quantity is the width average fluid velocity defined by

$$v_x^*(t,x) = \frac{1}{h}\int_0^{h(t,x)} v_x(t,x,y)\,dy = \frac{1}{2h}Q(t,x). \tag{3.45}$$

Equation (3.44) becomes, using (3.45)

$$v_x^*(t,x) = -\frac{1}{3\mu b}h^2(t,x)\frac{\partial}{\partial x}P(t,x). \tag{3.46}$$

## 3.5 Nondimensional variables

We introduce nondimensional variables and make the two partial differential equations (3.5) and (3.42) dimensionless. We define the nondimensional variables

$$\bar{t} = \frac{Ut}{L}, \qquad \bar{x} = \frac{x}{L}, \qquad \bar{h} = \frac{h}{H}, \qquad \bar{P} = \frac{P}{P_0}, \qquad \bar{Q} = \frac{Q}{Q_0}, \qquad \bar{v}_x^* = \frac{v_x^*}{U}. \tag{3.47}$$

.

where

$$P_0 = \Big(\frac{\mu U L_0}{H^2} - \sigma_{yy}^{(\infty)}\Big) b, \qquad Q_0 = HU \tag{3.48}$$

Then equation (3.5) becomes

$$\frac{\partial \bar{h}^2}{\partial \bar{t}^2} + \frac{EI}{L^2 \hat{\rho} U^2} \frac{\partial^4 \bar{h}}{\partial \bar{x}^4} = \frac{\mu b}{\hat{\rho} U} \Big(\frac{L_0}{H}\Big)^3 \Big[1 - \frac{\sigma_{yy}^{(\infty)} H^2}{\mu U L_0}\Big] \bar{P}. \tag{3.49}$$

Define the dimensionless numbers

$$A = \frac{EI}{\hat{\rho} L^2 U^2}, \qquad B = \frac{\mu b}{\hat{\rho} U} \Big(\frac{L_0}{H}\Big)^3 \Big[1 - \frac{\sigma_{yy}^{(\infty)} H^2}{\mu U L_0}\Big]. \tag{3.50}$$

Let $D$ denote the density of the rock in the beam. Then since $\hat{\rho}$ is the mass of the beam per unit length,

$$\hat{\rho} = Dbd. \tag{3.51}$$

where $d$ is the thickness of the beam. Also from (3.2),

$$I = \frac{bd^3}{12} \tag{3.52}$$

and from (3.48)

$$U = \frac{Q_0}{H}. \tag{3.53}$$

Using (3.2) and (3.53), the dimensionless number $A$ and $B$ are

$$A = \frac{Ed^2}{12 D Q_0^2} \Big(\frac{H}{L_0}\Big)^2, \qquad B = \frac{\mu H}{D d Q_0} \Big(\frac{L_0}{H}\Big)^3 \Big[1 - \frac{\sigma_{yy}^{(\infty)} H^3}{\mu L_0 Q_0}\Big]. \tag{3.54}$$

The dimensionless numbers $A$ and $B$ are independent of the breadth of the beam. Equation (3.49) becomes

$$A\frac{\partial^4 \bar{h}}{\partial \bar{x}^4} + \frac{\partial^2 \bar{h}}{\partial t^2} = B\bar{P}. \tag{3.55}$$

The thin fluid-film equation (3.42) in dimensionless form becomes

$$\frac{\partial \bar{h}}{\partial \bar{t}} = \frac{1}{3}\Big[1 - \frac{\sigma_{yy}^{(\infty)} H^3}{\mu L_0 Q_0}\Big]\frac{\partial}{\partial \bar{x}}\Big(\bar{h}^3 \frac{\partial \bar{P}}{\partial \bar{x}}\Big) \tag{3.56}$$

Equation (3.44) for the flux becomes

$$\bar{Q}(t,x) = -\frac{2}{3}\Big[1 - \frac{\sigma_{yy}^{(\infty)} H^3}{\mu L_0 Q_0}\Big]\bar{h}^3(t,x)\frac{\partial}{\partial x}\bar{P}(t,x). \tag{3.57}$$

and equation (3.46) for the width average fluid velocity is

$$\bar{v}_x^*(t,x) = -\frac{1}{3}\Big[1 - \frac{\sigma_{yy}^{(\infty)} H^3}{\mu L_0 Q_0}\Big]\bar{h}^2(t,x)\frac{\partial}{\partial x}\bar{P}(t,x). \tag{3.58}$$

The overhead bars are suppressed to keep the notation simple.

## 3.6 Boundary and initial conditions

Finally, consider the boundary conditions. The length of the fracture at time $t$ is $L(t)$. At $x = L(t)$, the half-width and the spatial gradient of the beam vanish,

$$x = L(t) \quad : \qquad h(t, L(t)) = 0, \tag{3.59}$$

$$x = L(t) \quad : \qquad \frac{\partial}{\partial x} h(t, L(t)) = 0, \tag{3.60}$$

In dimensional variables the bending moment about the origin has magnitude M given by [17]

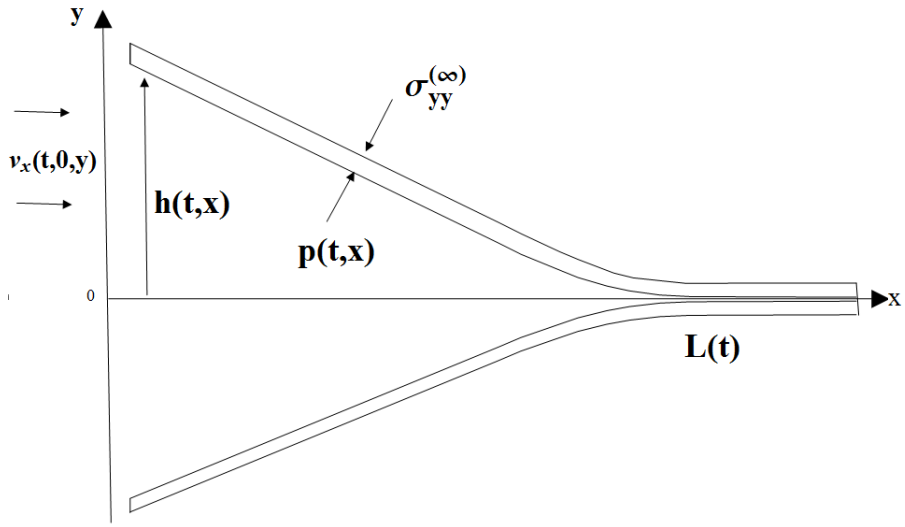



Figure 3.1: Bending beams due to injection of high pressure fluid

$$M(t,x) = EI\frac{\partial^2 h}{\partial x^2}, \tag{3.61}$$

where $E$ is the Young's modulus and $I$ is the second moment of area about the $z$-axis. We assume that the displacement gradient is small. The curvature of the neutral axis of the beam is then approximately equal to $\frac{\partial^2 h}{\partial x^2}$. Hence the bending moment is approximately proportional to the curvature of the beam.

Introduce dimensionless variable

$$\bar{M} = \frac{M}{M_0}. \tag{3.62}$$

Then (3.61) becomes

$$M = \frac{EIH}{L_0^2 M_0}\frac{\partial^2 \bar{h}}{\partial \bar{x}^2}. \tag{3.63}$$

Define

$$M_0 = \frac{EIH}{L_0^2}, \tag{3.64}$$

then

$$\bar{M} = \frac{\partial^2 \bar{h}}{\partial \bar{x}^2}. \tag{3.65}$$

Again will suppress the overhead bars in the calculations that follow.

Let $M(t)$ be the bending moment at the fracture tip. We consider only the case in which $M(t)$ is finite. When $M(t)$ is infinite the beam will crack at the tip and the model will no longer be valid. Thus

$$x = L(t): \qquad \frac{\partial^2 h}{\partial x^2}(t, L(t)) = M(t). \tag{3.66}$$

The form of $M(t)$ is determined by the invariant solution which is obtained in Chapter 4.

The flux of the fluid vanishes at the fracture tip. Thus

$$x = L(t): \qquad Q(t, L(t)) = 0, \tag{3.67}$$

that is, using (3.57),

$$x = L(t): \qquad h^3(t, L(t)) \frac{\partial}{\partial x} P(t, L(t)) = 0. \tag{3.68}$$

Consider now the boundary conditions and the initial conditions at the fracture entry. Since the characteristic half-width $H$ is the initial half-width at the fracture entry,

$$x = 0: \qquad h(0,0) = 1. \tag{3.69}$$

The flux of the fluid at the fracture entry is specified as far as the invariant solution allows:

$$x = 0: \qquad Q(t,0) = Q_0(t), \tag{3.70}$$

where the form of $Q_0(t)$ is determined by the invariant solutions. Using (3.57), the boundary condition (3.70) becomes

$$x = 0: \qquad -\frac{2}{3}\Big[1 - \frac{\sigma_{yy}^{(\infty)} H^3}{\mu L_0 Q_0}\Big] h^3(t,0) \frac{\partial}{\partial x} P(t,0) = Q_0(t). \tag{3.71}$$

This completes the specification of the boundary and initial conditions.

## 3.7 Conclusions

The mathematical modelling of hydraulic fracturing is formulated in terms of two coupled partial differential equations. The Lie symmetry analysis will have to be performed on the system of two partial differential equations. The nonlinear diffusion equation is second order while the beam equation is fourth order. The prolongation of the Lie point symmetry to fourth order will therefore have to be considered.

We saw that instead of the fluid pressure $p(t,x)$, a more suitable variable to use is the pressure difference $\frac{P(t)}{b} = p(t,x) - \sigma_{yy}^{(\infty)}$ where $\sigma_{yy}^{(\infty)}$ is the normal compressive stress on the upper surface of the beam due to the surrounding rock. The pressure difference $P(t,x)$ occurs in the beam equation. Since $\sigma_{yy}^{(\infty)}$ is constant the pressure gradient in the nonlinear diffusion equation can be expressed in terms of $P$. The two partial differential equations can therefore be expressed in terms of the dependent variables $h(t,x)$ and $P(t,x)$. These variables will be used in the remainder of the dissertation.

At the fracture tip we noticed that the boundary conditions , $x = L(t)$, depends on the bending moment, which must be finite. We can expect that the properties of the solution will depend on the bending moment at $x = L(t)$.

The boundary condition at the fracture entry, $x = 0$, is in terms of the flux at the fracture entry. The flux can be prescribed at the entry but conditions may be placed on it by the form of the invariant solution.

# Chapter 4

# Lie point symmetries and invariant solutions

## 4.1 Introduction

In this chapter the Lie point symmetries of the system of two partial differential equations consisting of the thin fluid film equation (3.56) and the Euler-Bernoulli beam equation (3.55) are derived. The invariant solution for the half-width $h(t,x)$ and the pressure $P(t,x)$ are obtained. The boundary and initial conditions are also expressed in terms of the invariant solution.

## 4.2 Lie point symmetry

The thin fluid film equation and the Euler-Bernoulli beam equation are

$$\frac{\partial h}{\partial t} = \frac{k}{3}\frac{\partial}{\partial x}\Big(h^3\frac{\partial P}{\partial x}\Big) \tag{4.1}$$

and

$$A\frac{\partial^4 h}{\partial x^4} + \frac{\partial^2 h}{\partial t^2} = BP, \tag{4.2}$$

where

$$k = 1 - \frac{\sigma_{yy}^{(\infty)} H^3}{\mu Q_0 L_0}. \tag{4.3}$$

Equation (4.1) is expanded and expressed in terms of partial derivatives. The suffix notation will be used to denote the partial derivatives of $h$ and $P$ with respect to $t$ and $x$. The partial derivatives of $h$ and $P$ with respect to $t$ and $x$ are regarded as independent variables when deriving the Lie point symmetries and invariant solution. Expressed in terms of independent partial derivatives, (4.1) and (4.2) becomes

$$h_t = kh^2 h_x P_x + \frac{k}{3} h^3 P_{xx}, \tag{4.4}$$

$$Ah_{xxxx} + h_{tt} = BP. \tag{4.5}$$

A Lie point symmetry of the system of partial differential equations, (4.4) and (4.5), is of the form

$$X = \xi^1(t,x,h,P)\frac{\partial}{\partial t} + \xi^2(t,x,h,P)\frac{\partial}{\partial x} + \eta^1(t,x,h,P)\frac{\partial}{\partial h} + \eta^2(t,x,h,P)\frac{\partial}{\partial P}. \tag{4.6}$$

The invariance criteria for the system of partial differential equations, (4.4) and (4.5), are given by:

$$X^{[2]}(h_t - kh^2 h_x P_x - \frac{k}{3} h^3 P_{xx})|_{(4.4),(4.5)} = 0, \tag{4.7}$$

$$X^{[4]}(Ah_{xxxx} + h_{tt} - BP)|_{(4.4),(4.5)} = 0. \tag{4.8}$$

where $X^{[2]}$ and $X^{[4]}$ are the second and the fourth prolongations of X defined by

$$X^{[2]} = X + \zeta_1^1 \frac{\partial}{\partial h_t} + \zeta_2^1 \frac{\partial}{\partial h_x} + \zeta_2^2 \frac{\partial}{\partial P_x} + \zeta_{22}^2 \frac{\partial}{\partial P_{xx}}, \tag{4.9}$$

$$X^{[4]} = X + \zeta_{11}^1 \frac{\partial}{\partial h_{tt}} + \zeta_{2222}^1 \frac{\partial}{\partial h_{xxxx}} \tag{4.10}$$

and the coefficients $\zeta_i^\alpha$, $\zeta_{ij}^\alpha$ and $\zeta_{ijkl}^\alpha$ are defined by (2.9), (2.10) and (2.12). We consider first (4.7) because $X$ is prolongated only to second order. The results obtained from (4.7) will make it easier to calculate the fourth prolongation $X^{[4]}$. When expanded, the invariant condition (4.7) is

$$(-2khh_xP_x - kh^2P_{xx})\eta^1 + \zeta_1^1 + (-kh^2P_x)\zeta_2^1 + (-kh^2h_x)\zeta_2^2 + (-\frac{k}{3}h^3)\zeta_{22}^2|_{(4.4),(4.5)} = 0 \tag{4.11}$$

where

$$\zeta_1^1 = D_t(\eta^1) - h_t\, D_t(\xi^1) - h_x\, D_t(\xi^2), \tag{4.12}$$

$$\zeta_2^1 = D_x(\eta^1) - h_t\, D_x(\xi^1) - h_x\, D_x(\xi^2), \tag{4.13}$$

$$\zeta_2^2 = D_x(\eta^2) - P_t\, D_x(\xi^1) - P_x\, D_x(\xi^2), \tag{4.14}$$

$$\zeta_{22}^2 = D_x(\zeta_2^2) - P_{xt}\, D_x(\xi^1) - P_{xx}\, D_x(\xi^2). \tag{4.15}$$

Expanding equations (4.12) to (4.15), we obtain

$$\zeta_1^1 = \frac{\partial\eta^1}{\partial t} + \frac{\partial\eta^1}{\partial h}h_t + \frac{\partial\eta^1}{\partial P}P_t - h_t\Big(\frac{\partial\xi^1}{\partial t} + \frac{\partial\xi^1}{\partial h}h_t + \frac{\partial\xi^1}{\partial P}P_t\Big) - h_x\Big(\frac{\partial\xi^2}{\partial t} + \frac{\partial\xi^2}{\partial h}h_t + \frac{\partial\xi^2}{\partial P}P_t\Big), \tag{4.16}$$

$$\zeta_2^1 = \frac{\partial\eta^1}{\partial x} + \frac{\partial\eta^1}{\partial h}h_x + \frac{\partial\eta^1}{\partial P}P_x - h_t\Big(\frac{\partial\xi^1}{\partial x} + \frac{\partial\xi^1}{\partial h}h_x + \frac{\partial\xi^1}{\partial P}P_x\Big) - h_x\Big(\frac{\partial\xi^2}{\partial x} + \frac{\partial\xi^2}{\partial h}h_x + \frac{\partial\xi^2}{\partial P}P_x\Big), \tag{4.17}$$

$$\zeta_2^2 = \frac{\partial\eta^2}{\partial x} + \frac{\partial\eta^2}{\partial h}h_x + \frac{\partial\eta^2}{\partial P}P_x - P_t\Big(\frac{\partial\xi^1}{\partial x} + \frac{\partial\xi^1}{\partial h}h_x + \frac{\partial\xi^1}{\partial P}P_x\Big) - P_x\Big(\frac{\partial\xi^2}{\partial x} + \frac{\partial\xi^2}{\partial h}h_x + \frac{\partial\xi^2}{\partial P}P_x\Big), \tag{4.18}$$

$$
\begin{aligned}
\zeta_{22}^2 &= D_x\Big(\frac{\partial\eta^2}{\partial x}+\frac{\partial\eta^2}{\partial h}h_x+\frac{\partial\eta^2}{\partial P}P_x-P_t\Big(\frac{\partial\xi^1}{\partial x}+\frac{\partial\xi^1}{\partial h}h_x+\frac{\partial\xi^1}{\partial P}P_x\Big)-P_x\Big(\frac{\partial\xi^2}{\partial x}\\
&+ \frac{\partial\xi^2}{\partial h}h_x+\frac{\partial\xi^2}{\partial P}P_x\Big)\Big)-P_{xt}D_x(\xi^1)-P_{xx}D_x(\xi^2)\\
&= \frac{\partial\eta^2}{\partial x}+2\frac{\partial\eta^2}{\partial x\partial h}h_x+2\frac{\partial\eta^2}{\partial x\partial P}P_x+2\frac{\partial\eta^2}{\partial h\partial P}h_xP_x+\frac{\partial\eta^2}{\partial h^2}h_x^2+\frac{\partial\eta^2}{\partial P^2}P_x^2+\frac{\partial\eta^2}{\partial h}h_{xx}\\
&+ \frac{\partial\eta^2}{\partial P}P_{xx}-2P_{tx}\Big(\frac{\partial\xi^1}{\partial x}+\frac{\partial\xi^1}{\partial h}h_x+\frac{\partial\xi^1}{\partial P}P_x\Big)-2P_{xx}\Big(\frac{\partial\xi^2}{\partial x}+\frac{\partial\xi^2}{\partial h}h_x+\frac{\partial\xi^2}{\partial P}P_x\Big)\\
&- P_t\Big(\frac{\partial^2\xi^1}{\partial x^2}+2\frac{\partial^2\xi^1}{\partial x\partial h}h_x+2\frac{\partial^2\xi^1}{\partial x\partial P}P_x+2\frac{\partial^2\xi^1}{\partial h\partial P}h_xP_x+\frac{\partial^2\xi^1}{\partial h^2}h_x^2+\frac{\partial^2\xi^1}{\partial P^2}P_x^2\\
&+ \frac{\partial\xi^1}{\partial h}h_{xx}+\frac{\partial\xi^1}{\partial P}P_{xx}\Big)-P_x\Big(\frac{\partial^2\xi^2}{\partial x^2}+2\frac{\partial^2\xi^2}{\partial x\partial h}h_x+2\frac{\partial^2\xi^2}{\partial x\partial P}P_x+2\frac{\partial^2\xi^2}{\partial h\partial P}h_xP_x\\
&+ \frac{\partial^2\xi^2}{\partial h^2}h_x^2+\frac{\partial^2\xi^2}{\partial P^2}P_x^2+\frac{\partial\xi^2}{\partial h}h_{xx}+\frac{\partial^2\xi}{\partial P}P_{xx}\Big). \qquad (4.19)
\end{aligned}
$$

Now substituting into the determining equation (4.11) the expressions (4.16) to (4.19) for $\zeta_1^1$, $\zeta_2^1$, $\zeta_2^2$ and $\zeta_{22}^2$, we obtain

$$
\begin{aligned}
& \frac{\partial \eta^1}{\partial t} + \frac{\partial \eta^1}{\partial h} h_t + \frac{\partial \eta^1}{\partial P} P_t - h_t \Big( \frac{\partial \xi^1}{\partial t} + \frac{\partial \xi^1}{\partial h} h_t + \frac{\partial \xi^1}{\partial P} P_t \Big) - h_x \Big( \frac{\partial \xi^2}{\partial t} + \frac{\partial \xi^2}{\partial h} h_t \\
+ \quad & \frac{\partial \xi^2}{\partial P} P_t \Big) - k h^2 P_x \Big[ \frac{\partial \eta^1}{\partial x} + \frac{\partial \eta^1}{\partial h} h_x + \frac{\partial \eta^1}{\partial P} P_x - h_t \Big( \frac{\partial \xi^1}{\partial x} + \frac{\partial \xi^1}{\partial h} h_x + \frac{\partial \xi^1}{\partial P} P_x \Big) \\
- \quad & h_x \Big( \frac{\partial \xi^2}{\partial x} + \frac{\partial \xi^2}{\partial h} h_x + \frac{\partial \xi^2}{\partial P} P_x \Big) \Big] - k h^2 h_x \Big[ \frac{\partial \eta^2}{\partial x} + \frac{\partial \eta^2}{\partial h} h_x + \frac{\partial \eta^2}{\partial P} P_x - P_t \Big( \frac{\partial \xi^1}{\partial x} \\
+ \quad & \frac{\partial \xi^1}{\partial h} h_x + \frac{\partial \xi^1}{\partial P} P_x \Big) - P_x \Big( \frac{\partial \xi^2}{\partial x} + \frac{\partial \xi^2}{\partial h} h_x + \frac{\partial \xi^2}{\partial P} P_x \Big) \Big] - \frac{k}{3} h^3 \Big[ \frac{\partial^2 \eta^2}{\partial x^2} + 2 \frac{\partial^2 \eta^2}{\partial x \partial h} h_x \\
+ \quad & 2 \frac{\partial \eta^2}{\partial x \partial P} P_x + 2 \frac{\partial \eta^2}{\partial h \partial P} h_x P_x + \frac{\partial \eta^2}{\partial h^2} h_x^2 + \frac{\partial \eta^2}{\partial P^2} P_x^2 + \frac{\partial \eta^2}{\partial h} h_{xx} + \frac{\partial \eta^2}{\partial P} P_{xx} \\
- \quad & 2 P_{tx} \Big( \frac{\partial \xi^1}{\partial x} + \frac{\partial \xi^1}{\partial h} h_x + \frac{\partial \xi^1}{\partial P} P_x \Big) - 2 P_{xx} \Big( \frac{\partial \xi^2}{\partial x} + \frac{\partial \xi^2}{\partial h} h_x + \frac{\partial \xi^2}{\partial P} P_x \Big) - P_t \Big( \frac{\partial^2 \xi^1}{\partial x^2} \\
+ \quad & 2 \frac{\partial^2 \xi^1}{\partial x \partial h} h_x + 2 \frac{\partial^2 \xi^1}{\partial x \partial P} P_x + 2 \frac{\partial^2 \xi^1}{\partial h \partial P} h_x P_x + \frac{\partial^2 \xi^1}{\partial h^2} h_x^2 + \frac{\partial^2 \xi^1}{\partial P^2} P_x^2 + \frac{\partial \xi^1}{\partial h} h_{xx} \\
+ \quad & \frac{\partial \xi^1}{\partial P} P_{xx} \Big) - P_x \Big( \frac{\partial^2 \xi^2}{\partial x^2} + 2 \frac{\partial^2 \xi^2}{\partial x \partial h} h_x + 2 \frac{\partial^2 \xi^2}{\partial x \partial P} P_x + 2 \frac{\partial^2 \xi^2}{\partial h \partial P} h_x P_x + \frac{\partial^2 \xi^2}{\partial h^2} h_x^2 \\
+ \quad & \frac{\partial^2 \xi^2}{\partial P^2} P_x^2 + \frac{\partial \xi^2}{\partial h} h_{xx} + \frac{\partial \xi^2}{\partial P} P_{xx} \Big) \Big] - \eta^1 (2 k h h_x P_x + k h^2 P_{xx}) \Big|_{(4.4),(4.5)} = 0, \qquad (4.20)
\end{aligned}
$$

We now replace $h_t$ in (4.20) using (4.4). Since (4.20) does not depend on either $h_{tt}$ or $h_{xxxx}$ we cannot use (4.5) to replace $h_{tt}$ or $h_{xxxx}$ in (4.20). The Lie point symmetry which is derived is therefore a conditional symmetry of the partial differential equation (4.1). The condition is (4.5). Equation (4.20) becomes

$$
\begin{aligned}
&\frac{\partial \eta^1}{\partial t}+\frac{\partial \eta^1}{\partial h}(kh^2h_xP_x+\frac{k}{3}h^3P_{xx})+\frac{\partial \eta^1}{\partial P}P_t-(kh^2h_xP_x+\frac{k}{3}h^3P_{xx})\Big(\frac{\partial \xi^1}{\partial t}\\
+\;&\frac{\partial \xi^1}{\partial h}(kh^2h_xP_x+\frac{k}{3}h^3P_{xx})+\frac{\partial \xi^1}{\partial P}P_t\Big)-h_x\Big(\frac{\partial \xi^2}{\partial t}+\frac{\partial \xi^2}{\partial h}(kh^2h_xP_x+\frac{k}{3}h^3P_{xx})\\
+\;&\frac{\partial \xi^2}{\partial P}P_t\Big)-kh^2P_x\Big[\frac{\partial \eta^1}{\partial x}+\frac{\partial \eta^1}{\partial h}h_x+\frac{\partial \eta^1}{\partial P}P_x-(kh^2h_xP_x+\frac{k}{3}h^3P_{xx})\Big(\frac{\partial \xi^1}{\partial x}\\
+\;&\frac{\partial \xi^1}{\partial h}h_x+\frac{\partial \xi^1}{\partial P}P_x\Big)-h_x\Big(\frac{\partial \xi^2}{\partial x}+\frac{\partial \xi^2}{\partial h}h_x+\frac{\partial \xi^2}{\partial P}P_x\Big)\Big]-kh^2h_x\Big[\frac{\partial \eta^2}{\partial x}+\frac{\partial \eta^2}{\partial h}h_x\\
+\;&\frac{\partial \eta^2}{\partial P}P_x-P_t\Big(\frac{\partial \xi^1}{\partial x}+\frac{\partial \xi^1}{\partial h}h_x+\frac{\partial \xi^1}{\partial P}P_x\Big)-P_x\Big(\frac{\partial \xi^2}{\partial x}+\frac{\partial \xi^2}{\partial h}h_x+\frac{\partial \xi^2}{\partial P}P_x\Big)\Big]\\
-\;&\frac{k}{3}h^3\Big[\frac{\partial^2 \eta^2}{\partial x^2}+2\frac{\partial^2 \eta^2}{\partial x\partial h}h_x+2\frac{\partial^2 \eta^2}{\partial x\partial P}P_x+2\frac{\partial^2 \eta^2}{\partial h\partial P}h_xP_x+\frac{\partial^2 \eta^2}{\partial h^2}h_x^2+\frac{\partial^2 \eta^2}{\partial P^2}P_x^2\\
+\;&\frac{\partial \eta^2}{\partial h}h_{xx}+\frac{\partial \eta^2}{\partial P}P_{xx}-2P_{tx}\Big(\frac{\partial \xi^1}{\partial x}+\frac{\partial \xi^1}{\partial h}h_x+\frac{\partial \xi^1}{\partial P}P_x\Big)-2P_{xx}\Big(\frac{\partial \xi^2}{\partial x}+\frac{\partial \xi^2}{\partial h}h_x\\
+\;&\frac{\partial \xi^2}{\partial P}P_x\Big)-P_t\Big(\frac{\partial^2 \xi^1}{\partial^2 x^2}+2\frac{\partial^2 \xi^1}{\partial x\partial h}h_x+2\frac{\partial^2 \xi^1}{\partial x\partial P}P_x+2\frac{\partial^2 \xi^1}{\partial h\partial P}h_xP_x+\frac{\partial^2 \xi^1}{\partial h^2}h_x^2\\
+\;&\frac{\partial^2 \xi^1}{\partial P^2}P_x^2+\frac{\partial \xi^1}{\partial h}h_{xx}+\frac{\partial \xi^1}{\partial P}P_{xx}\Big)-P_x\Big(\frac{\partial^2 \xi^2}{\partial x^2}+2\frac{\partial^2 \xi^2}{\partial x\partial h}h_x+2\frac{\partial^2 \xi^2}{\partial x\partial P}P_x\\
+\;&2\frac{\partial^2 \xi^2}{\partial h\partial P}h_xP_x+\frac{\partial^2 \xi^2}{\partial h^2}h_x^2+\frac{\partial^2 \xi^2}{\partial P^2}P_x^2+\frac{\partial \xi^2}{\partial h}h_{xx}+\frac{\partial \xi^2}{\partial P}P_{xx}\Big)\Big]-\eta^1(2khh_xP_x\\
+\;&kh^2P_{xx})=0. \qquad (4.21)
\end{aligned}
$$

Since $t, x, h, P$ and the partial derivatives of $h$ and $P$ are regarded as independent variables we separate (4.21) according to the powers and products of the partial derivatives of $h$ and $P$. This gives

$$P_{tx} \quad : \quad \frac{\partial \xi^1}{\partial x} = 0, \tag{4.22}$$

$$P_{tx}h_x \quad : \quad \frac{\partial \xi^1}{\partial h} = 0, \tag{4.23}$$

$$P_{tx}P_x \quad : \quad \frac{\partial \xi^1}{\partial P} = 0, \tag{4.24}$$

$$P_x^3 \quad : \quad \frac{\partial^2 \xi^2}{\partial P^2} = 0, \tag{4.25}$$

$$P_t \quad : \quad \frac{\partial \eta^1}{\partial P} + \frac{k}{3}h^3 \frac{\partial^2 \xi^1}{\partial x^2} = 0, \tag{4.26}$$

$$P_x h_{xx} \quad : \quad \frac{\partial \xi^2}{\partial h} = 0, \tag{4.27}$$

$$P_x^2 \quad : \quad -h^2 \frac{\partial \eta^1}{\partial P} - \frac{1}{3}h^3 \frac{\partial^2 \eta^2}{\partial P^2} + \frac{2}{3}h^3 \frac{\partial^2 \xi^2}{\partial x \partial P} = 0, \tag{4.28}$$

$$h_{xx} \quad : \quad \frac{\partial \eta^2}{\partial h} = 0, \tag{4.29}$$

$$P_t h_x \quad : \quad h^2 \frac{\partial \xi^1}{\partial x} + \frac{2}{3}kh^3 \frac{\partial^2 \xi^1}{\partial x \partial h} - \frac{\partial \xi^2}{\partial P} = 0. \tag{4.30}$$

From (4.22) to (4.30) it follows that

$$\xi^1 \quad = \quad \xi^1(t), \tag{4.31}$$

$$\xi^2 \quad = \quad \xi^2(t,x), \tag{4.32}$$

$$\eta^1 \quad = \quad \eta(t,x,h), \tag{4.33}$$

$$\eta^2 \quad = \quad Pa_1(t,x) + a_2(t,x). \tag{4.34}$$

Using (4.31) to (4.34) the first determining equation becomes

$$
\begin{aligned}
&\frac{\partial \eta^1}{\partial t} + kh^2\frac{\partial \eta^1}{\partial h}h_xP_x + \frac{1}{3}kh^3\frac{\partial \eta^1}{\partial h}P_{xx} - kh^2\frac{d\xi^1}{dt}h_xP_x - \frac{1}{3}kh^3\frac{d\xi^1}{dt}P_{xx} - \frac{\partial \xi^2}{\partial t}h_x \\
- \quad & kh^2\frac{\partial \eta^1}{\partial x}P_x - kh^2\frac{\partial \eta^1}{\partial h}P_xh_x + kh^2\frac{\partial \xi^2}{\partial x}P_xh_x - kh^2P\frac{\partial a_1}{\partial x}h_x - kh^2\frac{\partial a_2}{\partial x}h_x + kh^2\frac{\partial \xi^2}{\partial x}h_xP_x \\
- \quad & kh^2a_1(t,x)P_xh_x - \frac{1}{3}h^3P\frac{\partial^2 a_1}{\partial x^2} - \frac{1}{3}kh^3\frac{\partial^2 a_2}{\partial x^2} - \frac{1}{3}kh^3\frac{\partial a_1}{\partial x}P_x + \frac{1}{3}kh^3a_1(t,x)P_{xx} \\
+ \quad & \frac{2}{3}kh^3\frac{\partial \xi^2}{\partial x}P_{xx} + \frac{1}{3}kh^3\frac{\partial^2 \xi^2}{\partial x^2}P_x - 2kh\eta^1h_xP_x - kh^2\eta^1P_{xx} = 0. \qquad (4.35)
\end{aligned}
$$

We separate by the remaining derivatives of $h$ and $P$

$$
\begin{aligned}
h_xP_x \quad &: \quad 2h^2\frac{\partial \xi^2}{\partial x} - h^2a_1(t,x) - h^2\frac{d\xi^1}{dt} - 2h\eta^1 = 0, \qquad (4.36)\\
P_{xx} \quad &: \quad \frac{1}{3}h^3\frac{\partial \eta^1}{\partial h} - \frac{h^3}{3}\frac{d\xi^1}{dt} - \frac{h^3}{3}a_1(t,x) + \frac{2}{3}h^3\frac{\partial \xi^2}{\partial x} - h^2\eta^1 = 0, \qquad (4.37)\\
h_x \quad &: \quad \frac{\partial \xi^2}{\partial t} + kh^2P\frac{\partial a_1}{\partial x} + kh^2\frac{\partial a_2}{\partial x} = 0, \qquad (4.38)\\
P_x \quad &: \quad \frac{h^3}{3}\frac{\partial^2 \xi^2}{\partial x^2} - \frac{2}{3}h^3\frac{\partial a_1}{\partial x} - h^2\frac{\partial \eta^1}{\partial x} = 0, \qquad (4.39)\\
Remainder \quad &: \quad \frac{\partial \eta^1}{\partial t} - \frac{1}{3}kh^3P\frac{\partial^2 a_1}{\partial x^2} - \frac{1}{3}kh^3\frac{\partial^2 a_2}{\partial x^2} = 0. \qquad (4.40)
\end{aligned}
$$

First we consider (4.38)

$$
\frac{\partial}{\partial t}\xi^2(t,x) + kh^2\Big[P\frac{\partial}{\partial x}a_1(t,x) + \frac{\partial}{\partial x}a_2(t,x)\Big] = 0. \qquad (4.41)
$$

Separate by the powers of $h$

$$
\begin{aligned}
h^2 \quad &: \quad P\frac{\partial}{\partial x}a_1(t,x) + \frac{\partial}{\partial x}a_2(t,x) = 0, \qquad (4.42)\\
h^0 \quad &: \quad \frac{\partial}{\partial t}\xi^2(t,x) = 0. \qquad (4.43)
\end{aligned}
$$

From (4.43),

$$\xi^2 = \xi^2(x). \tag{4.44}$$

Separate (4.40) by the powers of $P$.

$$P \quad : \qquad \frac{\partial}{\partial x} a_1(t,x) = 0, \tag{4.45}$$

$$P^0 \quad : \qquad \frac{\partial}{\partial x} a_2(t,x) = 0. \tag{4.46}$$

Thus

$$a_1 = a_1(t), \qquad a_2 = a_2(t). \tag{4.47}$$

Solving (4.36) and solve for $\eta^1$. This gives

$$\eta^1(t,x,h) = \frac{h}{2}\Big[2\frac{d\xi^2}{dx} - \frac{d\xi^1}{dt} - a_1(t)\Big]. \tag{4.48}$$

If we substitute (4.48) for $\eta^1(t,x,h)$ into (4.37), we find that (4.37) is identically satisfied. (4.39) becomes

$$\frac{d^2\xi^2}{dx^2} = 0 \tag{4.49}$$

and therefore

$$\xi^2(x) = c_3 x + c_4 \tag{4.50}$$

where $c_3$ and $c_4$ are constants. Thus (4.48) becomes

$$\eta^1(t,h) = \frac{h}{2}\Big[2c_3 - \frac{d\xi^1}{dt} - a_1(t)\Big]. \tag{4.51}$$

Finally (4.40) becomes

$$\frac{d^2\xi^1}{dt^2} + \frac{da_1}{dt} = 0. \tag{4.52}$$

Thus

$$\frac{d\xi^1}{dt} = -a_1(t) + c_5 \tag{4.53}$$

where $c_5$ is a constant. Equation (4.51) becomes

$$\eta^1(h) = \frac{h}{2}\Big[2c_3 - c_5\Big]. \tag{4.54}$$

The first determining equation therefore gives

$$\xi^1 = \xi^1(t), \tag{4.55}$$

$$\xi^2(x) = c_3 x + c_4, \tag{4.56}$$

$$\eta^1(h) = \frac{1}{2}(2c_3 - c_5)h, \tag{4.57}$$

$$\eta^2(t,P) = Pa_1(t) + a_2(t), \tag{4.58}$$

where $\xi^1(t)$ satisfies

$$\frac{d\xi^1}{dt} = -a_1(t) + c_5. \tag{4.59}$$

The Lie point symmetry determined from the first determining equation is therefore

$$X = \xi^1(t)\frac{\partial}{\partial t} + (c_3 x + c_4)\frac{\partial}{\partial x} + \frac{1}{2}(2c_3 - c_5)h\frac{\partial}{\partial h} + (Pa_1(t) + a_2(t))\frac{\partial}{\partial P}, \tag{4.60}$$

where $\xi^1(t)$ is related to $a_1(t)$ and $c_5$ by (4.59).

We now solve the second invariant condition

$$X^4(Ah_{xxxx} + h_{tt} - BP)|_{(4.4),(4.5)} = 0, \tag{4.61}$$

where

$$X^{[4]} = x + \zeta^1_{tt}\frac{\partial}{\partial h_{tt}} + \zeta^1_{xxxx}\frac{\partial}{\partial h_{xxxx}}. \tag{4.62}$$

Expanding (4.61) we obtain

$$A\zeta^1_{xxxx} + \zeta^1_{tt} - B\eta^2\Big|_{(4.4),(4.5)} = 0. \tag{4.63}$$

We first need to calculate $\zeta^1_{tt}$ and $\zeta^2_{xxxx}$. Now from (2.10)

$$\zeta^1_{11} = \zeta^1_{tt} = D_t(\zeta^1_t) - h_{tt}D_t(\xi^1) - h_{tx}D_t(\xi^2). \tag{4.64}$$

But from (2.9)

$$\zeta^1_1 = \zeta^1_t = D_t(\eta^1) - h_tD_t(\xi^1) - h_xD_t(\xi^2) \tag{4.65}$$

and therefore from (4.55) to (4.57)

$$\zeta^1_t = (a_1(t) + c_3 - \frac{3}{2}c_5)h_t. \tag{4.66}$$

Hence

$$\zeta^1_{tt} = \frac{da_1}{dt}h_t + \Big(2a_1(t) + c_3 - \frac{5}{2}c_5\Big)h_{tt}. \tag{4.67}$$

Also from (2.12),

$$\zeta^1_{xxxx} = D_x(\zeta^1_{xxx}) - h_{xxxt}D_x(\xi^1) - h_{xxxx}D_x(\xi^2) \tag{4.68}$$

and therefore

$$\zeta^1_{xxxx} = D_x(\zeta^1_{xxx}) - c_3 h_{xxxx} \tag{4.69}$$

Similarly using (2.9) to (2.11),

$$\begin{aligned} \zeta^1_{xxx} &= D_x(\zeta^1_{xx}) - c_3 h_{xxx}, & (4.70)\\ \zeta^1_{xx} &= D_x(\zeta^1_{x}) - c_3 h_{xx}, & (4.71)\\ \zeta^1_{x} &= D_x(\eta^1) - c_3 h_{x}. & (4.72) \end{aligned}$$

But from (4.57),

$$\zeta^1_x = -\frac{1}{2} c_5 h_x \tag{4.73}$$

and therefore

$$\begin{aligned} \zeta^1_{xx} &= -(c_3 + \frac{1}{2} c_5) h_{xx}, & (4.74)\\ \zeta^1_{xxx} &= -(2c_3 + \frac{1}{2} c_5) h_{xxx}, & (4.75)\\ \zeta^1_{xxxx} &= -(3c_3 + \frac{1}{2} c_5) h_{xxxx}. & (4.76) \end{aligned}$$

By using (4.67) and (4.76), the second determining equation (4.63) becomes

$$-A\Big(3c_3+\frac{1}{2}c_5\Big)h_{xxxx}+\frac{da_1}{dt}h_t+\Big(2a_1(t)+c_3-\frac{5}{2}c_5\Big)h_{tt}-Ba_1(t)P-Ba_2(t)\Big|_{(4.4),(4.5)} = 0. \tag{4.77}$$

Using (4.4) and (4.5) to replace $h_t$ and $h_{xxxx}$ in (4.77) gives the determining equation

$$- \quad \left(3c_3 + \frac{1}{2}c_5\right)\left(BP - h_{tt}\right) + \frac{da_1}{dt}\left(kh^2 h_x P_x + \frac{k}{3}h^3 P_{xx}\right) + \left(2a_1(t) + c_3 - \frac{5}{2}c_5\right)h_{tt}$$

$$- \quad Ba_1(t)P - Ba_2(t) = 0. \tag{4.78}$$

We separate (4.78) according to the powers and products of the partial derivatives of $h$ and $P$

$$P_{xx} \quad : \quad \frac{d}{dt}a_1(t) = 0, \tag{4.79}$$

$$h_x P_x \quad : \quad \frac{d}{dt}a_1(t) = 0, \tag{4.80}$$

$$h_{tt} \quad : \quad a_1(t) + 2c_3 - c_5 = 0, \tag{4.81}$$

$$Remainder \quad : \quad -Pa_1(t) - a_2(t) - P(3c_3 + \frac{1}{2}c_5) = 0. \tag{4.82}$$

From (4.79) and (4.80),

$$a_1(t) = c_1, \tag{4.83}$$

where $c_1$ is a constant. Separate (4.82) by the powers of $P$:

$$P \quad : \quad c_1 + 3c_3 + \frac{1}{2}c_5 = 0, \tag{4.84}$$

$$P^0 \quad : \quad a_2(t) = 0. \tag{4.85}$$

From (4.81) and (4.84)

$$c_3 = -\frac{3}{8}c_1, \qquad c_5 = \frac{1}{4}c_1. \tag{4.86}$$

and therefore by (4.59),

$$\frac{d\xi^1}{dt} = -\frac{3}{4}c_1. \tag{4.87}$$

Therefore

$$\xi^1(t) = -\frac{3}{4}c_1 t + c_6, \tag{4.88}$$

where $c_6$ is a constant. Thus (4.55) to (4.58) become

$$\xi^1(t) = c_6 - \frac{3}{4}c_1 t, \tag{4.89}$$

$$\xi^2(x) = c_4 - \frac{3}{8}c_1 x, \tag{4.90}$$

$$\eta^1(h) = -\frac{c_1}{2}h, \tag{4.91}$$

$$\eta^2(P) = c_1 P. \tag{4.92}$$

Next we rename the constants. Let

$$-\frac{3}{4}c_1 = c_2^*, \qquad c_6 = c_1^*, \qquad c_4 = c_3^* \tag{4.93}$$

and suppress the stars. Then

$$\xi^1(t) = c_1 + c_1 t, \tag{4.94}$$

$$\xi^2(x) = c_3 + \frac{1}{2}c_2 x, \tag{4.95}$$

$$\eta^1(h) = \frac{2}{3}c_2 h, \tag{4.96}$$

$$\eta^2(P) = -\frac{4}{3}P \tag{4.97}$$

and the Lie point symmetry is

$$X = (c_1 + c_2 t)\frac{\partial}{\partial t} + \Big(c_3 + \frac{1}{2}c_2 x\Big)\frac{\partial}{\partial x} + \frac{2}{3}c_2 h\frac{\partial}{\partial h} - \frac{4}{3}c_2 P\frac{\partial}{\partial P}. \tag{4.98}$$

The Lie point symmetry (4.98) is a conditional symmetry of the partial differential equation (4.1) because the determining equation (4.20) does not depend on either $h_{tt}$ or $h_{xxxx}$ which therefore could not be replaced using (4.5).

## 4.3 Invariant solution : general case $c_2 \neq 0$

We now derive the invariant solution. We first consider the general case in which $c_2 \neq 0$. The Lie point symmetry (4.98) can be written as

$$\frac{X}{c_2} = \Big(\frac{c_1}{c_2} + t\Big)\frac{\partial}{\partial t} + \frac{1}{2}\Big(\frac{2c_3}{c_2} + x\Big)\frac{\partial}{\partial x} + \frac{2}{3}h\frac{\partial}{\partial h} - \frac{4}{3}P\frac{\partial}{\partial P}. \tag{4.99}$$

Let

$$\frac{X}{c_2} = X^*, \qquad \frac{c_1}{c_2} = c_1^*, \qquad \frac{c_3}{c_2} = c_3^* \tag{4.100}$$

and suppress the star. Then

$$X = \Big(c_1 + t\Big)\frac{\partial}{\partial t} + \frac{1}{2}\Big(2c_3 + x\Big)\frac{\partial}{\partial x} + \frac{2}{3}h\frac{\partial}{\partial h} - \frac{4}{3}P\frac{\partial}{\partial P}. \tag{4.101}$$

Now $h = \psi(t,x)$ and $P = \phi(t,x)$ are invariant solutions of the system of partial differential equations (4.1) and (4.2) provided

$$X(h - \psi(t,x))_{h=\psi(t,x)} = 0, \tag{4.102}$$

$$X(P - \phi(t,x))_{P=\phi(t,x)} = 0. \tag{4.103}$$

Consider first (4.102). Using (4.101) we have

$$\left[\left(c_1+t\right)\frac{\partial}{\partial t}+\frac{1}{2}\left(2c_3+x\right)\frac{\partial}{\partial x}+\frac{2}{3}h\frac{\partial}{\partial h}-\frac{4}{3}P\frac{\partial}{\partial P}\right]\left[h-\psi(t,x)\right]\Big|_{h=\psi(t,x)}=0 \quad (4.104)$$

and expanding we obtain the first-order linear partial differential equation

$$(c_1+t)\frac{\partial\psi}{\partial t}+\frac{1}{2}\left(2c_3+x\right)\frac{\partial\psi}{\partial x}=\frac{2}{3}\psi. \quad (4.105)$$

The differential equations of the characteristic curves of (4.105) are

$$\frac{dt}{c_1+t}=\frac{2dx}{2c_3+x}=\frac{3d\psi}{2\psi}. \quad (4.106)$$

The first pair of terms gives

$$\frac{2c_3+x}{(c_1+t)^{\frac{1}{2}}}=a_1, \quad (4.107)$$

where $a_1$ is a constant. The first term and the third term give

$$\frac{\psi}{(c_1+t)^{\frac{2}{3}}}=a_2, \quad (4.108)$$

where $a_2$ is a constant. The general solution of the partial differential equation (4.105) is

$$a_2=F(a_1), \quad (4.109)$$

where $F$ is an arbitrary function. Thus since $\psi=h(t,x)$,

$$h(t,x)=(c_1+t)^{\frac{2}{3}}F(\xi), \quad (4.110)$$

where

$$\xi=\frac{2c_3+x}{(c_1+t)^{\frac{1}{2}}}. \quad (4.111)$$

Consider next (4.103) which is

$$\Big[\Big(c_1+t\Big)\frac{\partial}{\partial t}+\frac{1}{2}\Big(2c_3+x\Big)\frac{\partial}{\partial x}+\frac{2}{3}h\frac{\partial}{\partial h}-\frac{4}{3}P\frac{\partial}{\partial P}\Big]\Big[P-\phi(t,x)\Big]\Big|_{h=\psi(t,x)}=0 \quad (4.112)$$

and when expanded becomes the first order linear partial differential equation

$$(c_1+t)\frac{\partial\phi}{\partial t}+\frac{1}{2}\Big(2c_3+x\Big)\frac{\partial\phi}{\partial x}=-\frac{4}{3}\phi. \quad (4.113)$$

The differential equations of the characteristic curves of (4.113) are

$$\frac{dt}{c_1+t}=\frac{2dx}{2c_3+x}=-\frac{3d\phi}{4\phi}. \quad (4.114)$$

The first pair of terms again give the first integral (4.107). The first and third terms give

$$\phi(c_1+t)^{\frac{4}{3}}=a_3, \quad (4.115)$$

where $a_3$ is a constant. The general solution of the partial differential (4.113) is

$$a_3=G(a_1), \quad (4.116)$$

where G is an arbitrary function. Thus since $P=\phi(t,x)$ it follows that

$$P=(c_1+t)^{-\frac{4}{3}}G(\xi), \quad (4.117)$$

where $\xi$ is given by (4.111).

In summary the general form of the invariant solution of the system of partial differential equations(4.1) and (4.2) is

$$h(t,x)=(c_1+t)^{\frac{2}{3}}F(\xi), \quad (4.118)$$

$$P(t,x)=(c_1+t)^{-\frac{4}{3}}G(\xi), \quad (4.119)$$

where

$$\xi = \frac{2c_3 + x}{(c_1 + t)^{\frac{1}{2}}}. \tag{4.120}$$

Now we substitute the invariant solutions (4.118) and (4.119) for $h(t,x)$ and $P(t,x)$ into the (4.1) and (4.2). The partial differential equations are reduced to ordinary differential equations as follows.

Differentiating (4.118) and (4.119) with respect to $t$ and $x$, respectively, gives

$$\frac{\partial h}{\partial t} = (c_1 + t)^{-\frac{1}{3}}\Big[\frac{2}{3}F - \frac{1}{2}\xi\frac{dH}{d\xi}\Big], \tag{4.121}$$

$$\frac{\partial}{\partial x}\Big(h^3\frac{\partial P}{\partial x}\Big) = (c_1 + t)^{-\frac{1}{3}}\frac{d}{d\xi}\Big(F^3\frac{dG}{d\xi}\Big). \tag{4.122}$$

Thus substituting (4.118) and (4.119) into the partial differential equation (4.1) reduces it to the ordinary differential equation

$$k\frac{d}{d\xi}\Big(F^3\frac{dG}{d\xi}\Big) + \frac{3}{2}\xi\frac{dF}{d\xi} - 2F = 0. \tag{4.123}$$

Differentiating (4.118) twice and four times with respect to $t$ and $x$, respectively gives

$$\frac{\partial^2 h}{\partial t^2} = -\frac{1}{6}(c_1 + t)^{-\frac{4}{3}}\Big[\frac{4}{3}F - \frac{1}{2}\xi\frac{dF}{d\xi} - \frac{3}{2}\xi^2\frac{d^2F}{d\xi^2}\Big], \tag{4.124}$$

$$\frac{\partial^4 h}{\partial x^4} = (c_1 + t)^{-\frac{4}{3}}\frac{d^4F}{d\xi^4}. \tag{4.125}$$

Substituting (4.124) and (4.125) into the beam equation (4.2) reduces it to the ordinary differential equation

$$A\frac{d^4F}{d\xi^4}+\frac{1}{4}\xi^2\frac{d^2F}{d\xi^2}+\frac{1}{12}\xi\frac{dF}{d\xi}-\frac{2}{9}F=BG(\xi). \tag{4.126}$$

A summary of the invariant solution for the general case $c_2 \neq 0$ is as follows:

$$h(t,x) = (c_1+t)^{\frac{2}{3}}F(\xi), \tag{4.127}$$

$$P(t,x) = \frac{1}{(c_1+t)^{\frac{4}{3}}}G(\xi), \tag{4.128}$$

where

$$\xi=\frac{2c_3+x}{(c_1+t)^{\frac{1}{2}}} \tag{4.129}$$

and where $F(\xi)$ and $G(\xi)$ satisfy the system of two coupled ordinary differential equations

$$k\frac{d}{d\xi}\left(F^3\frac{dG}{d\xi}\right)+\frac{3}{2}\xi\frac{dF}{d\xi}-2F = 0, \tag{4.130}$$

$$A\frac{d^4F}{d\xi^4}+\frac{1}{4}\xi^2\frac{d^2F}{d\xi^2}+\frac{1}{12}\xi\frac{dF}{d\xi}-\frac{2}{9}F = BG(\xi). \tag{4.131}$$

## 4.4 Invariant solution: special case $c_2 = 0$

Solving the special case in which $c_2 = 0$. The Lie point symmetry (4.98) reduces to

$$X=c_1\frac{\partial}{\partial t}+c_3\frac{\partial}{\partial x}. \tag{4.132}$$

If either $c_1 = 0$ or $c_3 = 0$ the Lie point symmetry is trivial. Thus we consider $c_1 \neq 0$ and $c_3 \neq 0$. Divide (4.132) by $c_1$. Then

$$X = \frac{\partial}{\partial t} + c_3^* \frac{\partial}{\partial x}, \qquad c_3^* = \frac{c_3}{c_1}. \tag{4.133}$$

We suppress the star.

Now $h = \psi(t,x)$ and $P = \phi(t,x)$ are invariant solutions of the system of partial differential equations generated by the Lie point symmetry (4.133) provided

$$\Big(\frac{\partial}{\partial t} + c_3 \frac{\partial}{\partial x}\Big)\Big(h - \psi(t,x)\Big)\Big|_{h=\psi(t,x)} = 0, \tag{4.134}$$

$$,\Big(\frac{\partial}{\partial t} + c_3 \frac{\partial}{\partial x}\Big)\Big(P - \phi(t,x)\Big)\Big|_{P=\phi(t,x)} = 0, \tag{4.135}$$

that is, provided

$$\frac{\partial \psi}{\partial t} + c_3 \frac{\partial \psi}{\partial x} = 0, \tag{4.136}$$

$$\frac{\partial \phi}{\partial t} + c_3 \frac{\partial \phi}{\partial x} = 0. \tag{4.137}$$

The differential equations of the characteristic curves of (4.136) are

$$\frac{dt}{1} = \frac{dx}{c_3} = \frac{d\psi}{0}. \tag{4.138}$$

The first pair of terms in (4.138) give

$$x - c_3 t = a_1, \tag{4.139}$$

where $a_1$ is a constant. The last term in (4.138) gives

$$\psi = a_2, \tag{4.140}$$

where $a_2$ is a constant. The general solution of the first-order partial differential equation (4.136) is

$$a_2 = F(a_1), \tag{4.141}$$

where $F$ is an arbitrary function. Thus

$$\psi = F(x - c_3 t) \tag{4.142}$$

and, since $\psi = h(t,x)$, we obtain

$$h(t,x) = F(\xi), \tag{4.143}$$

where

$$\xi = x - c_3 t. \tag{4.144}$$

Similarly the general solution of the first-order partial differential equation (4.137) is

$$P(t,x) = G(\xi), \tag{4.145}$$

where $\xi$ is given by (4.144).

Substituting (4.143) and (4.145) into (4.1) and (4.2) reduces the two partial differential equations to the system of ordinary differential equations

$$k\frac{d}{d\xi}\left[F^3\frac{dG}{d\xi}\right] + 3c_3\frac{dF}{d\xi} = 0, \tag{4.146}$$

$$A\frac{d^4F}{d\xi^4} + c_3^2\frac{d^2F}{d\xi^2} = BG. \tag{4.147}$$

## 4.5 Boundary and initial conditions for the invariant solution: general case $c_2 \neq 0$

Consider now the boundary conditions formulated in Section 3.6 and express them in terms of the invariant solution, (4.127) and (4.128). We choose $c_3 = 0$

so that $\xi = 0$ when $x = 0$. Thus

$$\xi = \frac{x}{(c_1 + t)^{\frac{1}{2}}}. \tag{4.148}$$

Consider first the boundary condition (3.59) that the half-width is zero at the tip,

$$x = L(t): \qquad h(t, L(t)) = 0 \qquad for \;\; all \;\; t \geq 0. \tag{4.149}$$

Expressed in terms of the invariant solution (4.127) for $h(t,x)$, the boundary condition (4.149) becomes

$$F(w(t)) = 0, \tag{4.150}$$

where

$$w(t) = \frac{L(t)}{(c_1 + t)^{\frac{1}{2}}}. \tag{4.151}$$

Differentiate (4.150) with respect to $t$. Thus

$$\frac{dF}{dw}\frac{dw}{dt} = 0. \tag{4.152}$$

But $F(w)$ is not a constant function. Thus

$$\frac{dF}{dw} \neq 0 \tag{4.153}$$

and therefore

$$\frac{dw}{dt} = 0. \tag{4.154}$$

Hence

$$w(t) = a_1 \tag{4.155}$$

where $a_1$ is a constant. Thus

$$L(t) = a_1(c_1 + t)^{\frac{1}{2}}. \tag{4.156}$$

But

$$L(0) = 1 \tag{4.157}$$

and therefore

$$a_1 = c_1^{-\frac{1}{2}}. \tag{4.158}$$

Hence

$$L(t) = (1 + \frac{t}{c_1})^{\frac{1}{2}} \tag{4.159}$$

and the boundary condition (4.150) becomes

$$F(c_1^{-\frac{1}{2}}) = 0. \tag{4.160}$$

The similarity variable $\xi$ can be written as

$$\xi = \frac{x}{c_1^{\frac{1}{2}} L(t)}\cdot \tag{4.161}$$

Consider next the boundary condition (3.60)

$$x = L(t): \qquad \frac{\partial}{\partial x} h(t, L(t)) = 0. \tag{4.162}$$

Expressed in terms of the invariant solution, (4.162) becomes

$$\frac{d}{d\xi} F(c_1^{-\frac{1}{2}}) = 0. \tag{4.163}$$

The boundary condition on the bending moment $M(t)$ at the tip $x = L(t)$. We consider only finite bending moment at the fracture tip. When the bending

moment is infinite the beams will crack and the model no longer applies. From (3.65)

$$x = L(t): \qquad \frac{\partial^2}{\partial x^2} h(t, L(t)) = M(t). \tag{4.164}$$

Expressed in terms of the invariant solution, equation (4.164) becomes

$$c_1^{-\frac{1}{3}} \frac{d^2}{d\xi^2} F(c_1^{-\frac{1}{2}}) \Big(1 + \frac{t}{c_1}\Big)^{-\frac{1}{3}} = M(t). \tag{4.165}$$

Thus for an invariant solution, $M(t)$ must be of the form

$$M(t) = M_0 (1 + \frac{t}{c_1})^{-\frac{1}{3}}, \tag{4.166}$$

where

$$M_0 = c_1^{-\frac{1}{3}} \frac{d^2}{d\xi^2} F(c_1^{-\frac{1}{2}}). \tag{4.167}$$

The constant $M_0$ is prescribed. For an invariant solution the bending moment $M(t)$ at the tip cannot be arbitrary. It must be of the form (4.166). Equation (4.167) can be expressed as the boundary condition

$$\frac{d^2}{d\xi^2} F(c_1^{-\frac{1}{2}}) = c_1^{\frac{1}{3}} M_0. \tag{4.168}$$

Consider next the boundary condition on the flux of the fluid at the fracture tip. The flux of the fluid vanishes at the fracture tip, and hence from (3.67)

$$x = L(t): \qquad h^3(t, L(t)) \frac{\partial}{\partial x} P(t, L(t)) = 0. \tag{4.169}$$

Expressed in terms of the invariant solution, (4.127) and (4.128), equation (4.169) becomes

$$F^3(c_1^{-\frac{1}{2}}) \frac{d}{d\xi} G(c_1^{-\frac{1}{2}}) = 0. \tag{4.170}$$

From the boundary condition (4.160), $\frac{d}{d\xi}G(c_1^{-\frac{1}{2}})$ can be infinite at the fracture tip, $\xi = c_1^{-\frac{1}{2}}$.

Consider next the conditions at the fracture entry. Since the characteristic half-width is the initial half-width at the fracture entry, from (3.69),

$$x = 0: \qquad h(0,0) = 1. \tag{4.171}$$

Expressed in terms of the invariant solution, (4.171) gives the boundary condition

$$F(0) = c_1^{-\frac{2}{3}}. \tag{4.172}$$

Also the flux of fluid at the fracture entry is specified. From (3.70)

$$x = 0: \qquad -\frac{2}{3}kh^3(t,0)\frac{\partial}{\partial x}P(t,0) = Q(t), \tag{4.173}$$

where $Q(t)$ is specified as far as the invariant solution will allow. Expressed in terms of the invariant solution (4.127) and (4.128), (4.173) becomes

$$-\frac{2}{3}c_1^{\frac{1}{6}}kF^3(0)\frac{dG}{d\xi}(0)\Big(1+\frac{t}{c_1}\Big)^{\frac{1}{6}} = Q(t) \tag{4.174}$$

Thus $Q(t)$ must be of the form

$$Q(t) = Q_0\Big(1+\frac{t}{c_1}\Big)^{\frac{1}{6}} \tag{4.175}$$

where

$$Q_0 = -\frac{2}{3}c_1^{\frac{1}{6}}kF^3(0)\frac{dG}{d\xi}(0)\cdot \tag{4.176}$$

The constant $Q_0$ and $c_1$ are specified as far as the invariant solution will allow. For an invariant solution the flux of the fluid at the fracture entry cannot be arbitrary but it must be of the form (4.175) Using (4.172) for $F(0)$, (4.176) can be expressed as the boundary condition

$$\frac{dG}{d\xi}(0) = -\frac{3c_1^{\frac{11}{6}}Q_0}{2k}. \tag{4.177}$$

This completes writing the boundary and initial conditions in invariant form.

We make the transformation in order to immobilise the boundary

$$\xi = \frac{u}{c_1^{\frac{1}{2}}} \qquad \text{where} \qquad u = \frac{x}{L(t)}. \tag{4.178}$$

The fracture tip is now $u = 1$. Expressed in terms of $u$ the differential equations to be solved are

$$c_1 k \frac{d}{du}\left(F^3 \frac{dG}{du}\right) + \frac{3}{2}u\frac{dF}{du} - 2F = 0, \tag{4.179}$$

$$Ac_1^2 \frac{d^4F}{du^4} + \frac{1}{4}u^2\frac{d^2F}{du^2} + \frac{1}{12}u\frac{dF}{du} - \frac{2}{9}F = BG, \tag{4.180}$$

subject to the boundary conditions

$$u = 0: \qquad F(0) = c_1^{-\frac{2}{3}}, \tag{4.181}$$

$$\frac{dG}{du}(0) = -\frac{3c_1^{\frac{4}{3}}Q_0}{2k}, \tag{4.182}$$

$$u = 1: \qquad F(1) = 0 \tag{4.183}$$

$$\frac{dF}{du}(1) = 0, \tag{4.184}$$

$$\frac{d^2F}{du^2}(1) = c_1^{-\frac{2}{3}}M_0, \tag{4.185}$$

$$F^3(1)\frac{dG}{du}(1) = 0, \tag{4.186}$$

The fracture length, the bending moment at the fracture tip and the flux at the fracture entry satisfy

$$L(t) = \left(1+\frac{t}{c_1}\right)^{\frac{1}{2}}, \tag{4.187}$$

$$M(t) = M_0\left(1+\frac{t}{c_1}\right)^{-\frac{1}{3}}, \tag{4.188}$$

$$Q(t) = Q_0\left(1+\frac{t}{c_1}\right)^{\frac{1}{6}}, \tag{4.189}$$

where $c_1$, $M_0$ and $Q_0$ are constants. The half-width of the fracture and the pressure difference are

$$h(t,x) = c_1^{\frac{2}{3}}\left(1+\frac{t}{c_1}\right)^{\frac{2}{3}}F(u) \tag{4.190}$$

,

$$P(t,x) = c_1^{-\frac{4}{3}}\left(1+\frac{t}{c_1}\right)^{-\frac{4}{3}}G(u). \tag{4.191}$$

Consider the special case $c_1 = 0$. Equation (4.179) and (4.180) reduce to

$$\frac{3}{2}u\frac{dF}{du} - 2F = 0, \tag{4.192}$$

$$\frac{u^2}{4}\frac{d^2F}{du^2} + \frac{u}{12}\frac{dF}{du} - \frac{2}{9}F = BG. \tag{4.193}$$

The general solution of (4.192) is

$$F(u) = Du^{\frac{4}{3}} \tag{4.194}$$

where $D$ is a constant. Substituting (4.194) into (4.193) we obtain

$$G(u) = 0. \tag{4.195}$$

The boundary condition $F(1) = 0$ gives $D = 0$. Thus

$$F(u) = 0. \tag{4.196}$$

The solution for $c_1 = 0$ is therefore the trivial solution $F(u) = G(u) = 0$. We therefore do not consider the special case $c_1 = 0$.

It is shown in Appendix $A$ that the coupled system of ordinary differential equations,(4.179) and (4.180), does not admit a Lie point symmetry when $c_1 \neq 0$.

## 4.6 Boundary and initial conditions for the invariant solution : special case $c_2 = 0$

Consider again the boundary conditions formulated in Section 3.6 and imposed them on the solution for the special case $c_2 = 0$.

We first consider the boundary condition

$$x = L(t): \qquad h(t, L(t)) = 0. \tag{4.197}$$

Expressed in terms of the invariant solution (4.143) and (4.145), the boundary condition (4.197) becomes

$$F(w(t)) = 0, \tag{4.198}$$

where

$$w(t) = L(t) - c_3 t. \tag{4.199}$$

Differentiate (4.198) with respect to t. This gives

$$\frac{dF}{dw}\frac{dw}{dt} = 0 \tag{4.200}$$

and since $F(w)$ is not in general a constant function it follows that

$$\frac{dw}{dt} = 0. \tag{4.201}$$

Thus from (4.199)

$$\frac{dL}{dt} = c_3 \tag{4.202}$$

and therefore

$$L(t) = c_3 t + d \tag{4.203}$$

where $k$ is a constant. But $L(0) = 1$ and therefore $d = 1$. Thus

$$L(t) = 1 + c_3 t. \tag{4.204}$$

The boundary condition (4.198) becomes

$$F(1) = 0. \tag{4.205}$$

Next consider the boundary condition (3.60)

$$x = L(t): \qquad \frac{\partial}{\partial x} h(t, L(t)) = 0. \tag{4.206}$$

Expressed in terms of the invariant solution, (4.143) and (4.145), (4.206) is

$$\frac{dF}{d\xi}(1) = 0. \tag{4.207}$$

Consider next the boundary condition on the bending moment, $M(t)$, at the fracture tip, $x = L(t)$. The bending moment $M(t)$ is finite and prescribed. From (3.65),

$$x = L(t), \qquad \frac{\partial^2}{\partial x^2} h(t, L(t)) = M(t). \tag{4.208}$$

Using the similarity solution (4.143) and (4.145) and (4.204) for $L(t)$, (4.206) becomes

$$\frac{d^2F}{d\xi^2}(1) = M(t). \tag{4.209}$$

Thus $M(t)$ must be a constant, Say $M_0$. Thus

$$\frac{d^2F}{d\xi^2}(1) = M_0, \tag{4.210}$$

where $M_0$ is the prescribed bending moment at the fracture tip.

Consider next the boundary condition on the fluid flux at the fracture tip. Since the flux of fluid is zero at the tip, from (3.68),

$$x = L(t): \qquad h^3(t, L(t))\frac{\partial}{\partial x}P(t, L(t)) = 0. \tag{4.211}$$

Expressed in terms of the invariant solution (4.143), (4.145) and (4.204), equation (4.206) becomes

$$F^3(1)\frac{dG}{d\xi}(1) = 0. \tag{4.212}$$

Since $F(1) = 0$, it follows that $\frac{dG}{d\xi}(1)$ can be infinite and therefore $\frac{\partial P}{\partial x}$ can be infinite at the fracture tip.

Consider next the conditions at the entrance to the fracture, $x = 0$. Since the characteristic half-width is the initial half-width at the fracture entry

$$x = 0, \qquad t = 0: \qquad h(0,0) = 1. \tag{4.213}$$

Expressed in terms of the invariant solution (4.143) and (4.144), (4.213) becomes

$$F(0) = 1. \tag{4.214}$$

Also the flux of fluid at the fracture entry is specified. From (3.70)

$$x = 0: \qquad -\frac{2}{3}kh^3(t,0)\frac{\partial P}{\partial x}(t,0) = Q(t), \tag{4.215}$$

where $Q_0(t)$ is prescribed consistent with the invariant solution. Expressed in terms of the invariant solution, (4.215) becomes

$$-\frac{2}{3}kF^3(-c_3t)\frac{dG}{d\xi}(-c_3t) = Q(t). \tag{4.216}$$

Putting $t = 0$ and using (4.214)) gives

$$\frac{dG}{d\xi}(0) = -\frac{3}{2k}Q(0). \tag{4.217}$$

A summary of the problem for the special case $c_2 = 0$ is as follows. The half-width and pressure are of the form

$$h(t,x) = F(\xi), \tag{4.218}$$

$$P(t,x) = G(\xi), \tag{4.219}$$

where

$$\xi = x - c_3t, \tag{4.220}$$

and where $F(\xi)$ and $G(\xi)$ satisfy the coupled ordinary differential equations

$$k\frac{d}{d\xi}\left[F^3\frac{dG}{d\xi}\right] + 3c_3\frac{dF}{d\xi} = 0, \tag{4.221}$$

$$A\frac{d^4F}{d\xi^4} + c_3^2\frac{d^2F}{d\xi^2} = BG, \tag{4.222}$$

subject to the boundary conditions

$$F(0) = 1, \tag{4.223}$$

$$F(1) = 0, \tag{4.224}$$

$$\frac{dF}{d\xi}(1) = 0, \tag{4.225}$$

$$\frac{d^2F}{d\xi^2}(1) = M_0, \tag{4.226}$$

$$F^3(1)\frac{dG}{d\xi}(1) = 0, \tag{4.227}$$

where the constant $M_0$ is finite and prescribed. The fracture length, the bending moment at the fracture tip and the flux at the fracture entry satisfy

$$L(t) = 1 + c_3 t, \tag{4.228}$$

$$M(t) = M_0, \tag{4.229}$$

$$Q_0(t) = -\frac{2}{3}kF^3(-c_3 t)\frac{dG}{d\xi}(-c_3 t). \tag{4.230}$$

The constant $c_3$ has to be determined.

It is shown in Appendix B that the coupled system of ordinary differential equations, (4.221) and (4.222), does not admit any Lie point symmetry.

# Chapter 5

# Asymptotic and numerical solutions

## 5.1 Introduction

In this chapter the numerical solution for the hydraulic fracture of two closely spaced beams will be considered. The general case $c_2 \neq 0$ and finite bending moment will be considered which is the case of most interest in practical applications. We saw in Appendix A that the system of ordinary differential equations does not admit a Lie point symmetry when $c_1 \neq 0$ and therefore the differential equations may not have an analytical solution. The asymptotic solution at the fracture tip for the half-width, pressure difference and width average fluid velocity in the fracture will first be considered. The asymptotic solution will be used when deriving the numerical solution. A mathematical model of hydrofracture and magma fracture in geophysics is considered to determine values for the physical parameter and for the characteristic numbers $A$ and $B$. The numerical method is a shooting method which uses MATLAB ODE 45 for initial value problems.

## 5.2 Asymptotic solution at the fracture tip for $c_2 \neq 0$

We first consider the asymptotic solution for $F(u)$ as $u \to 1$. Let $u = 1-\delta$ where $0 < \delta \ll 1$. The Taylor expansion of $F(u)$ at $u = 1$ is

$$F(1-\delta) = F(1) - \delta \frac{dF}{du}(1) + \frac{\delta^2}{2!}\frac{d^2F}{du^2}(1) - \frac{\delta^3}{3!}\frac{d^3F}{du^3}(1) + \cdots \tag{5.1}$$

Define

$$E_0 = F(1), \quad E_n = \frac{(-1)^n}{n!}\frac{d^n F}{du^n}(1)\cdot \tag{5.2}$$

Then from the boundary conditions (4.183) and (4.185),

$$E_0 = F(1) = 0, \tag{5.3}$$

$$E_1 = -\frac{dF}{du}(1) = 0, \tag{5.4}$$

$$E_2 = \frac{1}{2}\frac{d^2F}{du}(1) = \frac{1}{2}c_1^{-\frac{2}{3}}M_0 \tag{5.5}$$

Thus since $u = 1-\delta$, (5.1) becomes

$$F(u) = E_2(1-u)^2 + E_3(1-u)^3 + E_4(1-u)^4 + E_5(1-u)^5 + O((1-u)^6), \tag{5.6}$$

as $u \to 1$, where $E_2$ is given by (5.5) and $E_3$, $E_4$ and $E_5$ are not yet determined.

Consider next asymptotic behaviour of $G(u)$ as $u \to 1$. From the beam equation (4.180)

$$G(u) = \frac{1}{B}\left[Ac_1^2\frac{d^4F}{du^4} + \frac{1}{4}u^2\frac{d^2F}{du^2} + \frac{u}{12}\frac{dF}{du} - \frac{2}{9}F\right] \tag{5.7}$$

and substituting (5.6) into (5.7) we obtain

$$G(u) = \frac{1}{B}\left[\frac{1}{2}E_2 + 24Ac_1^2E_4 + \left(-\frac{7}{6}E_2 + \frac{3}{2}E_3 + 120Ac_1^2E_5\right)(1-u) + O((1-u)^2)\right], \tag{5.8}$$

as $u \to 1$. Hence

$$\frac{dG}{du} = \frac{1}{B}\left[\left(\frac{7}{6}E_2 - \frac{3}{2}E_3 - 120Ac_1^2E_5\right) + O(1-u)\right], \tag{5.9}$$

as $u \to 1$.

The thin film equation (4.179),

$$c_1 k \frac{d}{du}\Big(F^3 \frac{dG}{du}\Big) + \frac{3}{2} u \frac{dF}{du} - 2F = 0 \tag{5.10}$$

has not been used in the derivation of the asymptotic results. We now check that the asymptotic results satisfy (5.10). Using (5.6) and (5.9),

$$\begin{aligned}
& c_1 k \frac{d}{du}\Big(F^3 \frac{dG}{du}\Big) + \frac{3}{2} u \frac{dF}{du} - 2F \\
= \;& c_1 k \Big[ -\frac{6}{B} E_2^3 \Big(\frac{7}{6} E_2 - \frac{3}{2} E_3 - 120 A c_1^2 E_5\Big)(1-u)^5 + O(1-u)^6 \Big] \\
- \;& \frac{3}{4} E_2 (1-u) + O((1-u)^2) \\
- \;& 2E_2 (1-u)^2 + O((1-u)^3) \\
= \;& \frac{3}{4} E_2 (1-u) + O((1-u)^2) \\
\to \;& 0 \qquad as \qquad u \to 1.
\end{aligned} \tag{5.11}$$

The thin fluid equation is therefore satisfied by the asymptotic results (5.6) and (5.8).

## 5.3 Width average fluid velocity: $c_2 \neq 0$.

Consider next the width average fluid velocity defined by (3.54). From (3.58) and suppressing the overhead bars, the width average fluid velocity in dimensionless form is

$$v_x^*(t,x) = -\frac{k}{3} h^2(t,x) \frac{\partial P}{\partial x}. \tag{5.12}$$

Using the invariant solution (4.190) and (4.191),

$$h(t,x) = c_1^{\frac{2}{3}}\Big[1+\frac{t}{c_1}\Big]^{\frac{2}{3}}F(u), \tag{5.13}$$

$$P(t,x) = c_1^{-\frac{4}{3}}\Big[1+\frac{t}{c_1}\Big]^{-\frac{4}{3}}G(u) \tag{5.14}$$

and

$$u=\frac{x}{L(t)}, \qquad L(t)=\Big(1+\frac{t}{c_1}\Big)^{\frac{1}{2}}, \tag{5.15}$$

equation (5.12) becomes

$$v_x^*(t,x) = -\frac{k}{3}\Big(1+\frac{t}{c_1}\Big)^{-\frac{1}{2}}F^2(u)\frac{dG}{du}(u)\cdot \tag{5.16}$$

Thus we obtain the mean velocity ratio

$$R(u)=\frac{v_x^*(t,x)}{\frac{dL}{dt}} = -\frac{2}{3}c_1kF^2(u)\frac{dG}{du}(u)\cdot \tag{5.17}$$

Consider now the asymptotic solution of $R(u)$ as $u\to 1$. Substituting (5.6) for $F(u)$ and (5.9) for $\frac{dG}{du}$ into (5.17) we obtain

$$R(u) = -\frac{2c_1kE_2^2}{3B}\Big[\frac{7}{6}E_2-\frac{3}{2}E_3-120Ac_1^2E_5\Big]\Big[(1-u)^4+O((1-u)^5)\Big], \tag{5.18}$$

as $u\to 1$. Thus

$$R(u)\to 0 \qquad \text{as} \qquad u\to 1. \tag{5.19}$$

The mean fluid velocity vanishes at the fracture tip because the half-width of the fracture gradually decreases as $u\to 1$. The viscous fluid sticks to the beams and the area of the cross-section with non-zero fluid velocity gradually decreases as $u\to 1$ leaving only the fluid with zero velocity sticking to the beams.

Consider finally the mean velocity ratio $R(u)$ at the fracture entrance u=0. From the boundary conditions (4.181) and (4.182)

$$F(0) = c_1^{-\frac{2}{3}}, \qquad \frac{dG}{du}(0) = -\frac{3}{2k} c_1^{\frac{4}{3}} Q_0. \tag{5.20}$$

Thus from (5.17),

$$R(0) = c_1 Q_0. \tag{5.21}$$

The results (5.21) is very useful in checking the numerical results. The two end points of the curve of $R(u)$ against $u$ for $0 \leq u \leq 1$ are known.

## 5.4 Numerical values for the parameters

In order to obtain values for the parameters $A$ and $B$ we will investigate the application of the beam fracture model to hydro-fracturing and also to magma fracturing in geophysics leading to the formation of sills. A sill is a tabular sheet of igneous rock that was intruded as magma between layers of sedimentary rock [7].

The model we have considered is for laminar flow in the fracture. We first consider the condition for the flow to be laminar. We define the Reynolds number for the flow in the fracture in terms of the width of the fracture as

$$Re = \frac{HU\rho}{\mu} = \frac{Q_0 \rho}{\mu} \tag{5.22}$$

where $Q_0$ is the characteristic fluid flux per unit breadth and $H$ is the characteristic half-width of the fracture,

$$Q_0 = HU. \tag{5.23}$$

We take the criteria for the flow to be laminar as [7]

$$Re \leq 10^3. \tag{5.24}$$

Thus for laminar flow

$$Q_0 \leq \frac{\mu}{\rho} 10^3, \quad U \leq \frac{\mu}{H\rho} 10^3. \tag{5.25}$$

The maximum value for $Q_0$ and $U$ for a laminar flow in a hydro-fracture and in a magma fracture with basalt and silicic magma are shown in Table 5.1. The numerical values for $\rho$ and $\mu$ are obtained from [7].

| | H | $\rho$ | $\mu$ | $Q_0$ | $U$ |
|---|---|---|---|---|---|
| Units | $m$ | $kg\ m^{-3}$ | $Pa\ s$ | $m^2\ s^{-1}$ | $m\ s^{-1}$ |
| Hydro-fracture (water) | $10^{-2}$ | $10^3$ | $10^{-4}$ | $10^{-4}$ | $10^{-2}$ |
| Basalt magma | $10^{-1}$ | 2.7x$10^3$ | $10^{-1}$ | 3.7x$10^{-2}$ | 0.37 |
| Silicic magma | $10^{-1}$ | 2.7x$10^3$ | $10^2$ | 37 | 370 |

Table 5.1: Maximum values for the characteristic volume flux per unit breadth $Q_0$ and the characteristic velocity $U$ along the fracture for the fluid flow in the fracture to be laminar [7].

A characteristic value for the maximum depth $W_{max}$ at which a fracture can propagate below the surface can be estimated as follows. The pressure at depth $W$ below the surface due to the overburden rock, which we assume has the same density as the beam, $D$, is

$$p = DgW. \tag{5.26}$$

But the characteristic pressure of the fluid in the thin fluid film is [1]

$$p = \frac{\mu LU}{H^2} \tag{5.27}$$

which using (5.23) for $U$ becomes

$$p = \frac{\mu LQ_0}{H^3}. \tag{5.28}$$

A fracture will propagate at a depth $W$ below the surface provide

$$DgW \lesssim \frac{\mu L Q_0}{H^3}, \tag{5.29}$$

that is, provided

$$W \lesssim \frac{\mu L Q_0}{DgH^3} = W_{max}. \tag{5.30}$$

Sills can form up to a few kilometers below the surface. We expect $W_{max}$ to be order of a kilometer. For smaller values of $W_{max}$ the model considered here for the hydraulic fracturing will not be applicable.

Consider now estimates of the characteristic numbers $A$ and $B$,

$$A = \frac{Ed^2}{12DQ_0^2}\Big(\frac{H}{L_0}\Big)^2, \tag{5.31}$$

$$B = \frac{\mu H}{DdQ_0}\Big(\frac{L_0}{H}\Big)^3\Big[1 - \frac{\sigma_{yy}^{(\infty)} H^3}{\mu L_0 Q_0}\Big], \tag{5.32}$$

where

$E$ = Young's modulus of the beam,

$\mu$ = coefficient of viscosity of the fluid,

$D$ = density of the rock,

$d$ = thickness of the beam ,

$H$ = characteristic half-width of the fracture,

$L_0$ = characteristic length of the fracture ,

$Q_0$ = characteristic flux of fluid per unit breath,

$\sigma_{yy}^{(\infty)} = DgW$ = normal compressive stress on the upper surface of the beam at depth $W$.

Thus using (5.30),

$$\frac{\sigma_{yy}^{(\infty)} H^3}{\mu L_0 Q_0} = \frac{DgWH^3}{\mu L_0 Q_0} = \frac{W}{W_{max}} \tag{5.33}$$

and (5.32) becomes

$$B = \frac{\mu H}{DdQ_0}\Big(\frac{L_0}{H}\Big)^3\Big[1 - \frac{W}{W_{max}}\Big]. \tag{5.34}$$

Estimate of the characteristic numbers $A$, $B$ and $W_{max}$ are presented in Table5.2

The value of $Q_0$ used in Table 5.2 is the maximum value for the flow to remain laminar. Since we expect a larger $Q_0$ to be better at opening the space between the beams, the values in Table 5.2 describe the best conditions for a fracture to propagate with laminar flow[7].

We see that for hydrofracture by a hydrothermal solution and for a basalt magma fracture the characteristic maximum depth below the surface for the sill to form $10^{-5}m$ and $10^{-2}m$ respectively. We conclude that sills will not form at physically significant depths. For silicic magma sills can form up to the depth of $10^4 m$, that is $10km$. We will therefore consider the solution with $A$ small , of order of magnitude $10^{-4}$, and $B$ large, of order of magnitude $10^5$. Hydraulic fracture of two closely spaced beams with laminar flow in the fracture can describe the formation of sills of silicic magma but not of basalt magma or the formation of hydrofractures. For basalt magma and hydrofractures to propagate a larger value of the volume flux $Q_0$ would be required which would produce a turbulent flow in the fracture.

## 5.5 Numerical solution for the general case: $c_2 \neq 0$ with finite bending moment at the fracture tip

The general case $c_2 \neq 0$ with a finite bending moment at the fracture tip is considered. The problem was formulated in Section 4.5. The problem is to solve the coupled ordinary differential equations

| | Hydro-fracture (water) | Basalt magma | Silicic magma |
|---|---|---|---|
| H<br>m | $10^{-2}$ | $10^{-1}$ | $10^{-1}$ |
| d<br>m | 5x$10^{-1}$ | 5x$10^{-1}$ | 5x$10^{-1}$ |
| L<br>m | $10^{2}$ | $10^{2}$ | $10^{2}$ |
| E<br>Pa | 2x$10^{10}$ | 2x$10^{10}$ | 2x$10^{10}$ |
| D<br>$kg\ m^{-3}$ | 2.4x$10^{3}$ | 2.4x$10^{3}$ | 2.4x$10^{3}$ |
| $Q_0$=UH<br>$m^2\ s^{-1}$ | $10^{-4}$ | 3.7 x $10^{-2}$ | 37 |
| $\mu$<br>Pa s | $10^{-4}$ | $10^{-1}$ | $10^{2}$ |
| $g$<br>$m\ s^{-2}$ | 9.8 | 9.8 | 9.8 |
| $A$ | 1.7x$10^{5}$ | 1.26x$10^{2}$ | 1.26x$10^{-4}$ |
| $W=\frac{\mu L Q_0}{DgH^3}$ | 4.25x$10^{-5}$ | 1.57x$10^{-2}$ | 1.57x$10^{4}$ |
| $B$ | 8.33x$10^{6}$ $\left(1-\frac{W}{W_{max}}\right)$ | 2.25x$10^{5}$ $\left(1-\frac{W}{W_{max}}\right)$ | 2.25x$10^{5}$ $\left(1-\frac{W}{W_{max}}\right)$ |

Table 5.2: Values of the characteristic numbers $A$ and $B$ and the characteristic maximum depth below the surface. The values of the parameters were taken from Emerman et al. [7].

$$c_1 k \frac{d}{du}\left(F^3 \frac{dG}{du}\right) + \frac{3}{2} u \frac{dF}{du} - 2F = 0, \tag{5.35}$$

$$A c_1^2 \frac{d^4F}{du^4} + \frac{1}{4} u^2 \frac{d^2F}{du^2} + \frac{1}{12} u \frac{dF}{du} - \frac{2}{9} F = BG, \tag{5.36}$$

for $F(u)$ and $G(u)$ subject to the boundary conditions

$$u = 0: \qquad F(0) = c_1^{-\frac{2}{3}}, \tag{5.37}$$

$$\frac{dG}{du}(0) = -\frac{3 c_1^{\frac{4}{3}} Q_0}{2k}, \tag{5.38}$$

$$u = 1: \qquad F(1) = 0, \tag{5.39}$$

$$\frac{dF}{du}(1) = 0, \tag{5.40}$$

$$\frac{d^2F}{du^2}(1) = c^{-\frac{2}{3}} M_0, \tag{5.41}$$

where $c_1$, $Q_0$ and $M_0$ are constants and from (4.3) and (5.33)

$$k = \left(1 - \frac{W}{W_{max}}\right). \tag{5.42}$$

From (5.34) we define $B_0$ by

$$B = B_0 k, \qquad B_0 = \frac{\mu H}{D d Q_0}\left(\frac{L_0}{H}\right)^3. \tag{5.43}$$

We rewrite (5.35) and (5.36) as the following system of six first-order ordinary differential equations. Let $F_1(u) = F(u)$ and $F_5(u) = G(u)$. Then

$$\frac{dF_1}{du} = F_2, \tag{5.44}$$

$$\frac{dF_2}{du} = F_3, \tag{5.45}$$

$$\frac{dF_3}{du} = F_4, \tag{5.46}$$

$$\frac{dF_4}{du} = \frac{1}{Ac_1^2}\Big[\frac{2}{9}F_1 - \frac{1}{12}uF_2 - \frac{1}{4}u^2F_3 + kB_0F_5\Big], \tag{5.47}$$

$$\frac{dF_5}{du} = F_6, \tag{5.48}$$

$$\frac{dF_6}{du} = \frac{2}{c_1kF_1^2} - \frac{3}{2}\frac{uF_2}{c_1kF_1^3} - \frac{3F_2F_6}{F_1}\cdot \tag{5.49}$$

The boundary conditions (5.37) to (5.41) become

$$u = 0: \qquad F_1(0) = c_1^{-\frac{2}{3}}, \tag{5.50}$$

$$F_6(0) = -\frac{3c_1^{\frac{4}{3}}Q_0}{2k}, \tag{5.51}$$

$$u = 1: \qquad F_1(1) = 0, \tag{5.52}$$

$$F_2(1) = 0, \tag{5.53}$$

$$F_3(1) = c^{-\frac{2}{3}}M_0. \tag{5.54}$$

The right hand side of the differential equation (5.49) is divided by $F_1(u)$ and is therefore singular at $u = 1$. The boundary conditions are therefore imposed at a small distance $\delta$ in from $u = 1$.

The problem is reformulated as an initial value problem at $u = 1-\delta$ and a shooting method is used to shoot from $u = 1-\delta$ to the boundary conditions (5.50) and (5.51) at $u = 0$. We propagate the solution from $u = 0.99$ to $u = 0$ using a MATLAB built in function ODE 45 to solve the higher order differential equations.

Initial conditions on the functions $F_1(u)$ to $F_6(u)$ are required at $u = 1-\delta$. Consider first the initial conditions on $F_1(u)$ to $F_4(u)$. From the asymptotic solution (5.6),

$$F_1(u) = E_2(1-u)^2 + E_3(1-u)^3 + E_4(1-u)^4 + E_5(1-u)^5 + O((1-u)^6), \quad (5.55)$$

as $u \to 1$. Differenting (5.55) with respect to u gives

$$\begin{aligned} F_2(u) = \frac{dF_1}{du} &= -2E_2(1-u) - 3E_3(1-u)^2 - 4E_4(1-u)^3 - 5E_5(1-u)^4 \\ &+ O(1-u)^5, \quad (5.56) \\ F_3(u) = \frac{d^2F_1}{du^2} &= 2E_2 + 6E_3(1-u) + 12E_4(1-u)^2 + 20E_5(1-u)^3 \\ &+ O((1-u)^4), \quad (5.57) \\ F_4(u) = \frac{d^3F_1}{du^3} &= -6E_3 - 24E_4(1-u) - 60E_5(1-u)^2 + O((1-u)^3), \quad (5.58) \end{aligned}$$

as $u \to 1$. Thus

$$F_1(1-\delta) = E_2\delta^2 + O(\delta^3), \tag{5.59}$$

$$F_2(1-\delta) = -2E_2\delta - 3E_3\delta^2 + O(\delta^3), \tag{5.60}$$

$$F_3(1-\delta) = 2E_2 + 6E_3\delta + 12E_4\delta^2 + O(\delta^3), \tag{5.61}$$

$$F_4(1-\delta) = -6E_3 - 24E_4\delta - 60E_5\delta^2 + O(\delta^3), \tag{5.62}$$

as $\delta \to 0$. Also from (5.8) and (5.9) for $G(u)$ and $\frac{dG}{du}$ we obtain

$$\begin{aligned} F_5(1-\delta) &= \frac{1}{2kB_0}\Big[E_2 + 48Ac_1^2E_4 + \Big(-\frac{7}{3}E_2 + 3E_3 + 240Ac_1^2E_5\Big)\delta \\ &+ O(\delta^2)\Big], \end{aligned} \tag{5.63}$$

$$F_6(1-\delta) = \frac{1}{2kB_0}\Big[\frac{7}{3}E_2 - 3E_3 - 240Ac_1^2E_5 + O(\delta)\Big], \tag{5.64}$$

as $\delta \to 0$. We calculate $F_5(1-\delta)$ and $F_6(1-\delta)$ only to the order $\delta$ and order 1 because to go to order $\delta^2$ introduces coefficients $E_6$ and $E_7$.

We see from (5.59) to (5.64) that the initial values of $F_1(u)$ to $F_6(u)$ at $u = 1-\delta$ depend on $E_2$ which is known from (5.5) and $E_3$, $E_4$ and $E_5$ which are unknown. In the shooting method, the values of $E_3$, $E_4$, and $E_5$ are varied until the boundary conditions (5.49) and (5.50) on $F_1(0)$ and $F_6(0)$ are satisfied.

From (5.17) the ratio of the width average fluid velocity to the speed of propagation of the fracture tip is

$$R(u) = \frac{v_x^*(t,x)}{\frac{dL}{dt}} = -\frac{2}{3}c_1kF_1^2(u)F_6(u). \tag{5.65}$$

From (5.18),

$$R(1-\delta) = -\frac{2c_1E_2^2}{3B_0}\Big[\frac{7}{6}E_2 - \frac{3}{2}E_3 - 120A_1c_1^2E_5\Big]\Big[\delta^4 + O(\delta^5)\Big], \tag{5.66}$$

as $\delta \to 0$ and $R(0)$ is given by (5.21).

The fluid flux at the fracture entry (4.189)

$$Q(t) = Q_0\Big(1 + \frac{t}{c_1}\Big)^{\frac{1}{6}} \tag{5.67}$$

is specified. Hence the values of $Q_0$ and $c_1$ can be specified. The characteristic numbers, $A$ and $B$, and the constant k are specified . The bending moment $M_0$ is also specified and from (5.54) and (5.61),

$$E_2 = \frac{1}{2} c_1^{-\frac{2}{3}} M_0. \tag{5.68}$$

The initial value problem for the six first order ordinary differential equations (5.44) to (5.49) is solved subject to the six initial values (5.59) to (5.64) using the MATLAB initial value solver ODE45 for higher order differential equations. The value $c_1$ is chosen. In practise it was found not to be possible to shoot to the two targets

$$c_1^{\frac{2}{3}} F_1(0) = 1, \tag{5.69}$$

$$F_6(0) = -\frac{3}{2} \frac{c_1^{\frac{4}{3}Q_0}}{k}\cdot \tag{5.70}$$

The value of $E_3$, $E_4$ and $E_5$ were adjusted until (5.69) was satisfied. The value obtained for $F_6(0)$ was used to determine the flux $Q_0$:

$$Q_0 = -\frac{2}{3} k c_1^{-\frac{4}{3}} F_6(0). \tag{5.71}$$

The bending moment $M_0$ is chosen and $E_2$ is calculated from (5.68). The shooting was done manually. The parameter $E_3$ was varied with $E_4 = 0$ and $E_5 = 0$. If a value of $E_3$ can be found then this gives the solution to the problem. If (5.69) cannot be satisfied then the value of $E_3$ for which $c_1^{\frac{2}{3}} F(0)$ is closest to unity is chosen. For this value of $E_3$, $E_4$ is varied with $E_5 = 0$, until (5.69) is satisfied. If (5.69) is not satisfied the the value of $E_4$ for which $c_1^{\frac{2}{3}} F(0)$ is closest to the unity is chosen and $E_5$ is varied for these values of $E_3$ and $E_4$. If a value of $E_5$ for which

(5.69) is satisfied cannot be found then it was concluded that the solution does not exist for the chosen values of $c_1$ and $M_0$.

Once the solutions for $F_1(u)$ to $F_5(u)$ are obtained the half- width $h(t,x)$ and the pressure difference $P(t,x)$ are obtained from (5.13) and (5.14),

$$h(t,x) = c_1^{\frac{2}{3}}\left[1+\frac{t}{c_1}\right]^{\frac{2}{3}} F_1(u), \tag{5.72}$$

$$P(t,x) = c_1^{-\frac{4}{3}}\left[1+\frac{t}{c_1}\right]^{-\frac{4}{3}} F_5(u) \tag{5.73}$$

and the velocity ratio is given by (5.66). The length of the fracture is given by

$$L(t) = \left(1+\frac{t}{c_1}\right)^{\frac{1}{2}}. \tag{5.74}$$

## 5.6 Results for the silicic magma fracture

The values chosen for the parameters are the values for the silicic magma fracture. From Table 5.2

$$A = 1.26 \text{ x } 10^{-4}, \qquad B = 2.25 \text{ x } 10^{5}.$$

We choose

$$k = 0.5, \qquad \delta = 0.01.$$

Since it was found to be easier to obtain laminar solutions for larger values of $c_1$ we considered $c_1 = 10^5$. Other cases were investigated but not as thoroughly as $c_1 = 10^5$. They are commented on briefly in Section 5.7.

**Case 1.** $c_1 = 10^5$

The bending moment $M_0$ was increased in powers of 10 from $M_0 = 1$ to $M_0 = 5$ x $10^7$. At values of $M_0$ as large as 5 x $10^7$ the beams themselves may crack and the model would cease to be valid. These large values are included to obtain a

| M_0 | E_2 | E_3 | c_1*(2/3)F_1(0) | E_4 | c_1*(2/3)F_1(0) | E_5 | c_1*(2/3)F_1(0) | P(0) | Q_0 | F_max | F_2(0) |
|---|---|---|---|---|---|---|---|---|---|---|---|
| 1 | 0.0002320079 | 87 | 375679.4522 | -174.3826671 | 1.000539233 | 0 | 1.000539233 | -0.00022412 | 0.2114 | 18940 | 83.46548825 |
| 10 | 0.0023207944 | 26.4 | 6463.866789 | -53.9298833 | 1.000851711 | 0 | 1.000851711 | -0.00677888 | 0.064527 | 5744 | 25.26858856 |
| 100 | 0.0232079444 | 4.6 | 26672.36289 | -12.4803391 | 1.000025077 | 0 | 1.000025077 | -0.0011125 | 0.010621 | 957.3 | 4.199539256 |
| 2*100 | 0.0464158888 | 1.1 | 1.000334971 | -5.8707985 | 1.000334971 | 0 | 1.000334971 | -215.0322213 | 0.002326898 | 206.1 | 0.88864659 |
| 2.1*100 | 0.0487368683 | 0.92 | 11584.3796 | -5.4807685 | 1.000050222 | 0 | 1.000050222 | -169.1254806 | 0.001910562 | 168.2 | 0.71772136 |
| 2.2*100 | 0.051057477 | 0.74 | 10807.64898 | -5.12012 | 1.000268747 | 0 | 1.000268747 | -122.574763 | 0.001486278 | 129.8 | 0.547765336 |
| 2.4*100 | 0.0556639066 | 0.45 | 9411.017777 | -4.468787 | 1.000801538 | 0 | 1.000801538 | -48.44667386 | 0.000820052 | 69.48 | 0.279876627 |
| 2.5*100 | 0.058001986 | 0.293 | 8780.626276 | -4.1793383 | 1.000151532 | 0 | 1.000151532 | -5.26538381 | 0.000447581 | 35.77 | 0.12919612 |
| 2.6*100 | 0.0603406555 | 0.171 | 8190.908167 | -3.9065506 | 1.000156314 | 0 | 1.000156314 | 48.32622892 | 0.000166543 | 12.26 | 0.01532178 |
| 2.61*100 | 0.0605727344 | 0.16 | 8131.193272 | -3.8802325 | 1.000071422 | 0 | 1.000071422 | 76.14471933 | 0.000141472 | 10.68 | 0.00434817 |
| 2.6105*100 | 0.0605843388 | 0.16 | 1.000070792 | -3.8788186 | 1.000070792 | 0 | 1.000070792 | 75.50530411 | 0.00014182 | 10.7 | 0.00508816 |
| 2.615*100 | 0.0606888774 | 0.15 | 8105.70466 | -3.8680726 | 1.000088668 | 0 | 1.000088668 | 293.5726269 | 0.000115275 | 9.233 | -0.0067373 |
| 2.617*100 | 0.060731519 | 0.15 | 8094.40394 | -3.8624185 | 1.000075151 | 0 | 1.000075151 | 253.0219517 | 0.000116774 | 9.313 | -0.0059764 |
| 2.6175*100 | 0.0607467394 | 0.15 | 8091.590249 | -3.8610074 | 1.000093043 | 0 | 1.000093043 | 244.5986242 | 0.000117133 | 9.333 | -0.0057946 |
| 2.618*100 | 0.0607583398 | 0.147 | 8088.763493 | -3.8603 | 1.058489831 | 0 | 1.058489831 | 1606.086812 | 9.08526E-05 | 8.893 | -0.0149237 |
| | | | | | | | | | | | |
| 1.05*10^3 | 0.24368344 | -0.48453 | 1.008172342 | 0 | 1.008172342 | 0 | 1.008172342 | 7565.845113 | 0.000364557 | 30.9 | -0.0237939 |
| 1.1*10^3 | 0.2552873 | -0.4739815 | 1.000085244 | 0 | 1.000085244 | 0 | 1.000085244 | 133.1618555 | 0.000482349 | 37.29 | 0.01775171 |
| 1.4*10^3 | 0.3249112 | -0.4584338 | 1.000086183 | 0 | 1.000086183 | 0 | 1.000086183 | 57.12584684 | 0.001004714 | 74.36 | 0.17927327 |
| 1.5*10^3 | 0.348119163 | -0.46417896 | 1.000065128 | 0 | 1.000065128 | 0 | 1.000065128 | 50.7103091 | 0.001149232 | 85.41 | 0.22129543 |
| 2*10^3 | 0.46415888 | -0.4641588 | 1.000088656 | 0 | 1.000088656 | 0 | 1.000088656 | 33.61174299 | 0.00177396 | 133.6 | 0.39251975 |
| 3*10^3 | 0.6962383 | -0.7247263 | 1.000082545 | 0 | 1.000082545 | 0 | 1.000082545 | 22.2897083 | 0.002844556 | 215.9 | 0.66363951 |
| 4*10^3 | 0.9283177 | -0.9441316 | 1.00002145 | 0 | 1.00002145 | 0 | 1.00002145 | 18.43908319 | 0.003852086 | 292.6 | 0.90941391 |
| 5*10^3 | 1.160397 | -1.1703497 | 1.000070552 | 0 | 1.000070552 | 0 | 1.000070552 | 16.67405554 | 0.004840783 | 368.2 | 1.14780116 |
| 6*10^3 | 1.392476 | -1.3992463 | 1.000058617 | 0 | 1.000058617 | 0 | 1.000058617 | 15.71646794 | 0.005821094 | 443 | 1.38330629 |
| 7*10^3 | 1.624556 | -1.6294069 | 1.000193238 | 0 | 1.000193238 | 0 | 1.000193238 | 15.13833676 | 0.006796109 | 517.6 | 1.61745107 |
| 8*10^3 | 1.856636 | -1.860241 | 1.000519263 | 0 | 1.000519263 | 0 | 1.000519263 | 14.75792212 | 0.007764546 | 591.8 | 1.85068708 |
| 9*10^3 | 2.088714 | -2.091467 | 1.000218631 | 0 | 1.000218631 | 0 | 1.000218631 | 14.5114113 | 0.008746378 | 665.9 | 2.08387005 |
| 10^4 | 2.320794 | -2.322936 | 1.000136172 | 0 | 1.000136172 | 0 | 1.000136172 | 14.33212944 | 0.009723387 | 740 | 2.31660742 |
| 10^5 | 23.32079 | -23.20754 | 1.000065821 | 0 | 1.000065821 | 0 | 1.000065821 | 13.55880059 | 0.097297039 | 7402 | 23.20659 |
| 10^6 | 232.0794 | -232.079 | 1.000342721 | 0 | 1.000342721 | 0 | 1.000342721 | 13.24212544 | 0.950565477 | 74060 | 232.0787 |
| 10^7 | 2320.794 | -2320.796 | 1.000913741 | 0 | 1.000913741 | 0 | 1.000913741 | 12.06368 | 8.648653137 | 740700 | 2320.79395 |
| 1.5*10^7 | 3481.191 | -3481.194 | 1.000028242 | 0 | 1.000028242 | 0 | 1.000028242 | 7.012396399 | 7.538080162 | 1110000 | 3481.20062 |
| 2*10^7 | 4641.589 | -4641.593 | 1.000006539 | 0 | 1.000006539 | 0 | 1.000006539 | 4.052701011 | 5.793100036 | 1481000 | 4641.60129 |
| 2.1*10^7 | 4873.668 | -4873.672 | 1.000066916 | 0 | 1.000066916 | 0 | 1.000066916 | 2.478843514 | 3.707544482 | 1555000 | 4873.68143 |
| 2.2*10^7 | 5105.747 | -5105.752 | 1.000041143 | 0 | 1.000041143 | 0 | 1.000041143 | 0.556277054 | 0.845288465 | 1628000 | 5105.76156 |
| 2.22*10^7 | 5152.163 | -5152.168 | 1.000066152 | 0 | 1.000066152 | 0 | 1.000066152 | 0.122743985 | 0.16151409 | 1643000 | 5152.17753 |
| 2.225*10^7 | 5163.781 | -5163.772 | 1.00000724 | 0 | 1.00000724 | 0 | 1.00000724 | 0.013635357 | -0.012529718 | 1647000 | 5163.7816 |
| 2.23*10^7 | 5175.376 | -5175.376 | 1.000078654 | 0 | 1.000078654 | 0 | 1.000078654 | -0.096558495 | -0.189093008 | 1650000 | 5175.3856 |
| 2.25*10^7 | 5221.787 | -5221.792 | 1.000017482 | 0 | 1.000017482 | 0 | 1.000017482 | -0.55643179 | -0.934176513 | 1665000 | 5221.80163 |
| 2.3*10^7 | 5337.827 | -5337.832 | 1.000080007 | 0 | 1.000080007 | 0 | 1.000080007 | -1.7831329 | -2.981639157 | 1703000 | 5337.8417 |
| 2.5*10^7 | 5801.986 | -5801.991 | 1.000093146 | 0 | 1.000093146 | 0 | 1.000093146 | -6.253264948 | -11.26917887 | 1852000 | 5802.00197 |
| 3*10^7 | 6962.383 | -6962.389 | 1.000072265 | 0 | 1.000072265 | 0 | 1.000072265 | -17.16928494 | -37.04390746 | 2222000 | 6962.40264 |
| 5*10^7 | 11603.97 | -11603.98 | 1.000097139 | 0 | 1.000097139 | 0 | 1.000097139 | -104.0467405 | -373.7411855 | 3704000 | 11604.0053 |

Table 5.3: The values of the parameters in the numerical solution for $c_1 = 10^5$

complete picture of the effect of $M_0$ on the solution. The results are shown in Table 5.3 When $M_0$ and $c_1$ are specified, $E_2$ is given by (5.68)

**Case 1.1** $\quad 1 \leqslant M_0 \lesssim 2.618 \text{ x } 10^2$

For $1 \leqslant M_0 \lesssim 2.618$ x $10^2$ both $E_3$ and $E_4$ had to be varied in the shooting method to obtain a numerical solution. The parameter $E_3$ was always positive and decreased from $E_3 = 87$ for $M_0 = 1$ to $E_3 = 0.147$ for $M_0 = 2.618$ x $10^2$. For a given value of $M_0$ in this range, we first take $E_3 = 0$, $E_4 = 0$ and $E_5 = 0$. The value of $c_1^{\frac{2}{3}} F_1(0)$ was calculated and found to be large and positive, of order of magnitude $10^3$. Keeping $E_4 = 0$ and $E_5 = 0$, $E_3$ was varied. It was found that as $E_3$ increased through positive values, $c_1^{\frac{2}{3}} F_1(0)$ decreased, reached a minimum value greater that one and started increasing again. This is illustrated in Figure 5.1 for $M_0 = 10^2$. The value of $E_3$ which makes $c_1^{\frac{2}{3}} F_1(0)$ a minimum is chosen and $E_3$ is fixed at this value. The parameter $E_4$ is then varied with $E_5 = 0$. It was found that as $E_4$ decreased through negative values, $c_1^{\frac{2}{3}} F_1(0)$ decrease to 1 and continued through 1. This is illustrated in Figure 5.2. The value of $E_4$ for which

$$c_1^{\frac{2}{3}} F_1(0) = 1 \tag{5.75}$$

is chosen. The parameter $E_5$ was not required and we took $E_5 = 0$. This was the solution of the numerical problem. As $M_0$ increased from $M_0 = 1$ to $M_0 = 2.618$ x $10^2$. $E_4$ increased from -174 to -3.86.

For $1 \leqslant M_0 \lesssim 2.618$ x $10^2$, the flux $Q_0$ decreased from 2.11 x $10^{-1}$ to 9.08 x $10^{-4}$ which is in the range for laminar flow in the fracture. The pressure difference at the fracture entry, $P(0)$,is negative for small $1 \lesssim M_0 \lesssim 2.5$ x $10^2$ but it becomes positive for $2.6\text{x}10^2 \lesssim M_0 \lesssim 2.618$ x $10^2$.

In Figures 5.3 to 5.7, we consider $M_0 = 2.2\text{x}10^2$ for which $P(0) < 0$. In Figure 5.3

$$h(o,u) = c_1^{\frac{2}{3}} F_1(u) \tag{5.76}$$

is plotted against $u$ for $0 \leq u \leq 1$ and in Figure 5.4 $h(t,u)$ is plotted against $u$ for a range of values of time. We see that the beams "buckle" in the fundamental mode as fluid is injected between the two beams. The length of the beams increases at a finite speed $\frac{dL}{dt}$ which is not sufficiently great to prevent the buckling which we see from Figure 5.4 grows steadily with time.

In Figure 5.5 the pressure difference

$$P(0,u) = c_1^{-\frac{4}{3}} G(u) \tag{5.77}$$

is plotted against $u$ for $0 \le u \le 1$ while in Figure 5.6, $P(t,u)$ is plotted against $u$ for a range of time. As fluid is injected into the fracture the magnitude of the pressure difference decrease with time, as the injected fluid provides support for the beam, and tends to zero as time tends to infinity. These results are consistent with (5.14)

In Figure 5.7 the ratio, $R(u)$, of the width average fluid velocity $v_x^*(t,x)$, to the speed of propagation of the fracture , $\frac{dL}{dt}$, is plotted against $u$ for $0 \le u \le 1$. Since $c_1 = 10^5$ and $Q_0 = 1.48628$ from Table 5.3, theory gives by (5.21)

$$R(0) = c_1 Q_0 = 1.48628 \text{ x } 10^2. \tag{5.78}$$

This compares very well with the computed value

$$R(0) = 1.48707 \text{ x } 10^2. \tag{5.79}$$

The theoretical limit $R(1) = 0$ given in (5.19) agrees with the computed value in Figure 5.7. The width average fluid velocity decreases very rapidly near the entrance to the fracture and is small over most of the fracture length. Conservation of the flux of the incompressible fluid requires the beams to buckle in the fracture.

In Figure 5.8, the fracture length $L(t)$ given by

$$L(t) = \left(1 + \frac{t}{c_1}\right)^{\frac{1}{2}} \tag{5.80}$$

is plotted against $t$ for $c_1 = 10^5$. The length grows steadily with time from the initial value $L(0) = 1$ of the pre-existing fracture. The length depends only on $c_1$ and is independent of the flux at the fracture entry and the bending moment $M_0$. This may help to explain why the beams "buckle". The injected fluid requires an increase in the volume of the fracture and if the length is not growing sufficiently rapidly the only way an increase in volume can occur if the beams "buckle".

In Figure 5.9 to 5.13 we consider $M_0 = 2.6105$ for which $P(0) > 0$. In Figure 5.9, $h(0,u)$ is plotted against $u$ and in Figure 5.10 $h(t,u)$ is plotted against u for

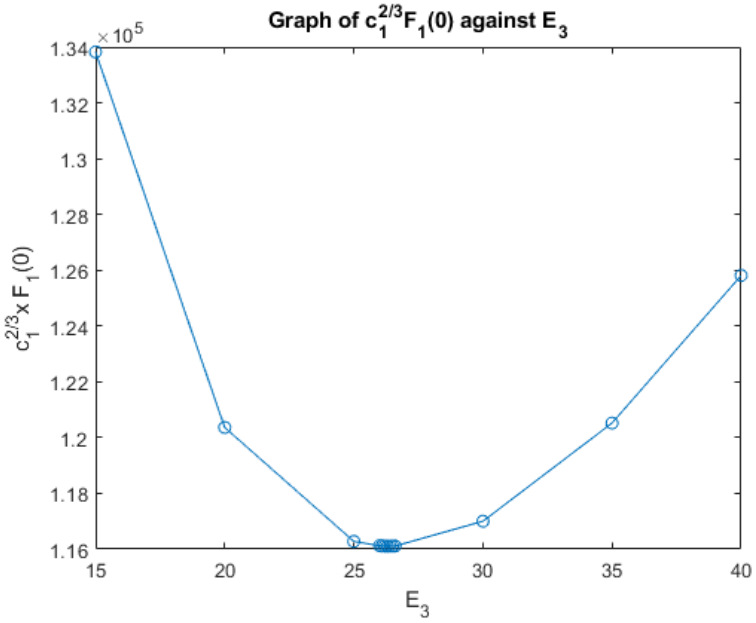



Figure 5.1: Graph of $c_1^{\frac{2}{3}} F(0)$ plotted against $E_3$ for $M_0 = 10^2$ and $c_1 = 10^5$.

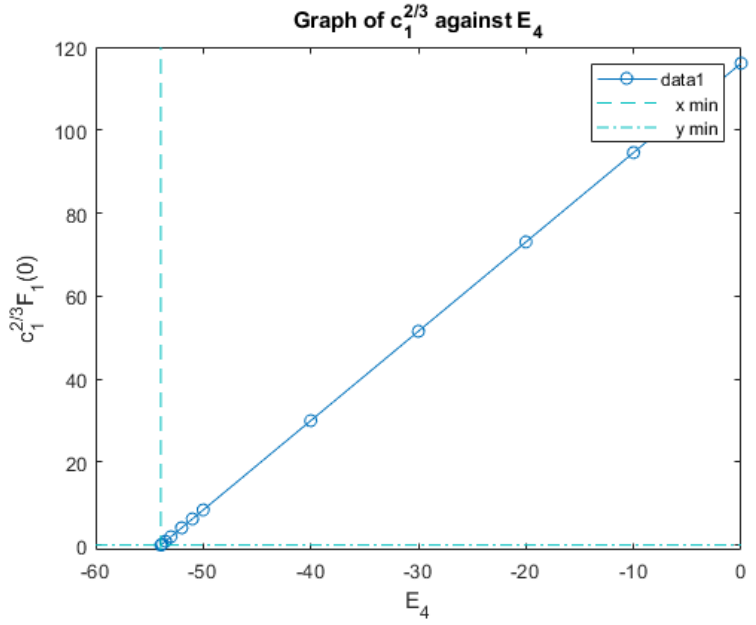



Figure 5.2: Graph of $c_1^{\frac{2}{3}} F(0)$ x $10^3$ plotted against $E_4$ for $M_0 = 10^2$ and $c_1 = 10^5$.

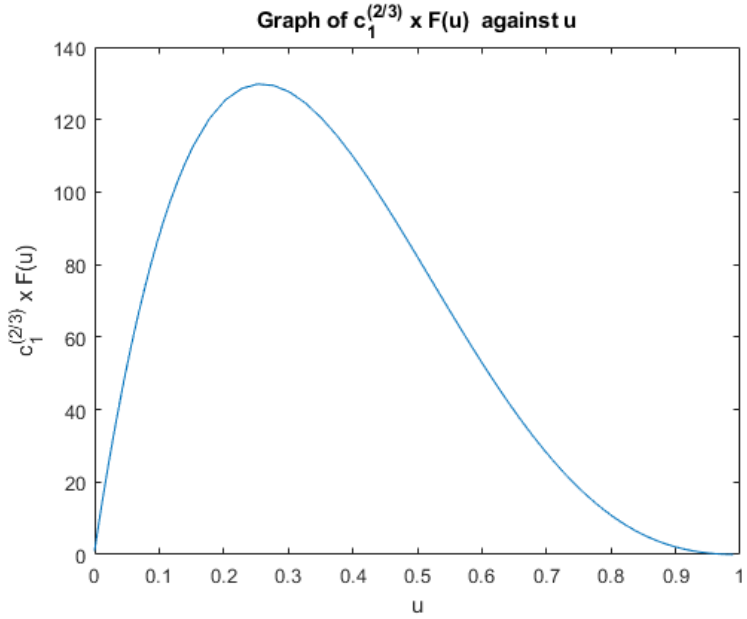



Figure 5.3: Graph of $c_1^{\frac{2}{3}} F(u)$ plotted against $u$ for $M_0 = 2.2$ x $10^2$ for a silicic magma fracture.

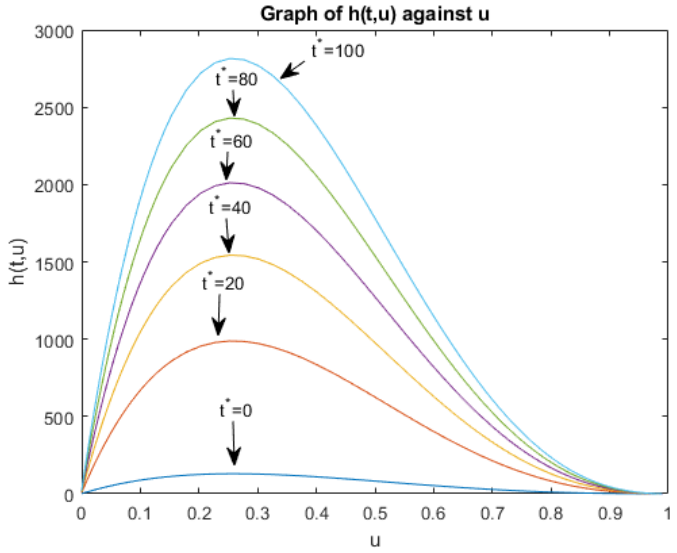



Figure 5.4: Graph of half-width $h(t,u)$ plotted against $u$ for $M_0 = 2.2$ x $10^2$ for a silicic magma fracture at times $t^* = \frac{t}{c_1} = 0.\ 20, 40, 60, 80.\ 100$

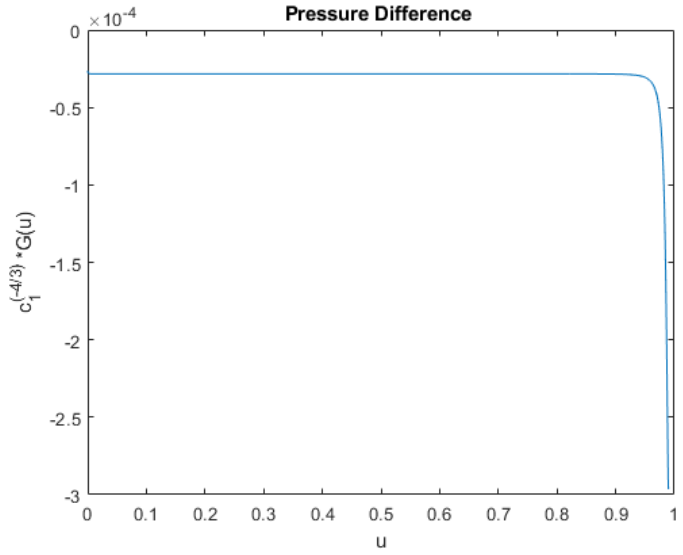



Figure 5.5: Graph of $c_1^{-\frac{4}{3}} G(u)$ plotted against $u$ for $M_0$ = 2.2 x $10^2$ for a silicic magma fracture

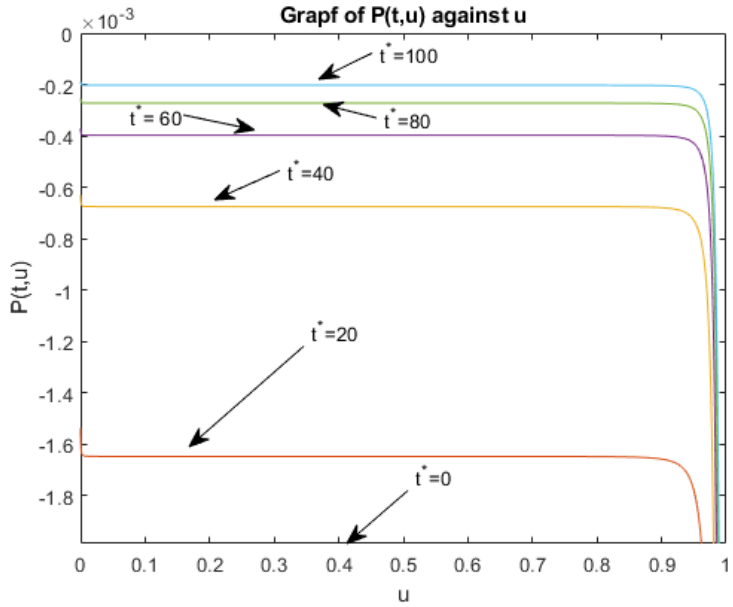



Figure 5.6: Graph of pressure difference $P(t,u)$ plotted against $u$ for $M_0$ = 2.2 x $10^2$ and $t^* = \frac{t}{c_1}$ = 0, 20, 40, 60, 80. 100 for a silicic magma fracture.

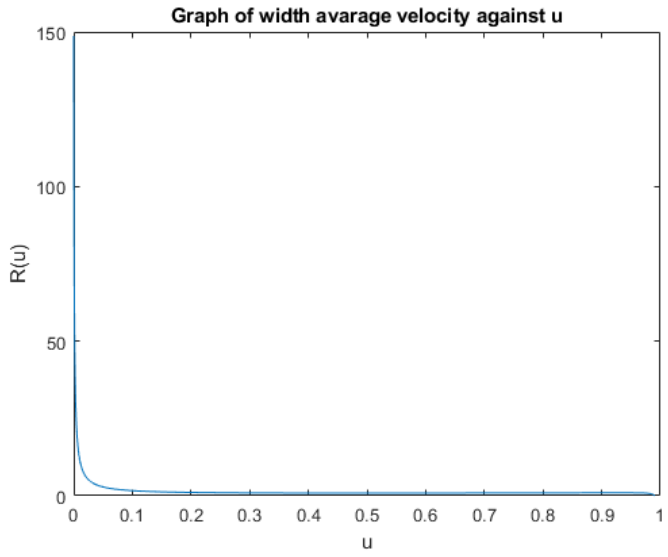



Figure 5.7: Graph of ratio of width average fluid velocity to the speed of propagation of the fracture $\frac{dL}{dt}$ plotted against $u$ for a silicic magma fracture. At the end points, $R(0) = 1.487 \text{ x } 10^2$ and $R(1) = 0$.

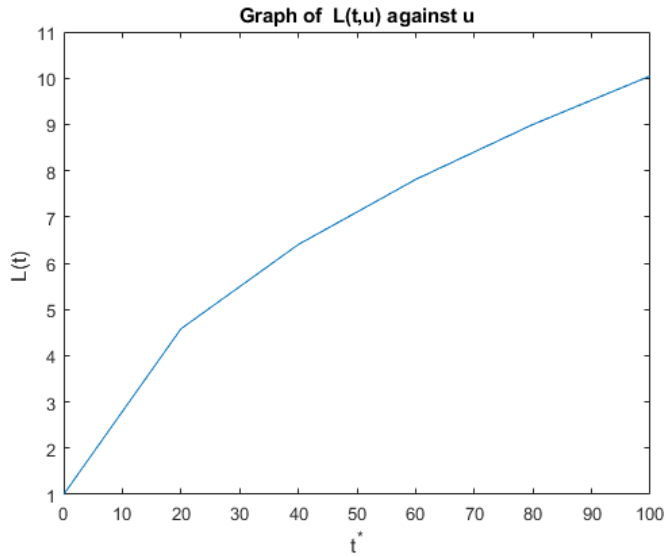



Figure 5.8: The length $L(t)$ of the fracture plotted against time $t^* = \frac{t}{c_1}$ for $c_1 = 10^5$. The length is independent of $M_0$ and $L(0) = 1$.

the range of values of time. The general shape of the beam is similar to that in Figures 5.3 and 5.4 but the position of the maximum displacement of the buckled beam has moved further from the entrance, from approximately 0.25 in Figure 5.4 to 0.45 in Figure 5.10. A pre-existing fracture with a half-width of $1cm$ at the entry at $\frac{t}{c} = 0$ will have a maximum half-with of $10cm$ at $\frac{t}{c} = 0$ which will grow to about $2.2m$ by dimensionless time $\frac{t}{c} = 100$ .

In Figure 5.11 the pressure difference $P(0,u)$ is plotted against $u$ while in Figure 5.12 $P(t,u)$ is plotted against $u$ for a range of values of time. We see that the pressure difference decrease rapidly at the fracture entry and is then approximately uniform over most of the length of the fracture. It again decrease rapidly at the fracture tip and becomes negative.

In Figure 5.13 the ration of the width average fluid velocity to the speed of propagation of the fracture is plotted against $u$. The decrease in $R(u)$ at the fracture entry is not as sharp as in Figure 5.7 but there still is a significant length of the fracture over which the width average fluid velocity is u uniform, before decreasing rapidly to zero at the fracture tip. From Table 5.3 $Q_0 = 1.4182$ x$10^{-4}$ and since $c_1 = 10^5$,

$$R(0) = c_1 Q_0 = 14.182 \tag{5.81}$$

This is in good agreement with the computed value in Figure 5.13,

$$R(0) = 14.18402. \tag{5.82}$$

At $u = 1$, the graph tends rapidly to $R(1) = 0$ in agreement with the theoretical limit (5.19),

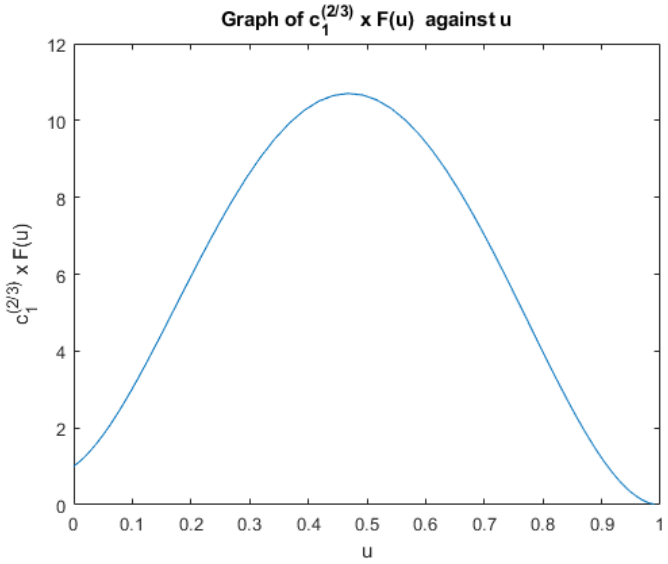



Figure 5.9: Graph of $c_1^{\frac{2}{3}} F(u)$ plotted against $u$ for $M_0 = 2.6105$ x $10^2$ for a silicic magma fracture.

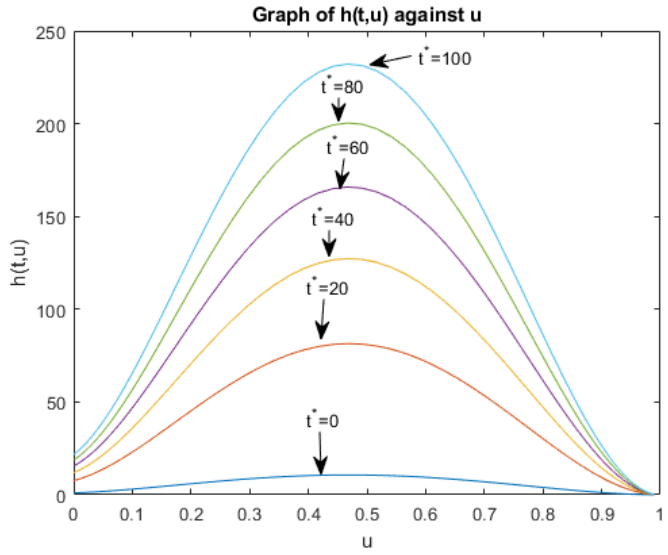



Figure 5.10: Graph of half-width $h(t,u)$ plotted against $u$ for $M_0 = 2.6105$ x $10^2$ for a silicic magma fracture at times and $t^* = \frac{t}{c} = 0$, 20, 40, 60, 80 and 100

.

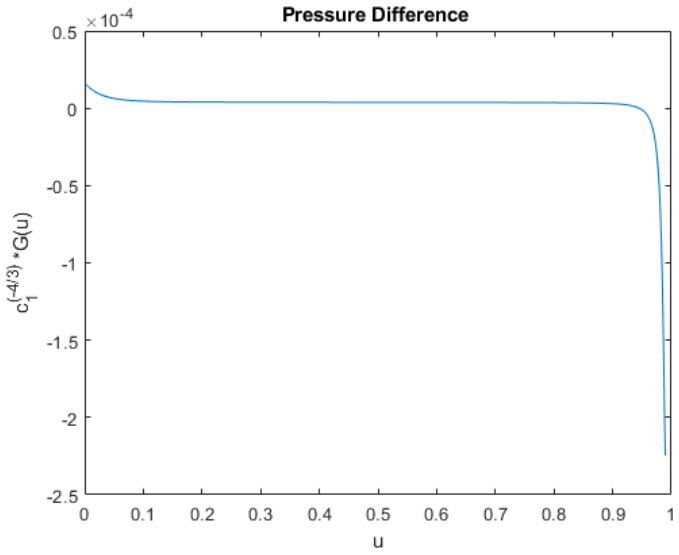



Figure 5.11: Graph of $c_1^{-\frac{4}{3}}G(u)$ plotted against $u$ for $M_0$ = 2.26105 x $10^2$ for a silicic magma fracture

.

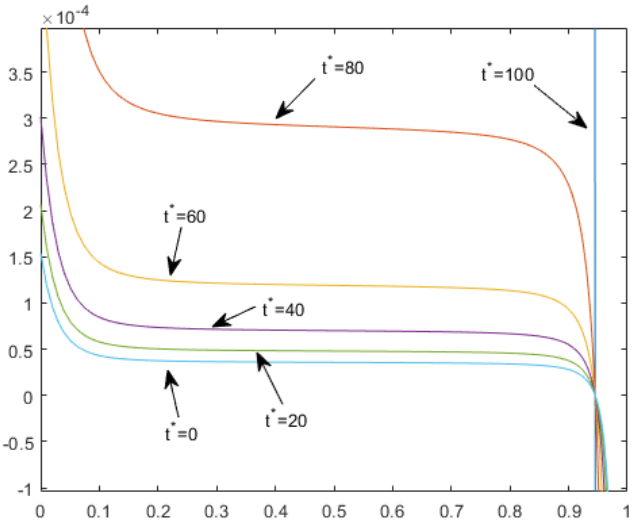



Figure 5.12: Graph of pressure difference $P(t,u)$ plotted against $u$ for $M_0$ = 2.6105 x $10^2$ and $t^* = \frac{t}{c}$ = 0, 20, 40, 60, 80 and 100 for a silicic magma fracture.

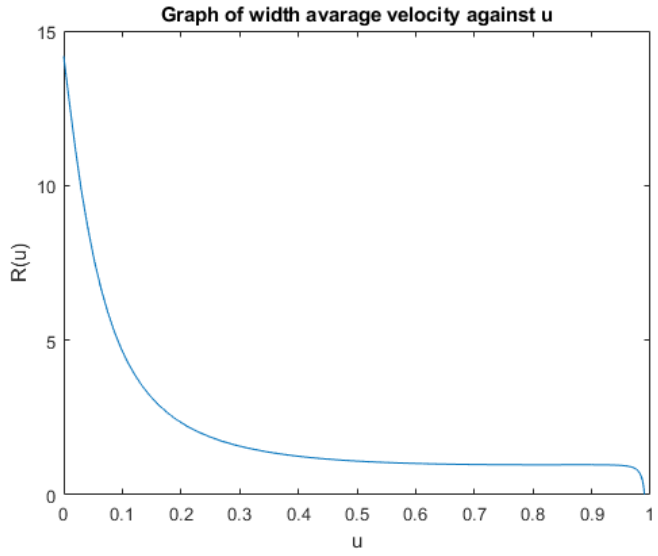



Figure 5.13: Graph of ratio of width average fluid velocity to the speed of propagation of the fracture $\frac{dL}{dt}$ plotted against $u$ for $M_0 = 2.6105 \text{ x } 10^2$ for a silicic magma fracture. At the end points, $R(0) = 14.184028$ and $R(1) = 0$.

**Case 1.2** $2.618 \text{ x } 10^2 \lesssim M_0 \lesssim 1.05 \text{ x } 10^3$

For this range of $M_0$ the numerical solution using the shooting method does not exist. By varying $E_3$, $E_4$ and $E_5$ it was not possible to reach $c_1^{\frac{2}{3}} F_1(0) = 1$. For example when $M_0 = 2.8 \text{ x } 10^2$, by varying $E_3$ with $E_4 = E_5 = 0$, a minimum value 314.20817 for $c_1^{\frac{2}{3}} F_1(0)$ was found at $E_3 = -0.05$. Fixing $E_3$ at this value it was found that $c_1^{\frac{2}{3}} F_1(0)$ increased for both less than and greater than $E_4 = -3.28$ This is illustrated in Figures 5.14 and 5.15.

In order to investigate why the shooting method does not give a numerical solution the limiting cases $M_0 = 2.618 \text{ x } 10^2$ and $M_0 = 1.05 \text{ x } 10^3$ were considered. The solution $M_0 = 2.618 \text{ x } 10^2$ is presented in Figure 5.16 to 5.19. In Figure 5.16 and 5.17, in which the half-width is plotted against u, we see that the half-width has a minimum value near the entry and that the upper and lower beams almost touch leaving little space for the fluid to flow. The beam may have buckled in the next higher mode. The reason the numerical method does not work in the range $2.618 \text{ x } 10^2 \lesssim M_0 \lesssim 1.05 \text{ x } 10^3$ may be because the upper and lower beams touch in this range preventing shooting in the numerical solution from $u = 1 - \delta$ to $u = 0$. From Figure 5.18 we see that there is a large pressure gradient

in the fluid forcing it through the narrow space between the two beams. From 5.19 we see that there is a sharp increase in the width average fluid velocity as the fluid is forced through the narrow space. The solution for $M_0 = 1.05\text{x } 10^3$, which is the value of $M_0$ for which the solution again exist is shown in Figures 5.20 to 5.23. These four Figures have the same features as Figures 5.16 to 5.19 for $M_0 = 2.618 \text{ x } 10^2$ but the magnitudes of the Quantities are an order of magnitude greater. The upper and lower beams almost touch near the fracture entry.

To illustrate the results when $2.618 \text{ x } 10^2 < M_0 < 1.05 \text{ x } 10^3$ the results obtained for $M_0 = 2.8 \text{ x } 10^2$ are shown in Figure 5.24 to 5.27. The shooting method cannot reach $c_1^{\frac{2}{3}} F_1(0) = 1$ which is clear from Figure 5.24 and 5.25 for the half-width. In Figure 5.27 for the width average fluid velocity the analytical results $R(0) = c_1 Q_0$ is not satisfied, even approximately. The numerical solution gives $R(0) = 0.33979$ while.

$Q_0 = 3.4417 \text{ x } 10^{-11}, \quad c_1 = 10^5, \quad Q_0 = 3.4417 \text{ x } 10^{-11}, \quad c_1 Q_0 = 3.44174 \text{ x } 10^{-6}$

**Case 1.3** $\quad 1.05 \text{ x } 10^3 \lesssim M_0 \lesssim 2.22 \text{ x } 10^7$

For $M_0 \gtrsim 1.05 \text{ x } 10^3$ the shooting method requires only $E_3$ to be varied, with $E_4 = E_5 = 0$. This is illustrated in Figure 5.28 in which $c_1^{\frac{2}{3}} F_1(0)$ is plotted against $E_3$ for $M_0 = 6 \text{ x } 10^3$. Unlike the range $1 \leq M_0 \lesssim 2.618 \text{ x } 10^2$, we see from Table 5.3 that $E_3 < 0$. We also see from Table 5.3 that for $M_0 \gtrsim 1.05 \text{ x } 10^3$, a good starting value for $E_3$ in the shooting method is $E_3 = -E_2$ and that this estimate is very good for $M_0 \gtrsim 2 \text{ x } 10^3$.

The solution for this range of $M_0$ is illustrated in Figures 5.29 to 5.32 for $M_0 = 6$ x $10^3$. The solution is similar to the solution in the range $2.6 \text{ x } 10^2 \lesssim M_0 \lesssim 2.618$ x $10^2$ described by Figure 5.9 to 5.13 but the magnitude of the quantities is greater.

For $M_0 \backsimeq 2.22 \text{ x } 10^7$ we see from Table 5.3 that $P(0) = 0.12274$, $Q_0 = 0.16151$ and that for $M_0 = 2.225 \text{ x } 10^7$, $Q_0$ is negative and that for $M_0 = 2.23 \text{ x } 10^7$, $P(0)$ is also negative. The value $M_0 = 2.22 \text{ x } 10^7$ therefore represents the limit for fluid inflow at the fracture entry.

**Case 1.4** $\quad M_0 \gtrsim 2.225 \text{ x } 10^7$

The magnitude of the bending moment $M_0$ is large which may lead to the fracturing of the beam. We include this case to cover all the types of solutions that

could occur.

Since the fluid flux $Q_0$ is negative there is fluid extraction at the fracture entry. The magnitude of $Q_0$ increases as $M_0$ increase. The fluid extraction therefore increases as $M_0$ increases. The pressure difference at the fracture entry is negative which contributes to the outflow of the fluid.

The solution for $M_0 = 2.5 \text{ x } 10^7$ is presented in Figures 5.33 to 5.37. The magnitude of the quantities are large with half-width order $10^6$ and may not be physical. The width average fluid velocity plotted in Figure 5.37 is negative, consistent with outflow of fluid. At the fracture entry the numerical solution gives $R(0) = -1.265 \text{ x } 10^6$ and the asymptotic results $c_1 Q_0 = -1.269 \text{ x } 10^6$ is also negative since $Q_0$ is negative and in good agreement with numerical results.

In Figure 5.34 the half-width grows steadily with time consistent with (5.72),

$$h(t,u) = c_1^{\frac{2}{3}} \Big[ 1 + \frac{t}{c_1} \Big]^{\frac{2}{3}} F_1(u). \tag{5.83}$$

When there is outflow at the entry we would have expected the half- width to decrease with time. An explanation may be that the fluid has become detached from the beams and occupies only part of the space between the beams or that it remains attached and the boundary condition (3.31) remains valid but cavities form in the fluid along the axis. This may be due to the large bending moment $M_0 = 2.5 \text{ x } 10^7$. From (4.175) and (4.182) the fluid flux at the entry is given by

$$Q(t) = Q_0 \Big( 1 + \frac{t}{c_1} \Big)^{\frac{1}{6}}, \tag{5.84}$$

where

$$Q_0 = -\frac{2}{3} k c_1^{-\frac{4}{3}} \frac{dG}{du}(0) \cdot \tag{5.85}$$

For fluid inflow $Q_0 > 0$ and $\frac{dG}{du}(0) < 0$ while for fluid outflow $Q_0 < 0$ and $\frac{dG}{du}(0) > 0$. From Table 5.5 we see that there is a change in sign of $\frac{dG}{du}(0)$ as $M_0$ increases and $Q_0$ changes from positive to negative. From (5.73)

$$\frac{dP}{du}(t,0) = c_1^{-\frac{4}{3}} \Big( 1 + \frac{t}{c_1} \Big)^{-\frac{4}{3}} \frac{dG}{du}(0) \tag{5.86}$$

and for fluid inflow the pressure gradient is negative at the entry and for fluid outflow it is positive at the entry as expected.

From Table 5.2 for silicic lava the maximum value of $Q_0$ for laminar flow is $Q_0 \lesssim 37$. We see from Table 5.3 that the flow will be laminar for $M_0 \lesssim 3.1 \text{ x } 10^7$.

| $M_0$ | $F_6(0) = \frac{dG}{du}(0)$ | $Q_0$ |
|---|---|---|
| $1.5 \text{ x } 10^7$ | $-1.05 \text{ x } 10^8$ | $+7.54$ |
| $2.1 \text{ x } 10^7$ | $-4.33 \text{ x } 10^4$ | $+3.71$ |
| $2.25 \text{ x } 10^7$ | $+1.74 \text{ x } 10^5$ | $-0.93$ |
| $t.5 \text{ x } 10^7$ | $+1.57 \text{ x } 10^8$ | $-11.27$ |

Table 5.4: Numerical values for $\frac{dG}{du}(0)$ and $Q_0$ for a range of values of bending moment $M_0$.

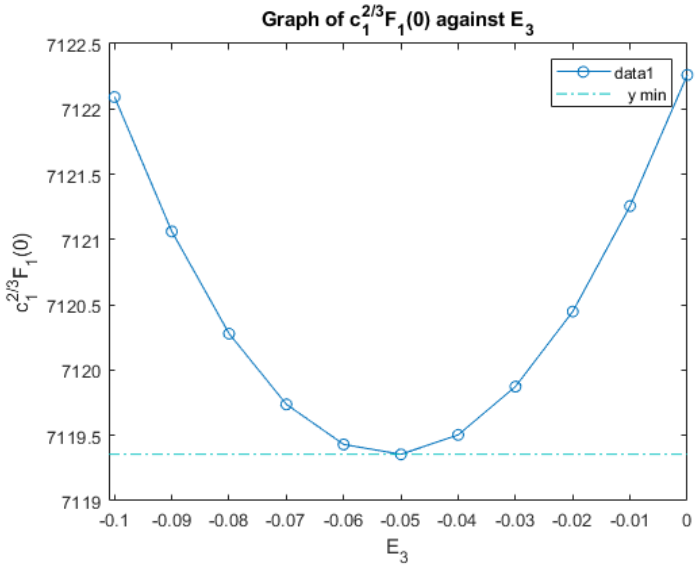



Figure 5.14: Graph of $c_1^{\frac{2}{3}}F_1(0)$ plotted against $E_3$ for $M_0 = 2.8 \text{ x } 10^2$ and $c_1 = 10^5$

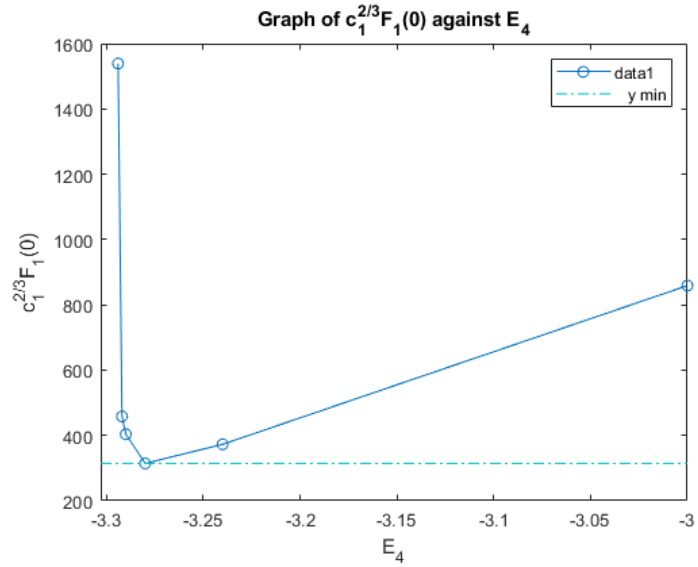



Figure 5.15: Graph of $c_1^{\frac{2}{3}}F_1(0) \text{ x } 10^{-3}$ plotted against $E_4$ for $M_0 = 2.8 \text{ x } 10^2$ and $c_1 = 10^5$

.

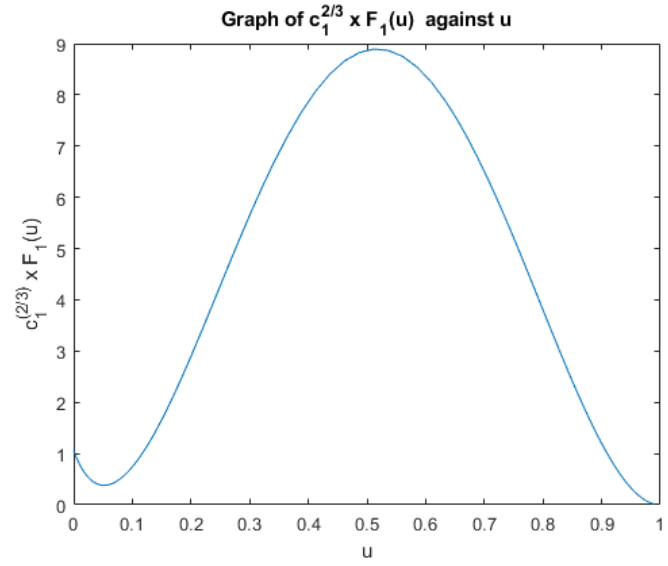



Figure 5.16: Graph of $h(0,u) = c_1^{\frac{2}{3}} F_1(u)$ plotted against $u$ for $M_0 = 2.618$ x $10^2$ for silicic magma fracture.

.

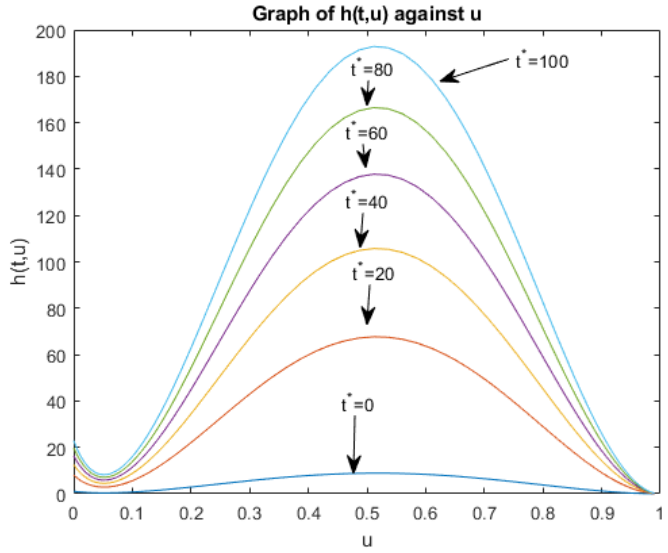



Figure 5.17: Graph of half-width $h(t,u)$ plotted against $u$ for $M_0 = 2.618$ x $10^2$ for a silicic magma fracture at a range of times from $t^* = \frac{t}{c_1} = 0$ to $t^* = \frac{t}{c_1} = 100$.

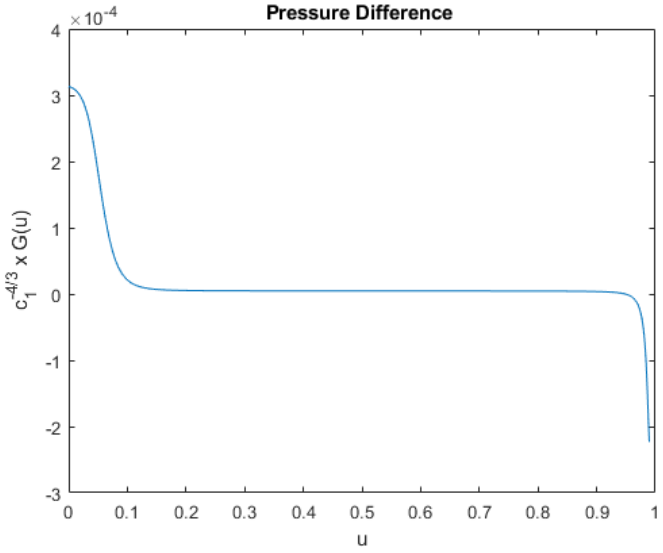



Figure 5.18: Graph of pressure difference $P(0,u) = c_1^{-\frac{4}{3}} G_1(u)$ plotted against $u$ for $M_0 = 2.618$ x $10^2$ for a silicic magma fracture.

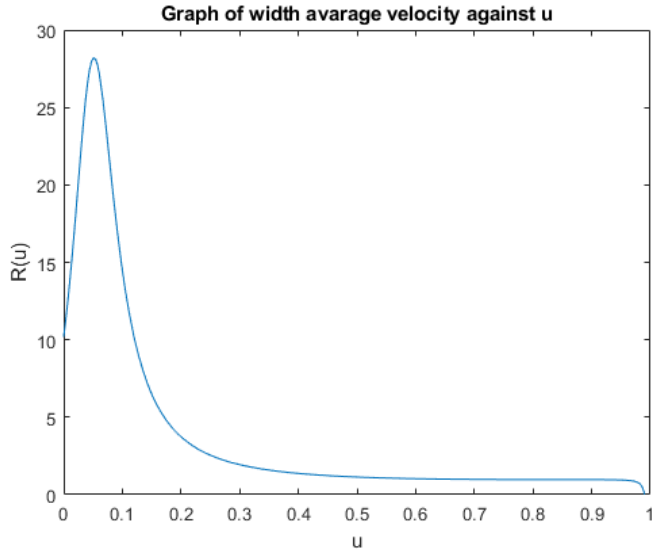



Figure 5.19: Graph of the ratio R(u) of the width average fluid velocity to the speed of propagation of the fracture $\frac{dL}{dt}$ plotted against $u$ for $M_0 = 2.618$ x $10^2$ for silicic magma fracture. At the entry $R(0) = 10.1851$ while the asymptotic results with $Q_0 = 9.0945$ x $10^{-5}$ gives $R(0) = c_1 Q_0 = 9.0945$.

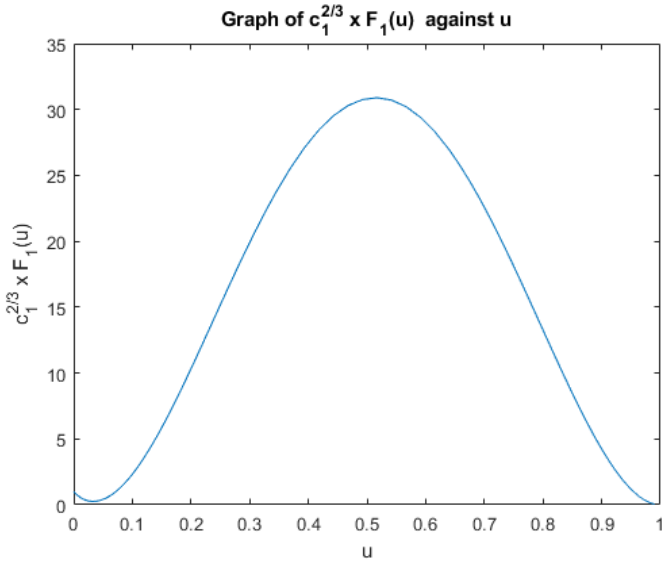



Figure 5.20: Graph of $h(0,u) = c_1^{\frac{2}{3}} F_1(u)$ plotted against $u$ for $M_0 = 1.05$ x $10^3$ for a silicic magma fracture.

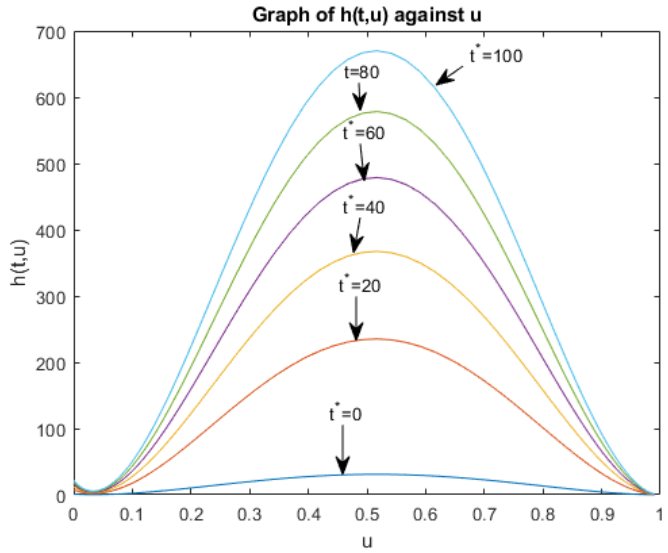



Figure 5.21: Graph of half-width $h(t,u)$ plotted against $u$ for $M_0 = 1.05$ x $10^3$ for a silicic magma fracture at a range of times from $t^* = \frac{t}{c_1} = 0$ to $t^* = \frac{t}{c_1} = 100$.

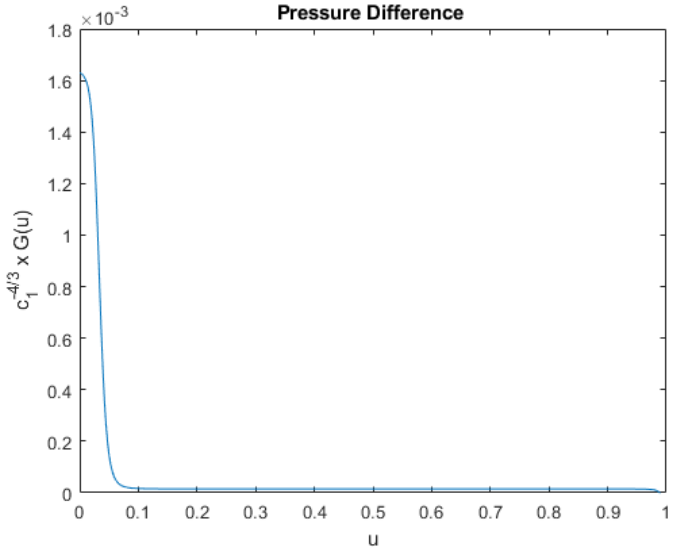



Figure 5.22: Graph of pressure difference $P(0,u) = c_1^{-\frac{4}{3}} G_1(u)$ plotted against $u$ for $M_0 = 1.05 \text{ x } 10^3$ for a silicic magma fracture.

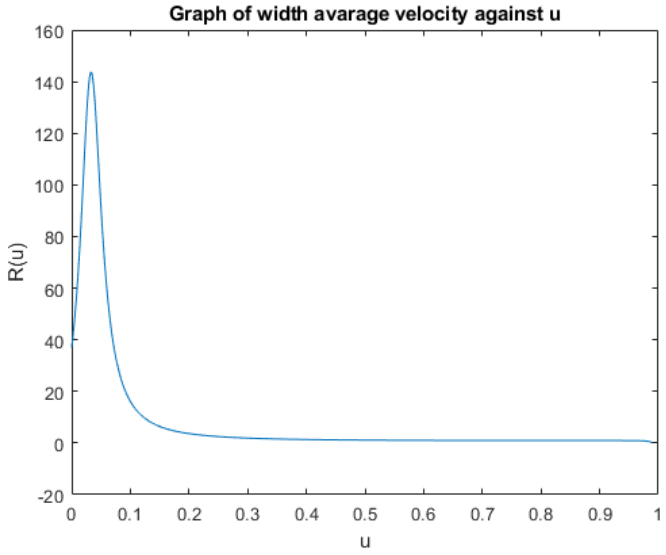



Figure 5.23: Graph of the ratio R(u) of the width average fluid velocity to the speed of propagation of the fracture $\frac{dL}{dt}$ plotted against $u$ for $M_0 = 1.05 \text{ x } 10^3$ for silicic magma fracture. At the entry $R(0) = 37.0540$ while the asymptotic results with $Q_0 = 3.64557 \text{ x } 10^{-4}$ gives $R(0) = c_1 Q_0 = 36.4557$.

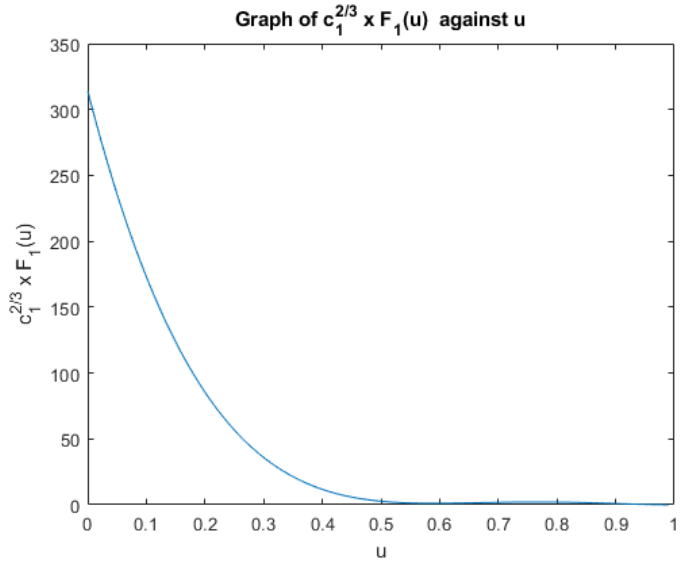



Figure 5.24: Graph of $h(0,u) = c_1^{\frac{2}{3}} F_1(u)$ plotted against $u$ for $M_0 = 2.8$ x $10^2$ for silicic magma fracture. The shooting method cannot reach $c_1^{\frac{2}{3}} F_1(0) = 1$ and the curve is not a numerical solution.

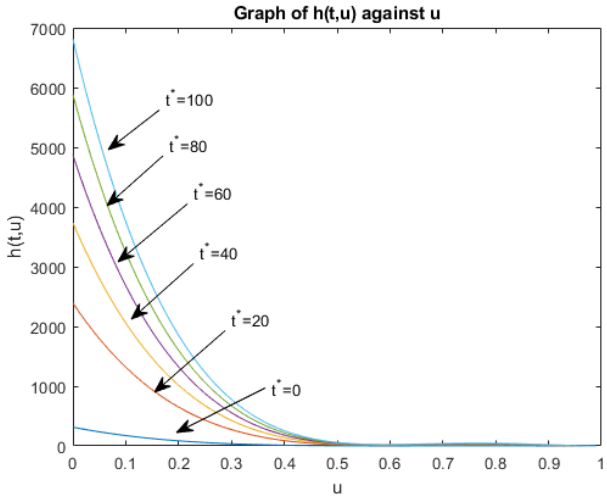



Figure 5.25: Graph of half-width $h(t,u)$ plotted against $u$ for $M_0 = 2.8$ x $10^2$ for a silicic magma fracture at a range of times from $t^* = \frac{t}{c_1} = 0$ to $t^* = \frac{t}{c_1} = 100$. The shooting method cannot reach $c_1^{\frac{2}{3}} F_1(0) = 1$ and the figure does not show a numerical solution.

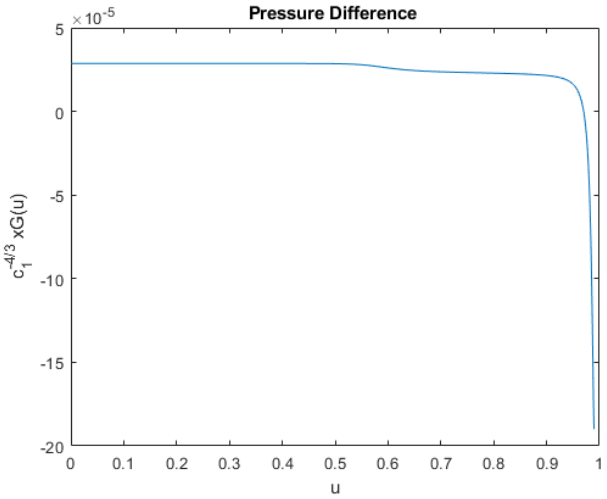



Figure 5.26: Graph of pressure difference $P(0,u) = c_1^{-\frac{4}{3}} G_1(u)$ plotted against $u$ for $M_0 = 2.8$ x $10^2$ for a silicic magma fracture. The curve does not describe a numerical solution because $c_1^{\frac{2}{3}} F_1(0) \neq 1$.

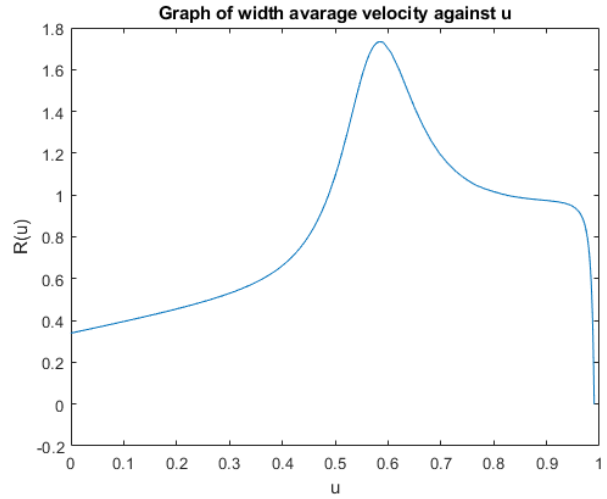



Figure 5.27: Graph of the ratio R(u) of the width average fluid velocity to the speed of propagation of the fracture $\frac{dL}{dt}$ plotted against $u$ for $M_0 = 2.8$ x $10^2$ for a silicic magma fracture. At the entry $R(0) = 0.339792$ while the asymptotic result with $Q_0 = 3.441743$ x $10^{-11}$ gives $R(0) = c_1 Q_0 = 3.441743$ x $10^{-6}$. The large difference is because the shooting method could not reach $c_1 F_1(0) = 1$.

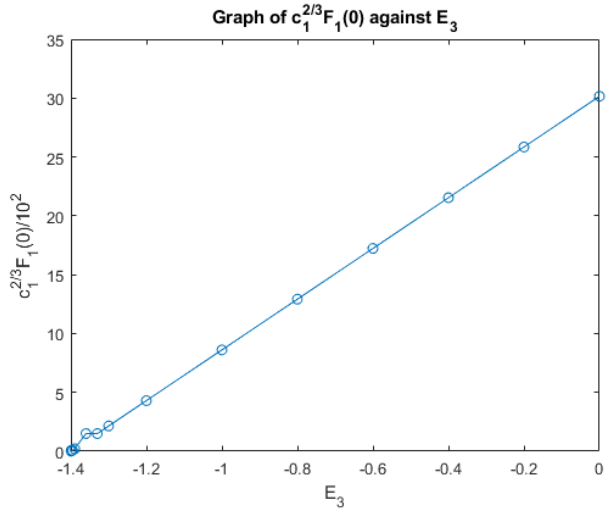



Figure 5.28: Graph of $c_1^{\frac{2}{3}}F_1(0)$ x $10^{-3}$ plotted against $E_3$ for $M_0$ = 6 x $10^3$ and $c_1 = 10^5$.

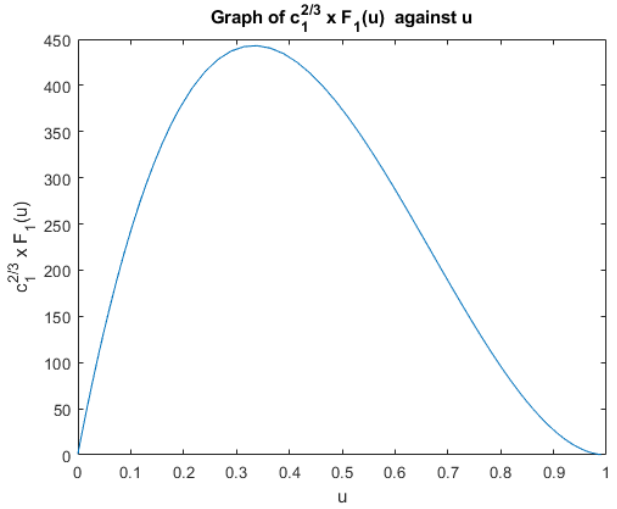



Figure 5.29: Graph of $h(0,u) = c_1^{\frac{2}{3}}F_1(u)$ plotted against $u$ for $M_0$ = 6 x $10^3$ for a silicic magma fracture.

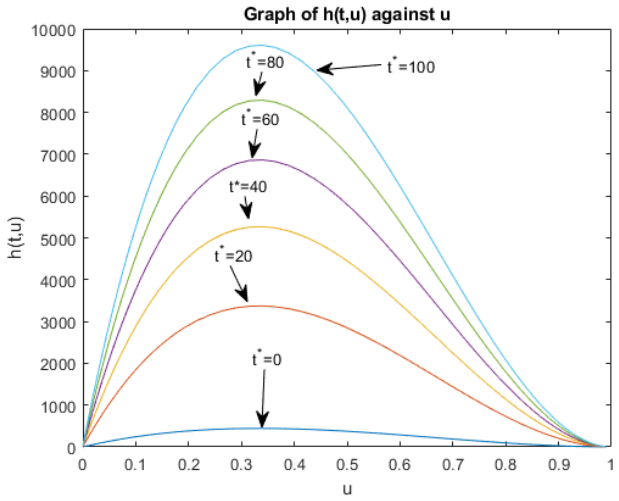



Figure 5.30: Graph of half-width $h(t,u)$ plotted against $u$ for $M_0 = 6$ x $10^3$ for a silicic magma fracture at a range of times from $t^* = \frac{t}{c_1} = 0$ to $t^* = \frac{t}{c_1}$.

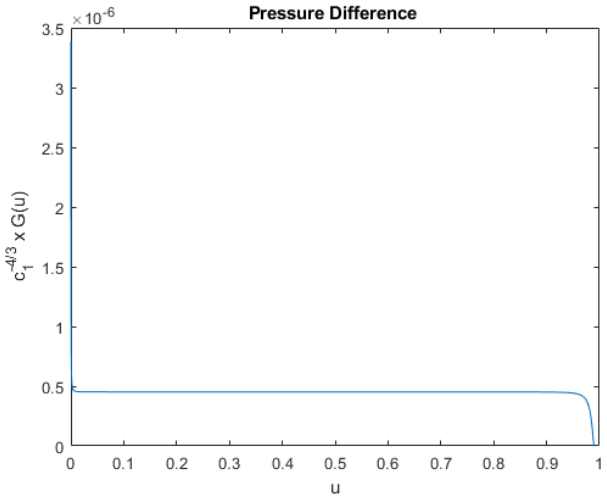



Figure 5.31: Graph of pressure difference $P(0,u) = c_1^{-\frac{4}{3}} G_1(u)$ plotted against $u$ for $M_0 = 6$ x $10^3$ for a silicic magma fracture. At the entry the pressure difference decrease rapidly from $P(0,0) = 15.355427$ to $P(0,u) = 0.5$ x $10^{-6}$

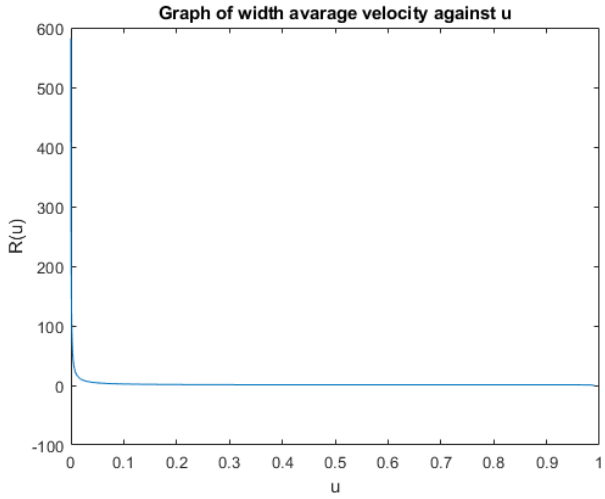



Figure 5.32: Graph of the ratio R(u) of the width average fluid velocity to the speed of propagation of the fracture $\frac{dL}{dt}$ plotted against $u$ for $M_0 = 6$ x $10^3$ for silicic magma fracture. At the entry $R(0) = 5.8217$ x $10^2$ while the asymptotic result with $Q_0 = 5.8211$ x $10^{-3}$ gives $R(0) = c_1 Q_0 = 5.8211$ x $10^{-3}$.

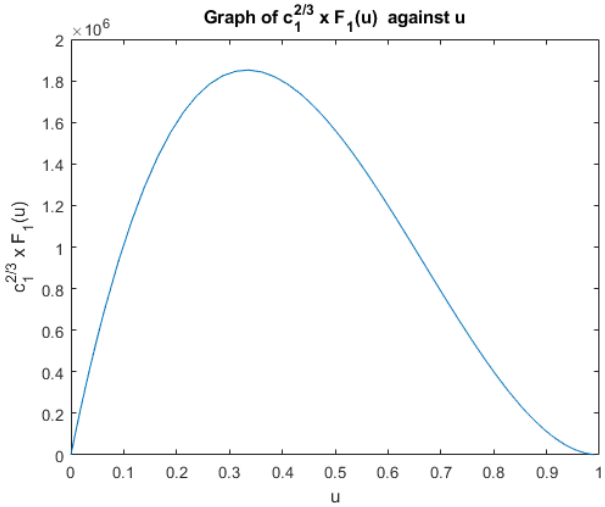



Figure 5.33: Graph of $h(0,u) = c_1^{\frac{2}{3}} F_1(u)$ plotted against $u$ for $M_0 = 2.5$ x $10^7$ for silicic magma fracture.

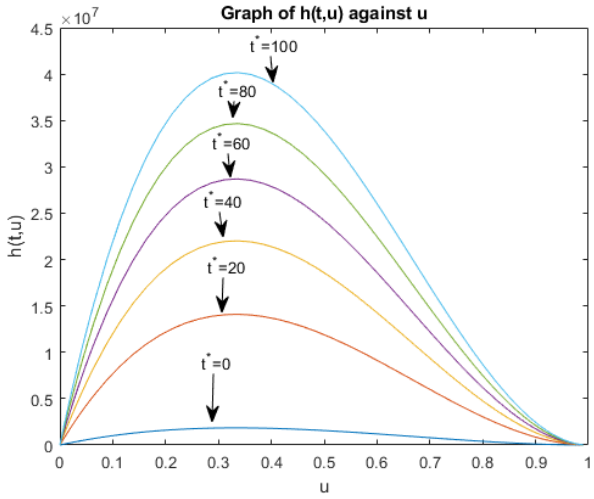



Figure 5.34: Graph of half-width $h(t,u)$ plotted against $u$ for $M_0 = 2.5$ x $10^7$ silicic magma fracture at a range of times from $t^* = \frac{t}{c_1} = 0$ to $t^* = \frac{t}{c_1} = 100$,. for fluid extraction at the fracture entry.

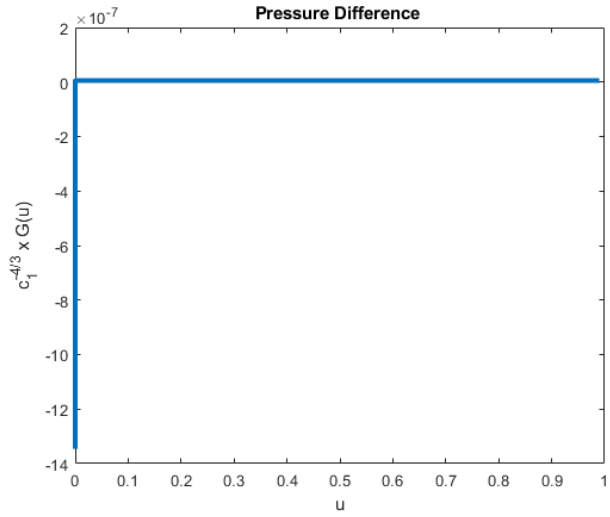



Figure 5.35: Graph of pressure difference $P(0,u) = c_1^{-\frac{4}{3}} G_1(u)$ plotted against $u$ for $M_0 = 2.5$ x $10^7$ for silicic magma fracture. At entry $P(0.0)$ - 6.26 but it increase rapidly to approximately zero. At the fracture tip $P(0,1) = 0$.

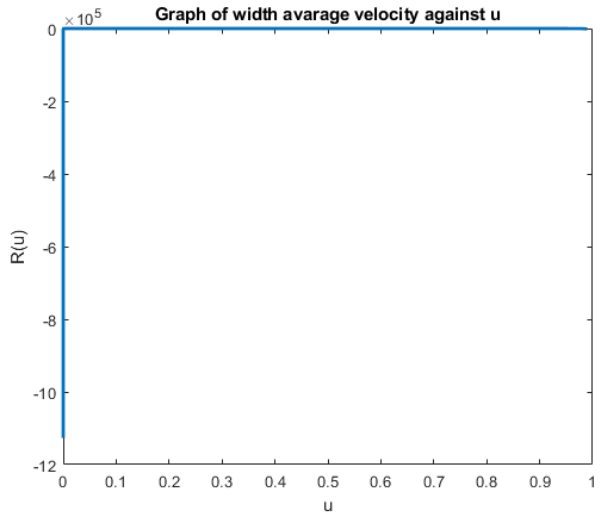



Figure 5.36: Graph of the ratio R(u) of the width average fluid velocity to the speed of propagation of the fracture $\frac{dL}{dt}$ plotted against $u$ for $M_0 = 2.5$ x $10^7$ for silicic magma fracture. At the entry $R(0) = -1.1265$ x $10^6$ while the asymptotic results with $Q_0 = -11.269$ gives $R(0) = c_1 Q_0 = -1.1269$ x $10^6$.

## 5.7 Conclusions

The asymptotic solution for finite bending moment for $F(u)$ and $G(u)$ as $u \to 1$ was useful in formulating the numerical solution. For the velocity ratio $R(u)$ we found that $R(u) \to 0$ as $u \to 1$ which showed that the width average fluid velocity vanished at the fracture tip because the gradient of the half-width tends to zero as $u \to 1$ and the viscous fluid sticks to the beams. Thus compares with the Perkin - Kern - Nordgren ($PKN$) models for hydraulic fracture for which the width average fluid velocity tends to the velocity of propagation of the fracture tip as $u \to 1$ [2]. The result $R(0) = c_1 Q_0$, derived from the boundary conditions, was very useful in checking the numerical solution.

The problem of sill formation in geophysics was very useful to determine the values of the parameters $A$ and $B$. Sill formation can be modelled as the injection of fluid between two beams. It also gave a condition on the physical parameters for the fluid flow to be laminar which was a condition made in the mathematical model. The numerical method could therefore be tested on a

practical problem.

When the bending moment at the fracture tip is finite the hydraulic fracturing problem was formulated as a boundary value problem for six ordinary differential equations subject to boundary conditions. A shooting method for the system of nonlinaer ordinary differential equations was considered. The initial conditions were calculated using the asymptotic solution at the fracture tip. We used the MATLAB built- in function ODE45 for Initial Value Problems. We shoot to the target

$$c_1^{-\frac{2}{3}} F_1(0) = 1. \tag{5.87}$$

The solution for $c_1 = 10^5$ was considered in detail. It was found that for small values of $M_0$ two parameters, $E_3$ which was positive and $E_4$ which was negative were required in the shooting method but after the range of $M_0$ for which there was no solution, only one parameter $E_3$ was needed which changed sign and become negative. For the range of $M_0$ a good initial estimate for $E_3$ was $E_3 = -E_2$ which improved as $M_0$ increased. We also see from the Table 5.3 that for

$$M_0 \gtrsim 3\text{x}10^3 \qquad F_2(0) = \frac{dF(0)}{du} \simeq E_2, \tag{5.88}$$

which improved as $M_0$ increased. The numerical solution for other value of $c_1$ were similar to the solution for $c_1 = 10^5$

The numerical results obtained described a large range of physical application which depend on the value of $M_0$ and $c_1$. They are different from the numerical results obtained by Zvyagin and Gevorkyan [20] for which the width of the fracture decreased steadily from the entry to the fracture tip. Our numerical results showed that the beams tended to "buckle" during the process of hydraulic fracturing and that the upper and lower beams could touch for which the shooting method did not give a solution. It was also found that the fluid extraction could occur for high bending moment.

In this dissertation the case $c_1 = 10^5$ only was considered. This value illustrated the wide range of possible solutions and the fluid flow was laminar with $Q_0 \lesssim 37$. Other values of $c_1$ were briefly investigated. For $c_1 = 10^4$ and $10^3$ the results were similar to the results of $c_1 = 10^5$. For $c_1 = 10^2$ and 1 there were more regions in which the numerical solution using the shooting method did not exist, especially for the small values of the bending moment $M_0$, which suggested

there was more touching of the beams. When the solution existed the values of $Q_0$ were larger showing that the flow was turbulent

# Chapter 6

# Conclusions

## 6.1 Mathematical model

The model of a hydraulic fracture using Euler-Bernoulli beams was first formulated by Zvyagin and Gevorkyan [20]. The application of lubrication theory to the thin fluid film between the two closely spaced beams greatly simplified the Navier-Stokes equation. A nonlinear diffusion equation was derived relating the half-width to the pressure difference between the fluid pressure and the normal compressive stress on the upper surface of the beam. The fourth order Euler-Bernoulli beam equation gave the second partial differential equation between the half-width and pressure difference. The partial differential equations in dimensionless form a depended essentially on two dimensionless numbers, $A$ and $B$. The number $A$ multiplied the highest derivative, of fourth order, in the beam equation.

The boundary conditions at the fracture tip depended critically on whether the bending moment $M_0$ is finite or infinite. We considered finite bending moment only because an infinite bending moment would crack the beam. The boundary condition at the fracture entry prescribed the fluid flux into the fracture.

The ratio of the width average fluid velocity to the speed of propagation of the fracture depend only on the variable $u = \frac{x}{L(t)}$ and was independent of time explicitly. The ratio was useful to check numerical results and interpret the flow of fluid in the fracture.

## 6.2 Lie group analysis

A Lie point symmetry analysis was done on the system of two coupled partial differential equations. The invariance condition for the second order nonlinear diffusion equation was first considered. Prolongation formulae only to second order had to be calculated. The results greatly simplified the Lie point symmetry which made it not too difficult to calculate the fourth order prolongation formulae in the invariance condition for the fourth order Euler-Bernoulli beam equation. By performing the derivation of the Lie point symmetry in this order it could be calculated manually.

We considered two cases for the invariant solution, the general case $c_2 \neq 0$ and the special case $c_2 = 0$. For both cases the partial differential equations were reduced to ordinary differential equations and the boundary conditions were expressed in terms of the invariant variables. The ordinary differential equations did not have any Lie point symmetries for $c_2 \neq 0$ and only $x = \frac{\partial}{\partial u}$ for $c_2 = 0$. We were not able to solve the ordinary differential equations analytically but were able to formulate the problem for a numerical solution.

## 6.3 Numerical solution

The numerical solution for the general case $c_2 \neq 0$ was considered because it was more important in practice. The system of one second order ordinary differential equation and one fourth order ordinary differential equation was written as a system of six first order ordinary differential equations. A shooting method was used, shooting from the fracture tip at $u = 1$ towards the fracture entry at $u = 0$. Because one of the six first order differential equations was singular at $u = 1$, the shooting was done a small distance $\delta$ in from $u = 1$. The asymptotic solution as $u \to 1$ was very useful in calculating the values of the functions $F_1(u)$, $F_2(u)$, ..., $F_6(u)$ at $u = 1-\delta$. The MATLAB built-in function ODE 45 for Initial Value Problems was able to give the numerical solution.

## 6.4 Results

In order to obtain values for the physical parameters and dimensionless numbers a specific physical problem was considered. We considered the problem

from geophysics of the formation of sills by injection of silicic lava between layers of rock which were modelled as beams. Our results showed that the beams tended to "buckle" during the fluid injection process. This is different from the results of Zvyagin and Gevorkyan [20] for hydraulic fracturing of two closely spaced beams who found numerically that the width between the beams decreased steadily from the fracture entry to the fracture tip. The shooting method worked well for most cases but did not give a solution for the range of values of the bending moment $M_0$ for which the upper and the lower beams may be touching at an interior point.

## 6.5 Future work

We have seen that the theory may have application to geophysics. In the model considered the fluid flow in the fracture was laminar. For silicic lava the conditions for the flow to become turbulent was calculated. Turbulent fluid fracture of the two closely spaced beams could be considered. Two models of turbulence could be investigated and compared, the Blasius wall shear stress model [7, 2] and Prandtl's mixing length model.

# Appendix A

# Lie point symmetries of the system of ordinary differential equations for the general case $c_2 \neq 0$.

In this Appendix we investigate the Lie point symmetries of the coupled system of ordinary differential equations (4.179) and (4.180) ,

$$c_1 k \frac{d}{du}\left(F^3 \frac{dG}{du}\right) + \frac{3}{2} u \frac{dF}{du} - 2F = 0, \tag{A.1}$$

$$A c_1 \frac{d^4}{du^4} + \frac{1}{4} u^2 \frac{d^2F}{du^2} + \frac{1}{12} u \frac{dF}{du} - \frac{2}{9} F = BG, \tag{A.2}$$

for $c_1 \neq 0$. The determining equations for the Lie point symmetry

$$X = \xi(u,F,G)\frac{\partial}{\partial u} + \eta^1(u,F,G)\frac{\partial}{\partial F} + \eta^2(u,F,G)\frac{\partial}{\partial G} \tag{A.3}$$

of the system, (A.1) and (A.2, are

$$X^{[2]}\left(3c_1 kF^2 F'G' + c_1 kF^3 G'' + \frac{3}{2} uF' - 2F\right)\Big|_{ODE(A.1),\ ODE(A.2)} = 0 \tag{A.4}$$

and

$$X^{[4]}\left(Ac_1^2F^{iv}+\frac{u^2}{4}F''+\frac{u}{12}F'-\frac{2}{9}F-BG\right)\Big|_{ODE(A.1),\ ODE(A.2)}=0, \tag{A.5}$$

where dash ($\prime$) denotes differentiation with respect to $u$ and $X^{[2]}$ and $X^{[4]}$ are

$$X^{[2]}=X+\zeta_1^1\frac{\partial}{\partial F'}+\zeta_1^2\frac{\partial}{\partial G'}+\zeta_{11}^2\frac{\partial}{\partial G''}, \tag{A.6}$$

$$X^{[4]}=X+\zeta_1^1\frac{\partial}{\partial F'}+\zeta_{11}^1\frac{\partial}{\partial F''},+\zeta_{1111}^1\frac{\partial}{\partial F^{iv}}, \tag{A.7}$$

where only the terms not identically zero are included and

$$\zeta_1^1 = D(\eta^1)-F'D(\xi), \tag{A.8}$$

$$\zeta_1^2 = D(\eta^2)-G'D(\xi), \tag{A.9}$$

$$\zeta_{11}^1 = D(\zeta_1^1)-F''D(\xi), \tag{A.10}$$

$$\zeta_{11}^2 = D(\zeta_1^2)-G''D(\xi), \tag{A.11}$$

$$\zeta_{111}^1 = D(\zeta_{11}^1)-F'''D(\xi), \tag{A.12}$$

$$\zeta_{1111}^1 = D(\zeta_{111}^1)-F^{iv}D(\xi) \tag{A.13}$$

and

$$D=\frac{\partial}{\partial u}+F'\frac{\partial}{\partial F}+G'\frac{\partial}{\partial G}+F''\frac{\partial}{\partial F'}+G''\frac{\partial}{\partial G'}.... \tag{A.14}$$

Consider first the determining equation ($A.4$) which using ($A.6$) for $X^{[4]}$ is

$$\frac{3}{2}\xi F' + (6c_1kFF'G' + 3c_1kF^2G'' - 2)\eta^1 + \frac{3}{2}(2c_1kF^2G' + u)\zeta_1^1 + 3c_1kF^2F'\zeta_1^2$$

$$+ \quad c_1kF^3\zeta_{11}^2|_{ODE(A.1),\ ODE(A.2)} = 0 \tag{A.15}$$

The coefficients $\zeta_1^1$ , $\zeta_1^2$ and $\zeta_{11}^2$ are expanded.

The second derivatives $G''$ and $F''$ are replaced in the determining equation using the ordinary differential equations (A.1) and (A.2),

$$G'' = -\frac{3F'G'}{F} - \frac{3uF'}{2c_1kF^3} + \frac{2}{c_1kF^2}, \tag{A.16}$$

$$F'' = -\frac{4Ac_1^2}{u^2}F^{iv} - \frac{1}{3u}F' + \frac{8}{9u^2}F + \frac{4B}{u^2}G. \tag{A.17}$$

The determining equation is then separated according to the powers and the products of the partial derivatives of $F$ and $G$:

$$F^{iv}G' \quad : \qquad \frac{\partial\xi}{\partial F} = 0, \tag{A.18}$$

$$F^{(iv)} \quad : \qquad \frac{\partial\eta^2}{\partial F} = 0, \tag{A.19}$$

$$F'G'^2 \quad : \qquad \frac{\partial\xi}{\partial G} = 0. \tag{A.20}$$

Hence

$$\xi = \xi(u), \qquad \eta^1 = \eta^1(u,F,G), \qquad \eta^2 = \eta^1(u,G), \tag{A.21}$$

and separating further

$$F'G' \quad : \quad F\frac{\partial \eta^1}{\partial F} - \eta^1 = 0, \tag{A.22}$$

$$G'^2 \quad : \quad 3\frac{\partial \eta^1}{\partial G} + F\frac{\partial^2 \eta^2}{\partial G^2} = 0, \tag{A.23}$$

$$G' \quad : \quad c_1 kF^2\Big[3\frac{\partial \eta^1}{\partial u} + 2F\frac{\partial^2 \eta^2}{\partial G \partial u} - F\frac{d^2\xi}{du^2}\Big] + \frac{3}{2}u\frac{\partial \eta^1}{\partial G} = 0, \tag{A.24}$$

$$\begin{aligned} F' \quad : \quad & \frac{3}{2}\Big(\xi + u\frac{d\xi}{du}\Big) + \frac{3}{2}\frac{u}{F}\Big(F\frac{\partial \eta^1}{\partial F} - 3\eta^1\Big) + 3c_1 kF^2\frac{\partial \eta^2}{\partial u} \\ - \quad & \frac{3}{2}u\frac{\partial \eta^1}{\partial G} = 0, \end{aligned} \tag{A.25}$$

$$\begin{aligned} Remainder \quad : \quad & -4F\frac{d\xi}{du} + \frac{3}{2}u\frac{\partial \eta^1}{\partial u} + 4\eta^1 + c_1 kF^3\frac{\partial^2 \eta^2}{\partial u^2} \\ + \quad & 2F\frac{\partial \eta^2}{\partial G} = 0. \end{aligned} \tag{A.26}$$

From (A.22) it follows that

$$\eta^1(u,F,G) = FP(u,G) \tag{A.27}$$

where $P(u,G)$ is an arbitrary function. Equation $(A.23)$ becomes

$$\frac{\partial}{\partial G^2}\eta^2(u,G) + 3\frac{\partial}{\partial G}P(u,G) = 0 \tag{A.28}$$

and intergrating with respect to $G$ gives

$$P(u,G) = A(u) - \frac{1}{3}\frac{\partial^2}{\partial G}\eta^2(u,G) \tag{A.29}$$

where $A(u)$ is an arbitrary function. Thus from $(A.27)$,

$$\eta^1(u,F,G) = F\Big(A(u) - \frac{1}{3}\frac{\partial}{\partial G}\eta^2(u,G)\Big). \tag{A.30}$$

Substitute ($A$.30) into ($A$.24) which becomes

$$c_1 k\Big[3\frac{dA}{du}+\frac{\partial}{\partial u\partial G}\eta^2(u,G)-\frac{d^2\xi}{du^2}\Big]F^3-\frac{u}{2}F\frac{\partial^2}{\partial G^2}\eta^2(u,G)=0. \tag{A.31}$$

Separate by powers of $F$.

$$F \quad : \quad \frac{\partial^2}{\partial G^2}\eta^2(u,G)=0, \tag{A.32}$$

$$F^3 \quad : \quad 3\frac{dA}{du}+\frac{\partial^2}{\partial u\partial G}\eta^2(u,G)-\frac{d^2\xi}{du^2}=0. \tag{A.33}$$

From ($A$.32),

$$\eta^2(u,G)=GB(u)+D(u), \tag{A.34}$$

where $B(u)$ and $D(u)$ are arbitrary function. Substitute ($A$.34) into ($A$.33) which gives

$$3\frac{dA}{du}+\frac{dB}{du}-\frac{d^2\xi}{du^2}=0 \tag{A.35}$$

and integrating with respect to u we obtain

$$B(u)=\frac{d\xi}{du}-3A(u)+b_1, \tag{A.36}$$

where $b_1$ is a constant. Substituting ($A$.36) back into ($A$.34) gives

$$\eta^2(u,G)=\Big(b_1-3A(u)+\frac{d\xi}{du}\Big)G+D(u) \tag{A.37}$$

and ($A$.30) becomes

$$\eta^1(u,F)=\Big(-\frac{1}{3}b_1+2A(u)-\frac{1}{3}\frac{d\xi}{du}\Big)F. \tag{A.38}$$

Substituting ($A$.37) and ($A$.38) into ($A$.25) equation ($A$.25) becomes

$$\frac{3}{2}\Big(\xi + u\frac{d\xi}{du}\Big) + u\Big(b_1 - 6A(u) + \frac{d\xi}{du}\Big) + 3c_1kF^2\Big[G\Big(-3\frac{dA}{du} + \frac{d^2\xi}{du^2}\Big) + \frac{dD}{du}\Big]$$

$$- \quad \frac{3u}{2}\Big(b_1 - 3A(u) + \frac{d\xi}{du}\Big) \tag{A.39}$$

Separate by powers and product of $F$ and $G$.

$$F^2 \quad : \quad \frac{dD}{du} = 0 \tag{A.40}$$

$$F^2G \quad : \quad \frac{d^2\xi}{du^2} - 3\frac{dA}{du} = 0, \tag{A.41}$$

$$Remainder \quad : \quad \frac{3}{2}\xi + u\frac{d\xi}{du} - \frac{1}{2}ub_1 - \frac{3}{2}uA(u) = 0. \tag{A.42}$$

From $(A.40)$ and $(A.41)$

$$D(u) \quad = \quad b_2, \tag{A.43}$$

$$\frac{d\xi}{du} - 3A(u) \quad = \quad b_3 \tag{A.44}$$

where $b_2$ and $b_3$ are constants. By eliminating A(u), the $Remainder$ $(A.42)$ becomes the first order linear differential equation

$$\frac{d\xi}{du} + \frac{3}{u}\xi = b_1 - b_3. \tag{A.45}$$

Hence

$$\xi(u) = \frac{1}{4}(b_1 - b_3)u + \frac{b_4}{u^3}, \tag{A.46}$$

where $b_4$ is a constant and from $(A.44)$,

$$A(u) = \frac{1}{12}\Big[b_1 - 5b_3 - 12\frac{b_4}{u^4}\Big]. \tag{A.47}$$

Thus

$$\eta^1(u,F) = -\Big[\frac{1}{4}(b_1+3b_3) + \frac{b_4}{u^4}\Big]F, \tag{A.48}$$

$$\eta^2(u,G) = (b_1+b_3)G + b_2. \tag{A.49}$$

We now substitute $(A.46)$, $(A.48)$ and $(A.49)$ for $\xi(u)$, $\eta^1(u,F)$ and $(\eta^2(u,G)$ into the last equation $(A.42)$ which becomes

$$Fb_4u^{-4} = 0 \tag{A.50}$$

and therefore

$$b_4 = 0. \tag{A.51}$$

Thus, from the first determining equation we obtain

$$X = \xi(u)\frac{\partial}{\partial u} + \eta^1(F)\frac{\partial}{\partial F} + \eta^2(G)\frac{\partial}{\partial G} \tag{A.52}$$

where

$$\xi(u) = \frac{1}{4}(b_1 - b_3)u, \tag{A.53}$$

$$\eta^1(F) = -\frac{1}{4}(b_1+3b_3)F, \tag{A.54}$$

$$\eta^2(F) = (b_1+b_3)G + b_2. \tag{A.55}$$

Before we consider the second determining equation we rename the constants in (4.53) to (4.55). Let

$$\frac{1}{4}(b_1 - b_3) = a_1, \quad -\frac{1}{4}(b_1 + 3b_3) = a_2, \quad b_2 = a_3, \tag{A.56}$$

then

$$b_1 = 3a_1 - a_2, \quad b_3 = -(a_1 + a_2), \quad b_1 + b_3 = 2(a_1 - a_2). \tag{A.57}$$

Thus

$$X = a_1 u\frac{\partial}{\partial u} + a_2 F\frac{\partial}{\partial F} + \Big[2(a_1 - a_2)G + a_3\Big]\frac{\partial}{\partial G} \tag{A.58}$$

and

$$\xi(u) = a_1 u, \tag{A.59}$$

$$\eta^1(F) = a_2 F, \tag{A.60}$$

$$\eta^2(G) = 2(a_1 - a_2)G + a_3. \tag{A.61}$$

The second determining equation is (A.5) which when expanded is

$$\frac{1}{2}\Big(uF'' + \frac{1}{6}F'\Big)\xi - \frac{2}{9}\eta^1 - \eta^2 + \frac{u}{12}\zeta^1_1 + \frac{u^2}{4}\zeta^1_{11} + Ac_1^2\zeta^1_{1111}|_{ODE(A.1),\ ODE(A.2)} = 0. \tag{A.62}$$

Now using $(A.8)$ to $(A.14)$,

$$\zeta_1^1 = (a_2 - a_1)F', \tag{A.63}$$

$$\zeta_{11}^1 = (a_2 - 2a_1)F'', \tag{A.64}$$

$$\zeta_{111}^1 = (a_2 - 3a_1)F''', \tag{A.65}$$

$$\zeta_{1111}^1 = (a_2 - 4a_1)F'^{v}. \tag{A.66}$$

.

Equation $(A.62)$ becomes

$$\frac{1}{2}\Big(uF'' + \frac{1}{6}F'\Big)a_1 u - \frac{2}{9}a_2 F - \Big[2(a_1 - a_2)G + a_3\Big] + \frac{u}{12}(a_2 - a_1)F'$$

$$+ \quad \frac{u^2}{4}(a_2 - 2a_1)F'' + Ac_1^2(a_2 - 4a_1)F'^{v}\Big|_{ODE(A.1),\ ODE(A.2)} = 0. \tag{A.67}$$

Now from $(A.2)$.

$$Ac_1^2 F'^{v} = -\frac{u^2}{4}F'' - \frac{u}{12}F' + \frac{2}{9}F + BG \tag{A.68}$$

and substititing $(A.68)$ into $(A.67)$ we obtain

$$-\frac{8}{9}a_1 F + 3(a_2 - 2a_1)BG + \frac{1}{3}a_1 uF' + a_1 u^2 F'' - Ba_3\Big|_{ODE(A.1)} = 0 \tag{A.69}$$

Also, from $(A.1)$

$$F' = \frac{2(2F - c_1 kF^3 G'')}{3(u + 2c_1 kF^2 G')} \tag{A.70}$$

and replacing $F'$ in $(A.69)$ using $(A.70)$ gives

$$
\begin{aligned}
&- \frac{4}{9}a_1uF - \frac{16}{9}a_1c_1kF^3G' + 3(a_2-2a_1)uG + 6(a_2-2a_1)c_1kBGF^2G' \\
&+ a_1u^3F'' + 2a_1c_1ku^2F^2G'F'' - 2Ba_3c_1kF^2G' + a_1u^3F'' \\
&- \frac{2}{9}a_1c_1kuF^3G'' = 0. \qquad \text{(A.71)}
\end{aligned}
$$

We separate $(A.71)$ by the powers and products of the independent variables.

$$F^3G': \qquad a_1 = 0. \qquad \text{(A.72)}$$

Equation $(A.71)$ reduces to

$$3a_2uG + 6a_2c_1kGF^2G' - Ba_3u - 2Ba_3c_1kF^2G' = 0 \qquad \text{(A.73)}$$

and separating again gives

$$F^2GG': \qquad a_2 = 0, \qquad \text{(A.74)}$$

$$F^2G': \qquad a_3 = 0. \qquad \text{(A.75)}$$

Hence from $(A.58)$

$$X = 0 \qquad \text{(A.76)}$$

and the system $(A.1)$ and $(A.2)$ does not admit a Lie point symmetry when $c_1 \neq 0$,

# Appendix B

# Lie point symmetries of the system of ordinary differential equations for $c_2 = 0$.

In this Appendix we consider the Lie point symmetries of the coupled system of equations (4.219) and (4.220)

$$k\frac{d}{du}\left[F^3\frac{dG}{du}\right] + 3c_3\frac{dF}{du} = 0, \tag{B.1}$$

$$A\frac{d^4F}{du^4} + c_3^2\frac{d^2F}{du^2} = BG, \tag{B.2}$$

where $c_3 \neq 0$. The Lie Point symmetry of the system $(B1)$ and $(B.2)$ is

$$X = \xi(u,F,G)\frac{\partial}{\partial u} + \eta^1(u,F,G)\frac{\partial}{\partial F} + \eta^2(u,F,G)\frac{\partial}{\partial G} \tag{B.3}$$

and the determining equations are

$$X^{[2]}(kF^3G'' + 3kF^2F'G' + 3c_3F')\Big|_{ODE(B.1),\quad ODE(B.2)} = 0, \tag{B.4}$$

$$X^{[4]}(AF^4 + 3c_3^2F'' - BG)\Big|_{ODE(B.1),\quad ODE(B.2)} = 0, \tag{B.5}$$

where

$$X^{[2]} = X + \zeta_1^1 \frac{\partial}{\partial F'} + \zeta_1^2 \frac{\partial}{\partial G'} + \zeta_{11}^2 \frac{\partial}{\partial G''}, \tag{B.6}$$

$$X^{[4]} = X + \zeta_{11}^1 \frac{\partial}{\partial F''} + \zeta_{1111}^1 \frac{\partial}{\partial F'^{\nu}} \tag{B.7}$$

and $\zeta_1^1$, $\zeta_{11}^1$, $\zeta_{111}^1$ (which is required to calculate $\zeta_{1111}^1$), $\zeta_{1111}^1$, $\zeta_1^2$ $\zeta_{11}^2$, are given by ($A$.8) to (A.13) with $D$ given by ($A$.14).

The first determining equation ($B$.4) is

$$(3kF^2G''+6kFF'G')\eta^1+(3kF^2G'+3c_3)\zeta_1^1+3kF^2F'\zeta_1^2+kF^3\zeta_{11}^2\Big|_{ODE(B.1),\quad ODE(B.2)} = 0 \tag{B.8}$$

The coefficients $\zeta_1^1$, $\zeta_1^2$ and $\zeta_{11}^2$ are calculated. The ordinary differential equation(B.1) and (B.2) are used to replace the second derivatives in (B.8),

$$F'' = \frac{1}{c_3^2}\Big(BG - AF'^{\nu}\Big), \tag{B.9}$$

$$G'' = -3\frac{G'F'}{F} - 3c_3\frac{F'}{kF^3} \tag{B.10}$$

The determining equation is then separated by the powers and products of the partial derivatives of $F$ and $G$.

$$G'F'^{\nu} \quad : \qquad \frac{\partial \xi}{\partial F} = 0, \tag{B.11}$$

$$F'^{\nu} \quad : \qquad \frac{\partial \eta^2}{\partial F} = 0, \tag{B.12}$$

$$F'G'^2 \quad : \qquad \frac{\partial \xi}{\partial G} = 0. \tag{B.13}$$

Thus

$$\xi = \xi(u), \qquad \eta^1 = \eta^1(u,F,G), \qquad \eta^2 = \eta^2(u,G). \tag{B.14}$$

Separating the determining equation again gives

$$G'F' \quad : \quad F\frac{\partial \eta^1}{\partial F} - \eta^1 = 0, \tag{B.15}$$

$$G'^3 \quad : \quad 3\frac{\partial \eta^1}{\partial G} + F\frac{\partial^2 \eta^2}{\partial G^2} = 0, \tag{B.16}$$

$$G' \quad : \quad 3F^2\frac{\partial \eta^2}{\partial u} + \frac{3c_3}{k}\frac{\partial \eta^1}{\partial G} + 2F^3\frac{\partial^2 \eta^2}{\partial G \partial u} - F^3\frac{d^2\xi}{du^2} = 0, \tag{B.17}$$

$$F' \quad : \quad -\frac{9c_3}{F}\eta^1 + 3F^2\frac{\partial \eta^2}{\partial u} + \frac{3c_3}{k}\frac{\partial \eta^1}{\partial F} - \frac{3c_3}{k}\frac{\partial \eta^2}{\partial G} + \frac{3c_3}{k}\frac{\partial \xi}{\partial u} = 0, \tag{B.18}$$

$$R \quad : \quad \frac{3c_3}{k}\frac{\partial \eta^1}{\partial u} + F^3\frac{\partial \eta^2}{\partial u^2}. \tag{B.19}$$

Where $R$ is the remainder.

From (B.15),

$$\eta^1(u,F,G) = FP(u,G) \tag{B.20}$$

where $P(u,G)$ is an arbitrary function. Substituting into the remainder we obtain

$$\frac{3c_3}{k}F\frac{\partial}{\partial u}P(u,G) + F^3\frac{\partial^2}{\partial u^2}\eta^2(u,G) = 0 \tag{B.21}$$

and separating by $F$ gives

$$F \quad : \quad \frac{\partial}{\partial u}P(u,G) = 0, \tag{B.22}$$

$$F^3 \quad : \quad \frac{\partial^2}{\partial u^2}\eta^2(u,G) = 0, \tag{B.23}$$

and therefore

$$P = P(G) \tag{B.24}$$

$$\eta^2(u,G) = uD(G) + E(G) \tag{B.25}$$

In summary,

$$\xi = \xi(u), \quad \eta^1(F,G) = FP(G), \quad \eta^2(u,G) = uD(G) + E(G). \tag{B.26}$$

Equation $(B.18)$ now becomes

$$-6c_3P(G) + 3kF^2D(G) - 3c_3\frac{dD}{dG} - 3c_3\frac{dE}{dG} + 3c_3\frac{d\xi}{du} = 0 \tag{B.27}$$

and separating we obtain

$$F^2 : D(G) = 0, \tag{B.28}$$

$$Remainder : 2P(G) + \frac{dE}{dG} - \frac{d\xi}{du} = 0. \tag{B.29}$$

Differentiating (B.29) by $u$ gives

$$\frac{d^2\xi}{du^2} = 0 \tag{B.30}$$

and therefore

$$\xi(u) = b_1u + b_2, \tag{B.31}$$

where $b_1$ and $b_2$ are constants. Equation (B.29) becomes

$$2P(G) + \frac{dE}{dG} - b_1 = 0. \tag{B.32}$$

hence from (B.26)

$$\xi(u) = b_1 u + b_2, \quad \eta^1(F,G) = \frac{1}{2}\Big(b_1 - \frac{dE}{dG}\Big)F, \quad \eta^2(G) = E(G). \tag{B.33}$$

Equation(B.17) becomes

$$\frac{d^2E}{dG^2} = 0 \tag{B.34}$$

and therefore

$$E(G) = b_3 G + b_4. \tag{B.35}$$

Equation (B.33) becomes

$$\xi(u) = b_1 u + b_2, \quad \eta^1(F,G) = \frac{1}{2}\Big(b_1 - b_3\Big)F, \quad \eta^2(G) = b_3 G + b_4. \tag{B.36}$$

The remaining equation (B.16) is identically satisfied. We rename the constants,

$$b_2 = a_1, \quad b_1 = a_2, \quad \frac{1}{2}\Big(b_1 - b_3\Big) = a_3, \quad b_4 = a_4 \tag{B.37}$$

and therefore

$$\xi(u) = a_1 u + a_2, \quad \eta^1(F,G) = a_3 F, \quad \eta^2(G) = a_4 + (a_2 - 2a_3)G. \tag{B.38}$$

Hence

$$X = \Big(a_1 + a_2 u\Big)\frac{\partial}{\partial u} + a_3 F\frac{\partial}{\partial F} + \Big[a_4 + (a_2 - 2a_3)G\Big]\frac{\partial}{\partial G}. \tag{B.39}$$

The second determining equation, (B.5), when expanded is

$$\Big(-\eta^2 + c_3^2\zeta^1_{11} + A\zeta^1_{1111}\Big)\Big|_{ODE(B.1),\ ODE(B.2)} = 0 \tag{B.40}$$

using (A.8) to (A.14),

$$\zeta_1^1 = (a_3 - a_2)F', \tag{B.41}$$

$$\zeta_{11}^1 = (a_3 - a_2)F'', \tag{B.42}$$

$$\zeta_{111}^1 = (a_3 - a_2)F''', \tag{B.43}$$

$$\zeta_{1111}^1 = (a_3 - a_2)F'^{v}, \tag{B.44}$$

Equation(B.40) becomes

$$-\Big[a_4+(a_2-2a_3)G\Big]+c_3^2(a_3-2a_2)F''+A(a_3-4a_2)F'^{v}\Big|_{ODE(B.1),\ ODE(B.2)} = 0 \tag{B.45}$$

But from (B.2)

$$AF'^{v} = -c_3^2F'' + BG \tag{B.46}$$

and substituting (B.46) into (B.45) we obtain

$$-a_4 + B(3a_2 - 5a_3)G + 2a_2c_3^2F''\Big|_{ODE(B.1),\ ODE(B.2)} = 0 \tag{B.47}$$

But (B.1) depends only on $F$, $F'$, $G'$ and $G''$ which do not occur in (B.47). Thus (B.1) cannot be substituted into (B.47), The Lie point symmetry is therefore a conditional symmetry, the condition is

$$kF^3G'' + 3kF^2F'G' + 3c_3F' = 0. \tag{B.48}$$

Separate (B.47) by equating to zero the coefficients of the independent variables.

$$c_3^2F'' \ : \ a_2 = 0, \tag{B.49}$$

$$G \ : \ 3a_2 - 5a_3 = 0, \tag{B.50}$$

$$Remainder \ : \ a_4 = 0. \tag{B.51}$$

Thus

$$a_2 = 0, \qquad a_3 = 0, \qquad a_4 = 0 \tag{B.52}$$

and the Lie point symmetry (B.39) reduces to

$$X = \frac{\partial}{\partial u}. \tag{B.53}$$

For the special case $c_2 = 0$, the system of ordinary differential equations, (B.1) and (B.2), therefore admit one Lie point symmetry, (B.53). The system (B.1) and (B.2), does not depend explicitly on u. It is a conditional symmetry, the condition is (B.48), derived from equation (B.1)

# Bibliography


[1] D. J. Acheson. *Elementary Fluid Dynamics*. Oxford University Press, 1990, Chapter 7.

[2] M Anthonyrajah, D P Mason, and A G Fareo. Propagation of a pre-existing turbulent fluid fracture. *International Journal of Non-Linear Mechanics*, 54:105–114, 2013.

[3] G. Bluman and S. Anco. *Symmetry and Integration Methods for Differential Equations*, volume 154. Springer Science & Business Media, 2008.

[4] G. Bluman and J. D. Cole. *Similarity Methods for Differential Equations*, volume 13. Springer Science & Business Media, 2012.

[5] G. Bluman and S. Kumei. *Symmetries and Differential Equations*, volume 81. Springer Science & Business Media, 2013.

[6] M. S. Diederichs and P. K. Kaiser. Stability of large excavations in laminated hard rock masses: the voussoir analogue revisited. *International Journal of Rock Mechanics and Mining Sciences*, 36(1):97–117, 1999.

[7] S H Emerman, D L Turcotte, and D A Spence. Transport of magma and hydrothermal solutions by laminar and turbulent fluid fracture. *Physics of the Earth and Planetary Interiors*, 41(4):249–259, 1986.

[8] A. Fatima, H. Bokhari, F. M. Mahomed, and F. D. Zaman. A note on the integrability of a remarkable static euler-bernoulli beam equation. *Journal of Engineering Mathematics*, 82(1):101–108, 2013.

[9] R. P. Gillespie. *Integration*. Oliver and Boyd, Edinburgh and London, New York, 1959, 113-117.

[10] H. P. W. Gottlieb. *Isospectral Euler-Bernoulli beams with continuous density and rigidity functions*, volume 413. Proceedings of the Royal Society of London A: Mathematical, Physical and Engineering Sciences, 235–250, 1987.

[11] N. H. Ibragimov. *CRC Handbook of Lie Group Analysis of Differential Equations*, volume 3. CRC Press, Boca Raton, 1995.

[12] N. K. Ibragimov. *Elementary Lie Group Analysis and Ordinary Differential Equations*, volume 197. Wiley New York, 1999.

[13] A Labuschagne, N. F. J. van Rensburg, and A. J. Van der Merwe. Comparison of linear beam theories. *Mathematical and Computer Modelling*, 49(1):20–30, 2009.

[14] R. Naz and F. M. Mahomed. Dynamic euler-bernoulli beam equation: classification and reductions. *Mathematical Problems in Engineering*, 2015, Article ID 520491, 7 pages.

[15] J. C. Ndogmo. Equivalence transformations of the euler–bernoulli equation. *Nonlinear Analysis: Real World Applications*, 13(5):2172–2177, 2172–2177, 2012.

[16] C. P. Please, D. P. Mason, C. M. Khalique, J. M. T. Ngnotchouye, A. J. Hutchinson, J. N. van der Merwe, and H. Yilmaz. Fracturing of an euler-bernoulli beam in coal mine pillar extraction. *International Journal of Rock Mechanics and Mining Sciences*, 64:132–138, 132–138, 2013.

[17] L. Segel and G. Handelman. *Mathematics Applied to Continuum Mechanics*. Society for Industrial and Applied Mathematics, 2007 , Chapter 5.

[18] C. Wafo Soh. Euler-bernoulli beams from a symmetry standpoint-characterization of equivalent equations. *Journal of Mathematical Analysis and Applications*, 345(1):345:387–395, 387–395, 2008.

[19] A. V. Zvyagin. Motion of a viscous fluid in a channel with elastic boundaries. *Vestn. Mosk. Univ. Ser*, 1:50–54, 2005.

[20] A. V. Zvyagin and A. G. Gevorkyan. Self-similar solution of the hydraulic fracture problem for two closely spaced beams. *Moscow University Mechanics Bulletin*, 67(3):72–75, 2012.